Elsevier Editorial System(tm) for Progress in Materials Science
Manuscript Draft

Manuscript Number:

Title: Recent advances in fiber/matrix interphase engineering for polymer composites

Article Type: Full Review Article

Keywords: composites; interphase; sizing/coating; hierarchical fibers; nanofillers.

Corresponding Author: Prof. Alessandro Pegoretti,

Corresponding Author's Institution: University of Trento

First Author: József Karger-Kocsis

Order of Authors: József Karger-Kocsis; Haroon Mahmood; Alessandro Pegoretti

Abstract: This review summarizes the recent (from year 2000) advancements in the interphase tailoring of fiber-reinforced polymer composites. The scientific and technological achievements are classified on the basis of the selected strategies distinguishing between i) interphase tailoring via sizing/coating on fibers, ii) creation of hierarchical fibers by nanostructures, iii) fiber surface modifications by polymer deposition and iv) potential effects of matrix modifications on the interphase formation. Special attention was paid to report on efforts dedicated to the creation on (multi)functional interphase in polymer composites. This review is round up by listing current trends in the characterization and modelling of the interphase. In the final outlook, future opportunities and challenges in the engineering of fiber/matrix interphase are summarized.

UNIVERSITÀ DEGLI STUDI
DI TRENTO

Department of Industrial Engineering

Trento, October 31st 2014

Professor B. Cantor
Vice Chancellor University of Bradford
Richmond Road, Bradford, West Yorkshire, BD7 1DP

Dear Prof. Cantor

On behalf of my co-authors, prof. Karger-Kocsis and Mr. Mahmood, I hereby submit our draft manuscript for consideration for publication as a Review in Progress in Materials Science: "Recent advances in fiber/matrix interphase engineering for polymer composites".

Progress in Materials Science seems an ideal forum for a manuscript addressing the recent (from year 2000) advancements in the tailoring of interphase of fiber-reinforced polymer composites. The scientific and technological achievements are classified on the basis of the selected strategies distinguishing between i) interphase tailoring via sizing/coating on fibers, ii) creation of hierarchical fibers by nanostructures, iii) fiber surface modifications by polymer deposition and iv) potential effects of matrix modifications on the interphase formation. Special attention was paid to report on efforts dedicated to the creation on (multi)functional interphase in polymer composites. This review is round up by listing current trends in the characterization and modelling of the interphase. In the final outlook, future opportunities and challenges in the engineering of fiber/matrix interphase are summarized.

I trust, therefore, that you will consider our manuscript to be appropriate for your readership.
This is an original manuscript and has not been previously published.

I look forward to hearing from you.

Yours sincerely,

Prof. Alessandro Pegoretti

Prof. Alessandro Pegoretti
Director of the Doctoral School in Materials, Mechatronics and Systems Engineering

Department of Industrial Engineering
Via Sommarive, 9 - 38123 Trento
Tel. ++39-0461-282452
Fax ++39-0461-281977
E-mail: alessandro.pegoretti@unitn.it

Tuesday, February 3, 2015 at 4:25:07 PM Central European Standard Time

Subject: FW: Review manuscript: Recent advances in fiber/matrix interphase engineering for polymer composites
Date: Monday, February 2, 2015 at 5:33:53 PM Central European Standard Time
From: Kirsty Dales
To: Alessandro.Pegoretti@unitn.it
CC: Dora Moscatello, Eduard Arzt, Ke Lu, Kristi Anseth, Ted Massalski (Gosia Fortune), Tetsuo Mohri

Dear Professor Pegoretti,

Please see below message from Professor Cantor for your attention.

Regards

UNIVERSITY of BRADFORD

Kirsty Dales

PA to the Vice-Chancellor
Offices of the Vice-Chancellor

+44 (0) 1274 233091
+44 (0) 1274 233003
www.bradford.ac.uk

Dear Professor Pegoretti,

Thank you for submitting your manuscript entitled ³Recent advances in fiber/matrix interphase engineering for polymer composites².

I am writing to inform you that your manuscript has been accepted for publication in Progress in Materials Science. Please can I ask you to submit your manuscript through the electronic EES system: http://ees.elsevier.com/pms/default.asp. in order for me to progress to publication with Elsevier. Please choose my name when asked to select an editor.

Please don't hesitate to contact me if you require any further information.

Yours sincerely,

Brian Cantor

From: Pegoretti, Alessandro [mailto:Alessandro.Pegoretti@unitn.it]
Sent: 31 October 2014 13:55
To: vc-office
Subject: Review manuscript: Recent advances in fiber/matrix interphase engineering for polymer composites

Dear Prof. Cantor

On behalf of my co-authors, prof. Karger-Kocsis and Mr. Mahmood, I hereby submit our draft manuscript for consideration for publication as a Review in Progress in Materials Science: ³Recent advances in fiber/matrix interphase engineering for polymer composites².

Progress in Materials Science seems an ideal forum for a manuscript addressing the recent (from year 2000) advancements in the tailoring of interphase of fiber-reinforced polymer composites. The scientific and technological achievements are classified on the basis of the selected strategies distinguishing between i) interphase tailoring via sizing/coating on fibers, ii) creation of hierarchical fibers by nanostructures, iii) fiber surface modifications by polymer deposition and iv) potential effects of matrix modifications on the interphase formation. Special attention was paid to report on efforts dedicated to the creation on (multi)functional interphase in polymer composites. This review is round up by listing current trends in the characterization and modelling of the interphase. In the final outlook, future opportunities and challenges in the engineering of fiber/matrix interphase are summarized.

I trust, therefore, that you will consider our manuscript to be appropriate for your readership. This is an original manuscript and has not been previously published.

I look forward to hearing from you.

Yours sincerely,

Alessandro Pegoretti

Professor of Materials Science and Technology
Director of the Doctoral School in Materials, Mechatronics and Systems Engineering

University of Trento
Department of Industrial Engineering
Via Mesiano 77, 38123 Trento, ITALY

Phone +39 0461 282452
http://www.ing.unitn.it/~pegorett/

http://www.frontiersin.org/Composite_Materials/about

*Abstract (summary)

Abstract

This review summarizes the recent (from year 2000) advancements in the interphase tailoring of fiber-reinforced polymer composites. The scientific and technological achievements are classified on the basis of the selected strategies distinguishing between i) interphase tailoring via sizing/coating on fibers, ii) creation of hierarchical fibers by nanostructures, iii) fiber surface modifications by polymer deposition and iv) potential effects of matrix modifications on the interphase formation. Special attention was paid to report on efforts dedicated to the creation on (multi)functional interphase in polymer composites. This review is round up by listing current trends in the characterization and modelling of the interphase. In the final outlook, future opportunities and challenges in the engineering of fiber/matrix interphase are summarized.

Recent advances in fiber/matrix interphase engineering for polymer composites

József Karger-Kocsis[a,b], Haroon Mahmood[c], Alessandro Pegoretti[c*]

[a] Budapest University of Technology and Economics, Faculty of Mechanical Engineering, Department of Polymer Engineering, 1111 Budapest (Hungary)

[b] MTA–BME Research Group for Composite Science and Technology, Műegyetem rkp. 3, 1111 Budapest (Hungary)

[c] University of Trento, Department of Industrial Engineering, Via Sommarive 9, 38123 Trento (Italy)

[*] Corresponding author at: University of Trento, Department of Industrial Engineering, Via Sommarive 9, 38123 Trento (Italy). Tel.: +39 0461 282452; fax: +39 0461 281977.

E-mail address: alessandro.pegoretti@unitn.it (A. Pegoretti).

Abstract

This review summarizes the recent (from year 2000) advancements in the interphase tailoring of fiber-reinforced polymer composites. The scientific and technological achievements are classified on the basis of the selected strategies distinguishing between i) interphase tailoring via sizing/coating on fibers, ii) creation of hierarchical fibers by nanostructures, iii) fiber surface modifications by polymer deposition and iv) potential effects of matrix modifications on the interphase formation. Special attention was paid to report on efforts dedicated to the creation on (multi)functional interphase in polymer composites. This review is round up by listing current trends in the characterization and modelling of the interphase. In the final outlook, future opportunities and challenges in the engineering of fiber/matrix interphase are summarized.

KEYWORDS: composites; interphase; sizing/coating; hierarchical fibers; nanofillers.

Table of Contents:

List of symbols

AE	acoustic emission
AF	aramid fiber
AFM	atomic force microscopy
APTES	3-(aminopropyl)triethoxysilane
ARG	alkali resistant glass fiber
BET	Brunauer–Emmett–Teller
BMI	bismaleimide
CAB	cellulose acetate butyrate
CF	carbon fiber
CNF	carbon nanofiber
CNT	carbon nanotube
CVD	chemical vapor deposition
DA	Diels-Alder reaction
DGEBA	diglycidyl ether of bisphenol-A
DMA	dynamic mechanical analysis
DMF	dimethyl formamide
DWCNT	double-walled carbon nanotube
EFM	electric force microscopy
EP	epoxy
EPA	ethylphenyl acetate
EPD	electrophoretic deposition
EVA	ethylene vinylacetate
FBG	Bragg grated optical fibers
F-CNT	flame synthesized carbon nanotube
FE-SEM	field emission scanning electron microscopy
FGE	furfuryl glycidyl ether
FTIR	Fourier transform infrared spectroscopy
GF	glass fiber
G_{Ic}	interlaminar fracture toughness (mode I)
GO	graphene oxide
GNP	graphite nanoplatelets
GSD	graphitic structures by design
H-bonding	hydrogen bonding
IFSS	interfacial shear strength
IGC	inverse gas chromatography
ILSS	interlaminar shear strength
IPN	interpenetrating network
LCP	liquid crystalline polyesters
MA	maleic anhydride
MW	molecular weight
MWCNT	multi-walled carbon nanotube
NF	natural fiber
OM	optical microscopy
PA	polyamide
PACM	4,4,'-methylene biscyclohexanamine
PAEK	polyaryletherketone

PAN	polyacrylonitrile
PANI	polyaniline
PBO	polybenzoxazole
PEI	polyetherimide
PGE	phenyl glycidyl ether
phr	part per hundred (part) resin
PLLA	poly-L-lactide
PMMA	polymethyl-methacrylate
PP	polypropylene
PP-b-PS	polybutadiene-block-polystyrene
PP-g-MA	polypropylene grafted by maleic anhydride
PS	polystyrene
RISP	reaction induced phase separation
SAM	self assembled monolayer
SEM	scanning electron microscopy
Semi IPN	Semi interpenetrating network
SPM	scanning probe microscopy
SWCNT	single-walled carbon nanotube
TEM	transmission electron microscopy
T_g	glass transition temperature
TGA	thermogravimetric analysis
T_m	melting temperature
TMA	thermo-mechanical analysis
ToF-SIMS	time of flight secondary ion mass spectrometry
TPU	thermoplastic polyurethane
UD	unidirectional
UF	urea formaldehyde resin
UHMWPE	ultra high molecular weight polyethylene
UP	unsaturated polyester
UV	ultraviolet
VAP	vacuum assisted process
VARTM	vacuum assisted resin transfer molding
VE	vinyl ester resin
XPS	x-ray photoelectron spectroscopy

1. Introduction

Fiber-reinforced polymer composites are still an emerging class of engineering materials. They include a wide range of types generally grouped according to the appearance of the reinforcing fibers (discontinuous, continuous-aligned, (dis)continuous-textile, fiber assembly and architecture) and matrix characteristics (thermoplastics or thermosets), respectively. Composites are defined as materials consisting of two or more distinct phases with a recognizable interphase. Accordingly, composites consist of at least three phases. Fibers are inherently stronger than the bulk materials because the probability of imperfections (“flaws”) decreases with decreasing dimension. The stiffness and strength of the most important reinforcing fibers such as glass (GF), carbon (CF), aramid (AF), natural fibers (NF) are markedly higher than those of polymeric matrices. The reinforcing fibers will be grouped into inorganic and organic ones in this review. High-strength inorganic fibers include glass, carbon and ceramic fibers. Nevertheless, due to their practical importance in fiber-reinforced

polymer composites, the attention will be here focused on glass and carbon fibers. The matrix transfers the loads to the fibers and distributes the stresses among them. The matrix is also responsible for protecting the fibrous reinforcement from the environment and allows the necessary positioning of the fibers. The fiber/matrix interphase guarantees the stress transfer from the “weak” matrix to the “strong” fiber and from fiber to fiber through the matrix, as well. The term interphase, meaning a finite interlayer with distinct physico-chemical properties between the fiber and matrix, has been introduced in the 1970s [1]. The interphase controls the interactions between fiber and matrix and thus also the mechanical property profile of structural composites. The mechanical properties, such as tensile strength and modulus, are mainly controlled by the tensile properties of fiber, its volume fraction, orientation (relative to loading) and length. There are some general design concepts for interphase engineering. For example, a strong bonding between fiber and matrix is recommended to achieve high stiffness and strength, while a relatively weak interfacial bonding generally improve the energy absorbing performances under impact conditions. Nonetheless, the above conflicting trends make clear that the stress transfer and energy absorbing mechanisms are completely different in polymer composites.

The load transfer capability of the interphase depends on the fiber/matrix adhesion which can be physico-chemical or frictional (or both) in nature [2]. Physico-chemical contribution, including chemical reactions, intermolecular interactions, surface-induced crystallizations, phase separation phenomena etc. seem to be the more important in polymer composites than the frictional one. Some concepts, however, trigger the latter by “roughening” the fiber surface and tailor the differential thermal contraction of the fiber and matrix by suitable curing/cooling cycles. In many cases both chemical and frictional components are at work though not explicitly mentioned or addressed.

Since the interphase is the key factor of composite performance its engineering design ("build-up") is being under spot of interest from both academia and industry. Properties of the interphase should be tailored on the basis of various parameters such as the locally prevailing stress field, possible environmental attack, service temperature, etc. Moreover, considering the fact that the dominating failure mode in fiber-reinforced polymer is debonding under transverse (to fibers) component of loading, its early detection and even its healing are highly desired.

Different attributes have been coined to cover the latest developments in interphase modifications, such as adaptive (one-way reaction to environmental change) and smart (two-way “communication” upon environmental change) [3]. Our feeling is, however, that “interphase engineering” is a better suited term to cover the developments in this field. The aim of this review is to survey the most relevant achievements and trends from year 2000.

2. Interphase tailoring via sizing/coating

All reinforcing fibers used for the preparation of polymer composites are surface treated and/or coated, usually during their manufacturing steps. This kind of coating is usually referred to as sizing. Next we make a distinction between sizing and coating where the composition of the latter deviates from that of normal sizing, for example due to the incorporation of nanofillers.

2.1. Recent progresses

2.1.1. Inorganic fibers

GFs are usually sized immediately after their spinning to protect them from fracturing. The aqueous formulation of GF sizing contains an adhesion promoter (usually an organosilane compound as coupling agent), a film former along with a suitable emulsifier and a lubricant. The two latter components have protective functions during production and handling. In fact, Weibull analysis of single fiber tensile test data demonstrated that silane coupling agent and/or polymeric film-former may effectively reduce the population of inherent flaws on GFs [4].

The effect of the film former on the fiber/matrix adhesion cannot be neglected. This becomes obvious by considering the complexity of the polysiloxane network formed by hydrolysis and subsequent polycondensation of the organosilanes (see Fig. 1) in presence of additives, generally present in the sizing . Note that in the polycondensation process the surface hydroxyl groups of GF may react with the hydrolyzed organosilane. Because the film former is a linear polymer whereas the surface bonded polysiloxane is cross-linked, the final structure can be treated as a semi interpenetrating network (semi IPN) [5]. The film former should be able to diffuse into the matrix, and vice versa, the matrix is expected to diffuse into the semi IPN. As a consequence, the film former should be highly compatible with that of the matrix. This note holds for both thermoplastic and in situ cured thermosetting systems.

The effect of the build-up of a semi IPN sizing structure was studied by Tanoglu et al. [6] on a GF/amine cured epoxy (EP) system. The cross-links density of polysiloxane strongly affected the penetration of the EP constituents into the semi IPN that initially contained the film former. After curing, the initially semi IPN interphase may have turn into a full IPN one when the film former migrates completely in the bulk EP. This description highlights that the interphase development may also affect the diffusion and reactions kinetics which should be taken into account. A schematic sketch on the optimum interphase formation is given in Figure 1.

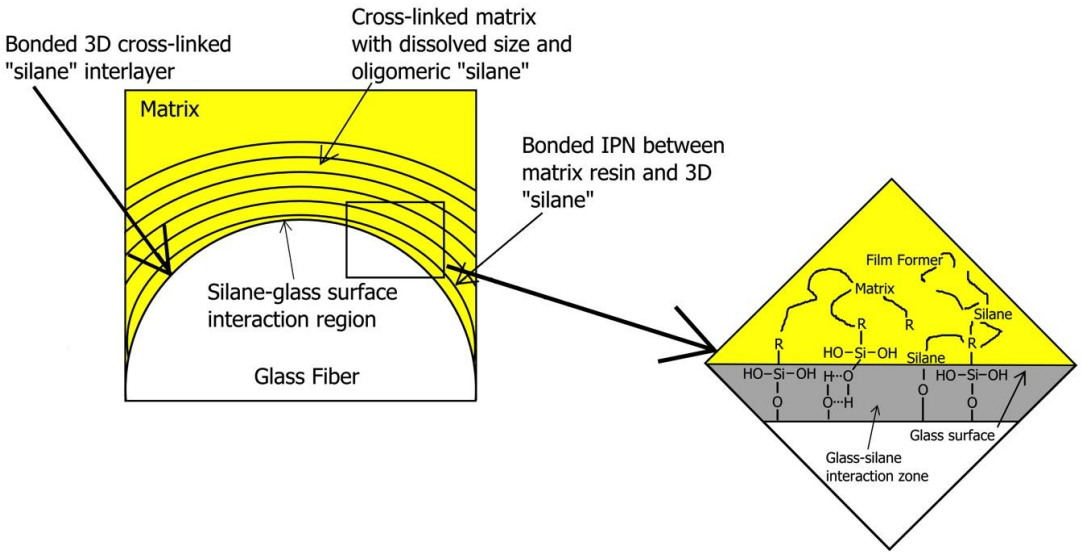

Figure 1. Scheme of the semi IPN structured interphase on GF. Note: the scheme highlights the effects of silane coupling agent and film former (based on Ref. [5]).

Dey et al. [7] studied the influence of film formers on GF/EP microcomposites through the microbond test. The authors concluded that matrix compatible (reactive) film former may be more efficient than epoxy functionalized silane in the sizing in improving fiber/matrix adhesion. Interestingly, a polyurethane film former yielding enhanced surface roughness proved to be as promising as a reactive one. This is a clear hint for the frictional contribution of adhesion bonding. Note that the microbond (microdroplet pull-off, microdroplet shear, microdebond) test is one of the preferred direct testing methods (on microcomposites) which are summarized in Figure 2. Figure 2 also displays some indirect test methods widely usedon macrocomposites to determine interphase effects. A detailed description of these testing methods is out of the scope of this review and the interested reader is addressed to the following reference [8, 9]

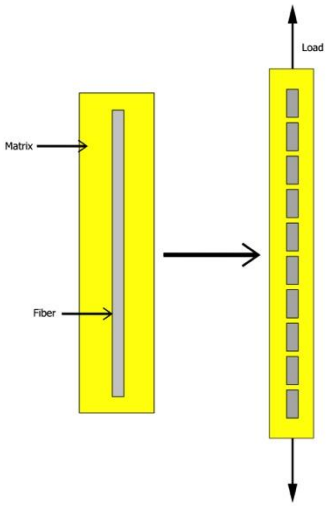

a)

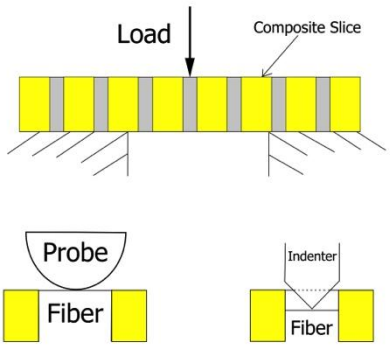

b)

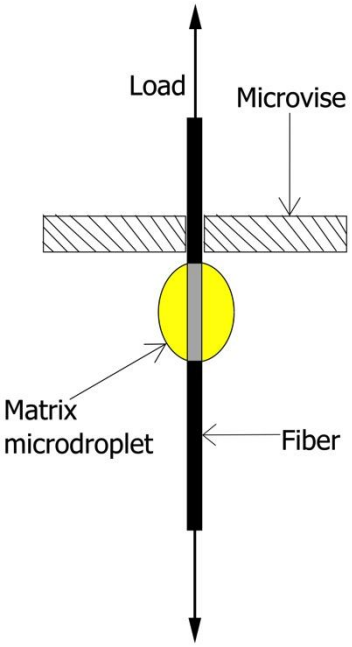

c)

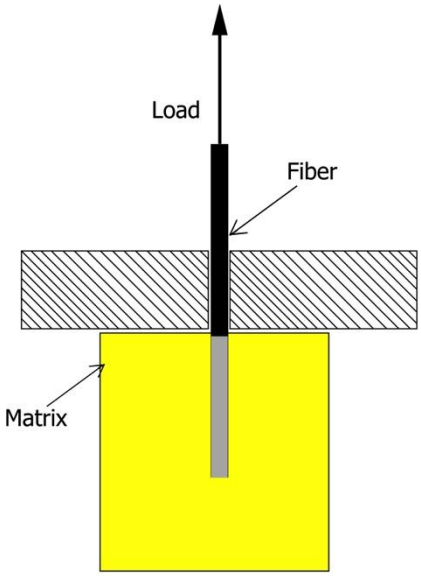

d)

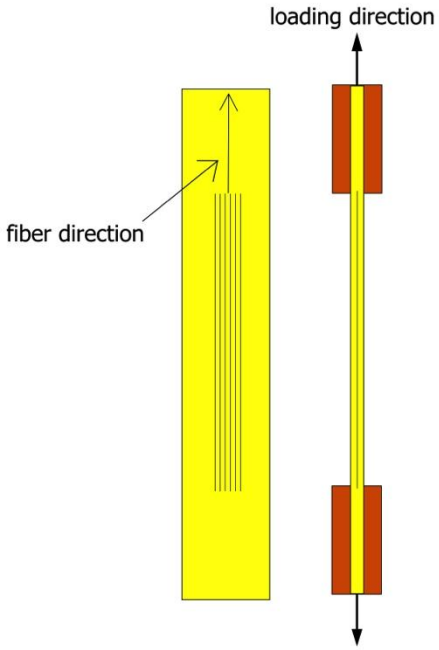
loading direction
fiber direction

e)

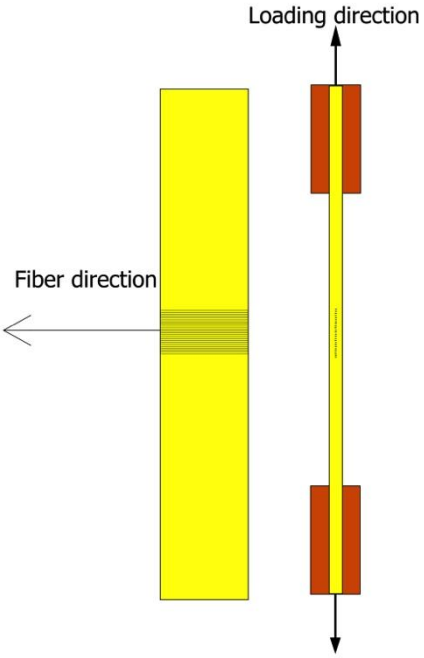
Loading direction
Fiber direction

f)

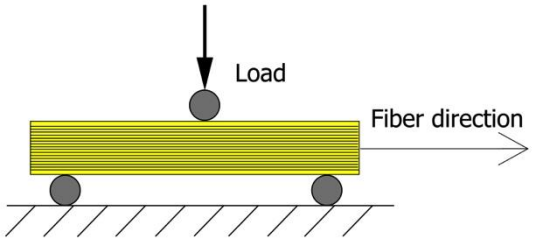
Load
Fiber direction

g)

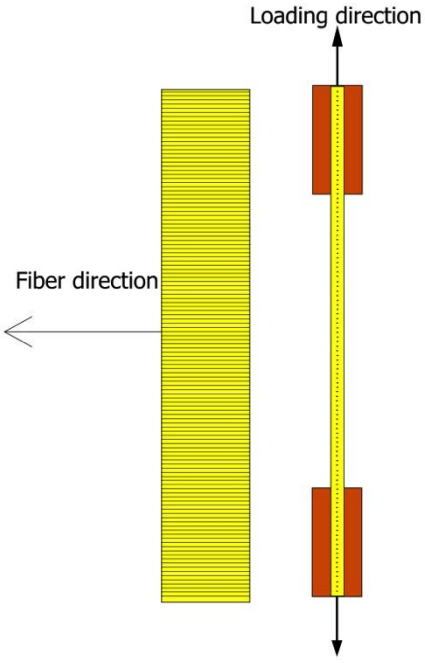
Loading direction
Fiber direction

h)

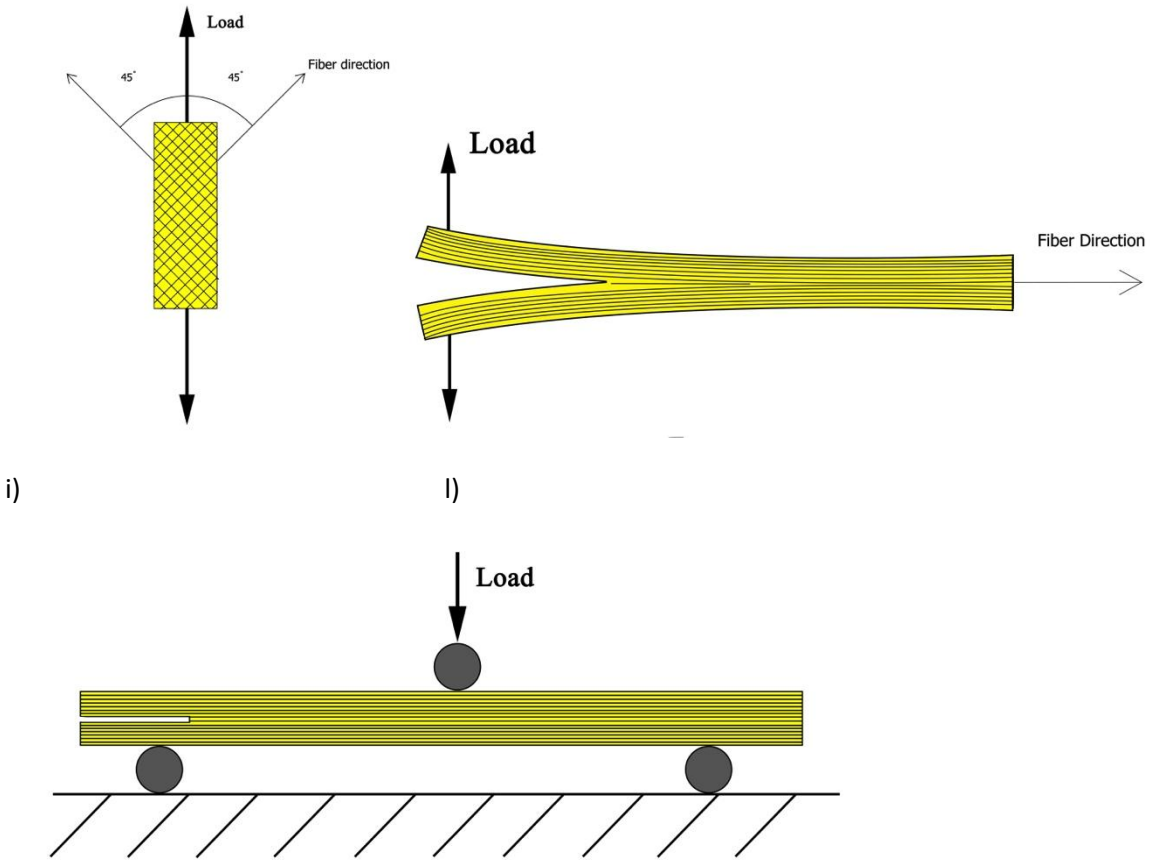

Figure 2. Direct single fiber (or fiber bundle) tests on microcomposites (model composites) to determine the interfacial shear (or tensile) strength values of the interphase, schematically: a) single-fiber fragmentation test b) single-fiber push-out test, c) microbond test, d) pull-out test, e) bundle fragmentation test f) bundle transverse tensile test. Indirect tests on macrocomposites (real composites) for the determination of the interlaminar shear (or tensile) strength, schematically: g) short beam shear test, h) transverse tensile test i) in-plane shear test (±45°), l) interlaminar delamination under mode I, m) interlaminar delamination under mode II.

Zinck and Gérard [10] recommended that hygrothermal resistant interphase in GF/anhydride cured EP should not have organosilane coupling agent reactive towards the anhydride. This was reasoned by surmising that an offset in stoichiometry favors the hygrothermal degradation of EP.

Sizing is commonly applied also for CFs. Note that CF is treated among the inorganic fibers throughout in this review though it is usually produced from an organic precursor, such as polyacrylonitrile (PAN). This grouping is reasoned by the fact that the distinction between organic and inorganic carbon compounds is somewhat arbitrary, and by this way, results on GF and CF can be introduced simultaneously. During their production, CFs may be subjected to various surface treatments in order to remove the weak outer layer and introduce oxygen containing functional groups [11]. The presence of functional groups governs the surface energetics (polar components) and improves the wettability [12]. For CF sizing the knowledge gained with thermoplastic modified EPs was adapted recently. Various thermoplastic polymers, including polyaryletherketones (PAEK), can be used as disperse phase toughening for EP [13]. When such polymers are used in the sizing then the interfacial fracture toughness may also be improved. Tensile tests on single fiber indicated

that PAEK coating eliminated the surface defects and improved the interfacial toughness. This has been proved by analyzing the force-displacement curves monitored in microbond tests [14].

2.1.2. Organic fibers

Organic fibers include aramid fiber (AF), ultra high molecular weight polyethylene (UHMWPE), polybenzoxazole-types (PBO), liquid crystalline polyesters (LCP) and various natural fibers (NF), as well. Except NF, they are also usually sized. Sizing is generally preceded by a suitable surface treatment, such as plasma, ion beam, laser [15]. In contrast to man-made reinforcing fibers, vivid research and development activity can be recently noticed for NFs. This is fueled by the "think green, go green" public philosophy and the polymer composite field is no exception in this respect.

NFs of different origin (bast, leaf, fruit, and seed) substantially differ from the man-made inorganic or organic counterparts. NFs are composed of bundles of elementary fibers (thus always discontinuous), contain voids and defects, their cross-section is irregular, and their quality is inconsistent (depending on cultivation, soil type, and climate). From the view point of chemical structure, NFs have varying surface energy and surface functional group populations even along a single technical fiber. Major constituents of plant (vegetable) fibers, preferentially used in polymer composites, are cellulose, hemicellulose and lignin in various amounts. The mechanical properties of plant fibers are controlled by the cellulose content. The non-cellulosic components bind and protect the cellulose fibers. The presence of these non-cellulosic constituents is generally undesired in order to get adequate fiber/matrix bonding. A further problem source is the hydrophilic (polar) nature of plant fibers, especially when embedded in hydrophobic (apolar) polymer matrices. To improve the fiber/matrix adhesion in NF-reinforced composites a large number of surface treatments have been explored. They have been classified as to physical and chemical treatments in a recent review by Fuqua et al. [16]. Among the physical treatments those linked with electric discharge (corona, plasma treatments) are the most explored [17]. Their effects range from surface "cleaning" and etching, changes in the chemical structure (functional groups, radicals and even crosslinking) to modification of the surface energy (a key factor for wettability).

A vast range of chemical treatments (alkaline, bleaching, coupling with silanes, acylation, grafting by monomers etc.) were tried to improve the interfacial adhesion [16]. Nevertheless, the alkaline treatment (mercerization) is the most widely applied.

The reason why the above short description appears under the heading "sizing/coating" is the surface coupling with silanes. This is similar to that of the silane adhesion promoter in GF sizing. Surface coatings of NFs are still at the very beginning. According to the authors' opinion, creation of a thick coating on NFs may be a promising route. A thick coating may efficiently "mask" fiber surface heterogeneities and via its build-up the wetting may be improved as well. Some works were done along this direction using water glass [18, 19]. Water glass is polysilic acid, widely used in the building industry, which undergoes a hydro/xerogel transition in air according to the following chemical equation [20, 21]:

Equation. 1

$$mNa_2O.nSiO_{2_{Na-WG}}.xH_2O + mCO_2 \rightarrow nSiO_2.(x-y)H_2O_{silica\ gel(Hydro-or\ xerogel)} + mNa_2CO_3 + yH_2O$$

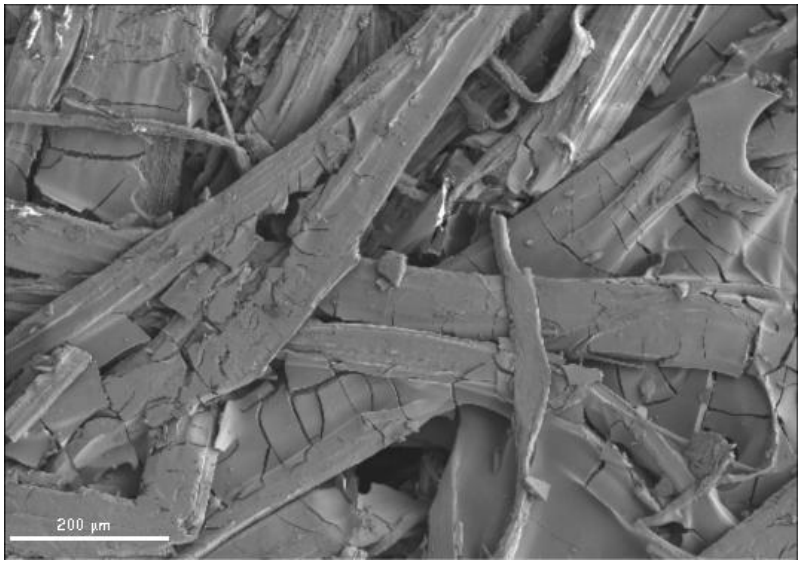

Figure 3. Flax mat with thick water glass-based polysilicate coating. Note: fissures are due to the hydro-xerogel transition.

The result is a polysilicate and thus a coating somewhat similar in composition to GF. Water glass treatment of NFs and related fabrics may occur by dip or spray coatings. Because water glass is highly alkaline, it may also work for the NF mercerization in-situ. Unfortunately, the polysilicate formed is very brittle (Figure 3) thus hampering the handling of the coated reinforcement. This drawback can be, however, circumvented by selecting suitable hybrid resins [20]. The feasibility of this approach has not been proved yet. Nonetheless, thick coating of NFs is the economic way when instead of matrix modification (e.g., polymer coupling agents reactive with the hydroxyl groups of NF) fiber treatment is the goal. This can hardly be avoided when, for example, the flame retardancy of NF-reinforced composites should be improved.

2.2. Effects of nanofillers in surface coatings

Incorporation of nanofillers into sizing formulations was pushed forward broadly by three main reasons. First, to enhance the surface roughness of the fiber, secondly, to increase the local modulus of the interphase and hence shear strength (thus decreasing the stress transfer length at a broken fibre), and finally, to exploit the possible structuring of nanofillers for sensing applications. Surface roughening is beneficial not only for improving the frictional component of adhesion, but also for toughening. The crack developed at the interface or in the interphase is forced to follow a zig-zag route owing to the nanofiller particles acting as obstacles. The higher the aspect ratio of the filler, the higher the crack deviation efficiency is. It is obvious that higher energy dissipation is involved in a zig-zag crack path (involving debonding, pull-out, fracture and various matrix-related failure events) rather than in a planar one. The sensing aspect with carbon nanotubes (CNT) was proposed by

Fiedler et al. [22]. It was early recognized that the in-situ sensing of stress, strain and damage would be a powerful tool for structural health monitoring. It has been already emphasized that, because stress transfer occurs through shear at the interface, the thermomechanical properties of the interphase determine the stress range which the composite can withstand before fracture [5]. This fact directed researchers to concentrate on sensing options in the interphase. At this regard, one of the straightforward strategies is to make use of the well-established sizing/coating techniques.

The type of nanofillers investigated so far for mechanical and sensing purposes, are exclusively high aspect ratio versions with platy (disk) or fibrous (needle) shapes. As platy reinforcements clay (layered silicate) and graphene derivatives, while as fibrous ones, CNT variants (single, double and multiwalled – SW, DW and MWCNT, respectively) were preferred in the sizing formulations. They were deposited on the fiber surfaces by dip coating, spraying and electrophoretic techniques. These processes are schematically depicted in Figure 4.

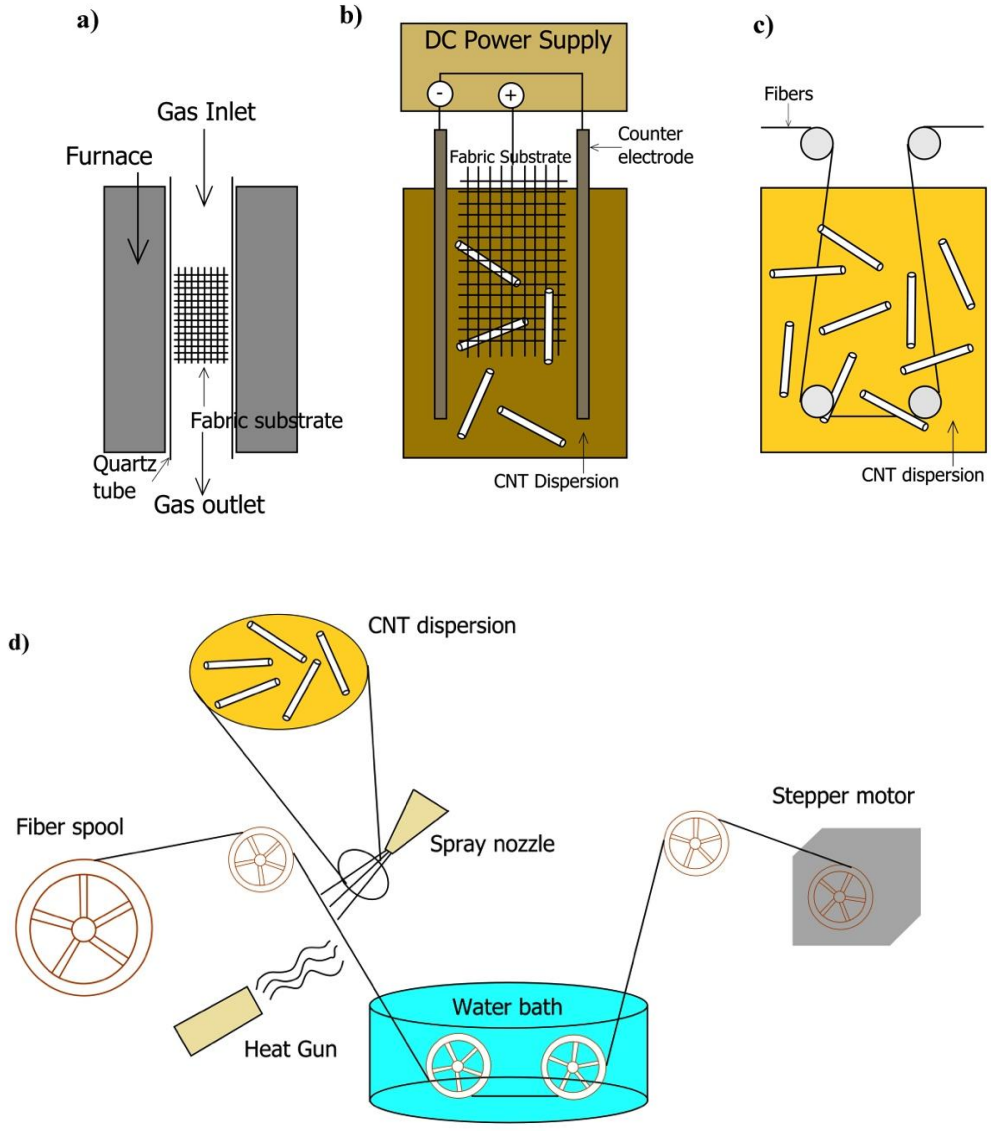

Figure 4. Schematics of typical surface coating techniques of fibers and related fabrics (based on Ref. [23]): a) CVD process, b) electrophoresis process c) sizing process, and d) spray coating process.

For the surface “coating” of NFs bacterial cellulose deposition was attempted, as well, as described later. It is noteworthy that the nanofillers are “physically absorbed” in the interlayer.

When sensing features are added to the interphase region, it is properly defined as functional interphase. Aspects of the latter are separately treated in section 6 of this review. Next, the main achievements with nanofiller coatings, grouped for inorganic and organic fibers, will be given in tabulated forms.

2.2.1. Inorganic Fibers

The most relevant literature information on the effects incorporation of nanofillers into sizing formulations on inorganic fibers are summarized In the following table.

Fiber type	Nanofiller type, amount in sizing medium	Sizing/Coating formulation	Matrix Composites	Sizing/Coating technique	Interphase		Sensing	Comments	Ref.
					Testing methods	Effects			
GF (E-glass)	SWCNT 0.5 wt% (solution)	Low MW EVA, PMMA, Poly(styrene-methyl-methacrylate)	PP Microcomposites	Solution coating	Single fiber fragmentation test	Variation in critical fiber length (l_c)	Strain sensor effect calibrated by Raman spectroscopy	Strain sensing proved. Adhesion improvement also due to SWCNT	[24]
GF (alkali resistant, ARG)	MWCNT with –COOH functionality 0.5 wt% (dispersion)	Aqueous dispersions with surfactants, sonicated MWCNT/surfactant = 2/3	EP (amine) Microcomposites	Dip coating	FE-ESEM, EFM, nanoindentation	Interphase region, 20-500 nm	Semiconductive interphase resulting from MWCNT network; piezoresistivity checked for sensing. The electrical conductivity depended also on temperature and humidity	First report on non GF-based composite. Conductive network capable to detect the T_g in the interphase.	[25]
GF (E-glass)	MWCNT 0.5 wt% (dispersion)	Aqueous EP-compatible phenoxy sizing with MWCNT applied for the as-received GF sizing	EP (amine) UD composites from prepregs	Dip coating	SEM TMA	T_g increase	-	Crack initiation energy (G_{Ic}) slightly increased, while propagation energy decreased in mode I interlaminar fracture test. Effect of CNT in the bulk matrix higher than in the sizing	[26]
GF (ARG)	MWCNT with –	Aqueous dispersion	EP (Amine)	Dip coating,	Single fiber	l_c was	Electrical	EPD coating is more	[27]

	COOH functionality, 0.5 wt% (dispersion)	with non-ionic surfactant and epoxy functional silane (coupling agent), sonicated	Microcomposites	electrophoretic deposition (EPD). Sizing amount: 1-2 wt%	tensile test, single fiber fragmentation test	smaller (IFSS higher) for EPD than for dip coated fibers	resistance of single fiber composite measured under tensile loading	beneficial than dip coating and yields a more homogenous interphase. Changes in the electrical resistivity of the interphase assigned to elastic and plastic deformations of the interphase	
GF (ECR)	F-CNT, SWCNT 0.021 wt%	Ethanol dispersion (0.5 mg/mL) sonicated	Vinyl ester (VE) UD composites	Spraying	SEM, TEM	Impact resistance (transverse to fiber direction) improved by 15%.	-	F-CNT out performed SWCNT having more defects and functional groups at the side-wall than SWCNT. This resulted in better dispersion and better interphase reinforcement	[28]
GF (ARG)	MWCNT with –COOH functionality, 0.05 wt% (dispersion)	Aqueous dispersion with non-ionic surfactant	EP (amine) Single and triple fiber microcomposites	EPD	-	-	Change in electrical resistance under tensile load measured, also as a function of temperature	Interphase probed as strain sensor and switch	[29]
GF fabric (E-glass)	MWCNT, also ozone treated and subsequently functionalized by polyethyleneimine, 1g/L (dispersion)	Dispersion, also containing epoxysilane	EP (amine) fabric Reinforced composite through VARTM	EPD	In-plane shear tests	In-plane shear strength doubled with MWCNT at 14 vol%	Change in the electrical resistivity as a function of MWCNT content and shear loading measured	EPD adapted for GF fabrics. Polyethyleneimine, linking the epoxy sized GF and the brittle EP matrix proved to be the right additive	[30]
GF (fabric)	SWCNT, MWCNT with –COOH functionality	Aqueous dispersion	EP (amine) Fabric-reinforced composites by VARTM	EPD	SEM, ILSS	ILSS improved by 27% due to 0.25%	In-plane and out-of-plane electrical conductivity measured	Electrophoresis is efficient to produce “multiscale hybrid composites” with enhanced ILSS and	[31]

						MWCNT in the composite		out-of-plane (transverse) mechanical and electrical properties	
CF (unsized then oxidized in air)	MWCNT with –COOH functionality	Solvent dispersion, 100mg/L (dispersion)	-	Chemichal grafting Dispersion deposition in several steps	SEM, TEM, FTIR	-	-	Chemical reactions (ester, anhydride and amide formation) supposed between the functional groups of MWCNT and oxidized CF, but not proved	[32]
CF	Clay	Aqueous ammonia solution	PEI Hand lay-up of prepregs and hot pressing	Immersion	Single fiber pull-out, SEM, XPS	ILSS and flexural strength increased	-	Improvements in ILSS and flexural strength attributed to surface roughening of CF (mechanical interlocking)	[33]
CF (woven fabric)	Carbon nanofiber (CNF) also with –COOH and $–NH_2$ functionalities	Aqueous dispersion	EP (amine) Composites by VARTM	EPD	Optical Microscopy (OM), SEM	ILSS enhanced	-	"Multiscale-reinforced" fabrics were used to produce "hierarchical composites". Panels with amine functionalized CNF showed the highest property improvements (ILSS=12%, compressive strength = 13%) compared to the composites without CNF.	[34]
CF (woven fabric)	CNF with $–NH_2$ functionality	Aqueous dispersion after sonication	-	EPD, two step EPD with potential change	OM, SEM	-	-	CNFs wrapped around the CF. Covalent bonding toward EP surmized through the $–NH_2$ of CNF. Enhancement	[35]

								in ILSS, compressive stress and delamination resistance predicted	
CF (unsized, sized)	CNF, with –COOH functionality	Aqueous dispersion	EP (amine) Microcomposite	EPD	FE-SEM, fragmentation	Changes in IFSS detected. Single fiber tensile tests performed and analyzed by the Weibull approach	-	Best IFSS achieved with sized CF coated with carboxyl functionalized CNF. Unsizing of CF reduced IFSS which was enhanced by CNF coating	[36]
CF (woven fabric)	MWCNT, also with carboxyl and acryl functionalities	Dispersion in matrix resin <1phr nanofiller (phr – part per hundred parts resin)	VE (bisphenol A-based) Hand lay-up and hot pressing	Dipping	TEM, XPS, SEM	Flexural strength, modulus and T_g increased	-	Improvements in the mechanical properties according to ranking MWCNT<carboxyl modified MWCNT<acryl grafted MWCNT. The acryl functional groups of the latter participated in the radical crosslinking. Properties improvements also with increasing MWCNT content.	[37]
CF (unsized)	MWCNT with carboxyl functionality	Aqueous dispersion with surfactant	EP (amine) UD laminates by VARTM	EPD continuous line	SEM, ILSS, single fiber push out	ILSS improved by 40%	-	EPD conditions on the MWCNT deposition studied. Improvement in ILSS did not correlate with MWCNT amount deposited (<1 wt%). According to single fiber push out (monotonic, cylic)	[38]

								the fiber/matrix bonding was not affected	
CF (low and high modulus)	SWCNT with carboxyl functionality	Ethanol dispersion (0.1 wt% dispersion) + silane solution	EP (amine)	Immersion	Single fiber composite, SEM, Raman spectroscopy	IFSS is markedly improved (>50%)	-	IFSS determined by calibration of the Raman shift of the 2D band in the model composite. IFSS improvement due to enhanced interfacial surface (SWCNT effect) and chemical bonding of the latter via –COOH to the epoxy groups of EP	[39]
CF (unsized)	MWCNT also with amine functionality	PAEK containing sizing MWCNT content: 1wt%	PAEK Microcomposites	Impregnation of CF tow	SEM, BET surface, wetting microbond test	IFSS enhanced by 60%	-	BET surface area of the MWCNT containing sizing was six times higher than without MWCNT. Presence of MWCNT improved both wetting of CF and IFSS	[40]
CF (unsized)	Graphene oxide (GO) also silanized	Aqueous dispersion, sonicated (3mg/ml, dispersion)	EP (anhydride) UD composite via RTM Microcomposites	Dipping (carbon nanoparticle content <1 wt%)	OM, AFM, XPS, SEM, FTIR microbond test	IFSS enhanced by <60%	-	A gradient interphase concluded. Its stiffness was lower than CF but higher than EP. The hierarchical composite with 0.5 wt% silanized GO showed the highest improvement (IFSS = 60%, ILSS = 19%, flexural strength, modulus and tensile strength by ca. 15% each)	[41]

GF (E-glass)	Capsules containing reactive EP and solvent	Aqueous dispersion of UF-walled capsules	EP (amine) Microcomposites	Dip coating	Repeated microbond tests after full debonding	Healing efficiency of the IFSS	-	Almost complete autonomic healing found. The mean capsule size was at about 2 and 0.6 µm, respectively, in the series	[42]
CF	Capsules containing reactive EP and solvent	Aqueous dispersion UF-walled capsules combined with binder in different ways	EP (amine) Microcomposites	Dip coating	Repeated microbond tests after full debonding	Healing efficiency of the IFSS	-	Autonomic healing demonstrated. The resin/solvent combination yielded up to 80% recovery of the IFSS as a function capsule coverage and binder method	[43]

Table 1: Interphases produced by nanofiller containing sizing/coating on inorganic fibers, their characteristics and effects

Sharma et al. [44] recently provided a comprehensive review on the research work carried out over the past couple of years in the area of CF surface modifications and CF/polymer interfacial adhesion. This paper provides a systematic and up-to-date account of various 'wet', 'dry' and 'multi-scale' fiber surface modification techniques, i.e., sizing, plasma, chemical treatments and carbon nano-tubes/nanoparticles coating, for increasing the wettability and interfacial adhesion with polymeric matrices. In particular, this review highlights strategies for retaining the mechanical strength of CF after surface modification.

2.2.2. Organic Fibers

The following table summarizes most of the literature information available on the subject of incorporation of nanofillers into sizing formulations for inorganic fibers are summarized In the following table.

Fiber type	**Nanofiller type, amount in sizing medium**	**Sizing/Coating formulation**	**Matrix Composites**	**Sizing/Coating technique**	**Interphase**		**Sensing**	**Comments**	**Ref.**
					Testing methods	**Effects**			
NF (jute) Single fiber fabric	MWCNT with carboxyl functionality	Aqueous dispersion with non-ionic surfactant	EP (amine) Microcomposites, Fabric-reinforced composite via VAP	Dip coating	FE-SEM, EFM, DMA	-	Sensing behavior of the MWCNT coated jute fibers for temperature, humidity and stress/strain response checked	Interconnected MWCNT network in the interphase proved for multifunctional sensing. Single MWCNT coated jute fiber exhibited high humidity sensitivity. Controllable anisotropic dielectric properties noticed for MWCNT coated fabric reinforced composite	[45]
TPU (yarn)	MWCNT with amine functionality	MWCNT dispersion in solvent, sonicated and “thickened” by TPU solution	-	Roll coating	SEM	-	Relative electrical resistance as a function of strain, applied also cyclically, measured	The elastic TPU yarn showed good strain sensing ability at an equivalent MWCNT concentration of as low as 0.015 wt%.	[46]

NF (hemp, sisal)	Nanocellulose, cellulose nanofibrils	Cellulose producing bacteria	PLLA, CAB	Bacterial deposition via static culture, fermentation	OM, SEM, XPS, single fiber pull-out test	IFSS improvement depended on NF type	-	"Green" method to modify the surface of NFs presented. Adhesion of nanocellulose (5-6%) to NF is via H-bonding. NF type and fermentation process conditions should be properly selected. Change in the surface energy of the modified NF with "hierarchical structure" may serve for improved wetting.	[47, 48]

Table 2: Interphases produced by nanofiller containing sizing/coating on organic fibers, their characteristics and effects

Surveying the recent progresses according to Tables 1 and 2, one can recognize a clear change from concepts aiming at enhancing the surface of the fibers toward the creation of a smart interphase. Several different terminologies were introduced for defining the scenario when nanofillers are used for interphase modification in composite material reinforced with traditional microfibers. In fact, almost independently from the specific method adopted, the terms “multiscale”, “hierarchical”, and “hybrid” are used. The latter is improper as already reserved to indicate composites containing two or more different reinforcements. Composites with multiscale reinforcements are typically those which contain nano- and microscale reinforcements (which may be of different types and thus also hybrids) simultaneously [49].

The term hierarchical may be misleading since generally reserved to indicate the structural hierarchy of composite structures [50] which comprises several levels: macro (part), meso (plies, tows, yarns), and micro (fibers). Nonetheless, we shall keep the terms hierarchically structured fiber or interphase due to the wide acceptance they received by the community. Moreover, the hierarchical build-up can be defined as a combination of microscale fibers and nanoscale additives which are in "intimate" contact with each others. Apart from the sizing/coating approach summarized in this section, this contact can be achieved also in other ways, such as chemical vapor deposition (CVD) techniques and alike. The above definition implies that the load bearing capacity of the microscale fibers is not jeopardized by the nanoadditives, just the opposite occurs.

To sum up, tailoring of the interphase for sensing is absolutely straightforward because the onset of mechanical damage occurs in this region. Until now relatively less attention has been paid to the potential offered by graphene or other two-dimensional carbon materials. Their very high aspect ratio (allowing folding, wrapping), versatile chemical modification along with the high electrical and thermal conductivities may open a new horizon for the nano-engineering of (multi)functional interphase via sizing/coating procedures. The deposition of bacterial nanocellulose is an elegant way to produce hierarchical structured NFs. This approach would be more appealing when it could be combined with other “green” technologies replacing the standard chemical treatments generally required in NFs to separate the fibrils from the naturally occurring bundle.

3. Creation of hierarchical fibers

As shown before, sizing/coating with formulations containing nanofillers proved to be a very promising route for interphase engineering. The next logical step is to “anchor” the nanofillers on the fiber surface. This may be achieved by chemical reaction between functionalized carbonaceous nanofillers (CNT, CNF and graphene) and fibers bearing reactive groups. The alternative way is to let CNT or CNF grow directly on the fiber surface. For the latter purpose, chemical vapor deposition (CVD) processes have been adopted with success. Both the chemical coupling and CVD are often termed as “grafting”. There are, in fact, some similarities with grafting of polymers (covalently bonding monomers to the main chain without affecting its length) though the mechanisms are highly different, as demonstrated later.

3.1. Chemical grafting of nanofillers

The huge surface area of CNT, CNF and graphene can be exploited to enhance the specific surface area of the reinforcing fiber provided that a covalent bond can be assured. Basic learning from the

bulk modification of polymers with carbonaceous nanofillers was that the latter should be functionalized in order to be properly dispersed in the investigated matrices.

Though various functionalization methods have been tried, the most efficient have been proven to be the oxidative treatments via wet chemistry. These usually started with the Hummers method, or similar ones, and the resulting functional groups (-COOH, -OH) were converted into the desired ones by further reactions [51]. Compared to CNT, graphene sheets have less entanglement, larger specific area and lower production cost, and thus they are ideal candidates for the surface nano-engineering of fibers, especially GF.

GF generally has hydroxyl groups on the surface which can be converted easily into amine groups. The amine groups may react with the carboxyl ones of graphene oxide thus yielding an amide coupling between GF and graphene oxide. This chemical route, applicable for CNT as well, is summarized in Figure 5.

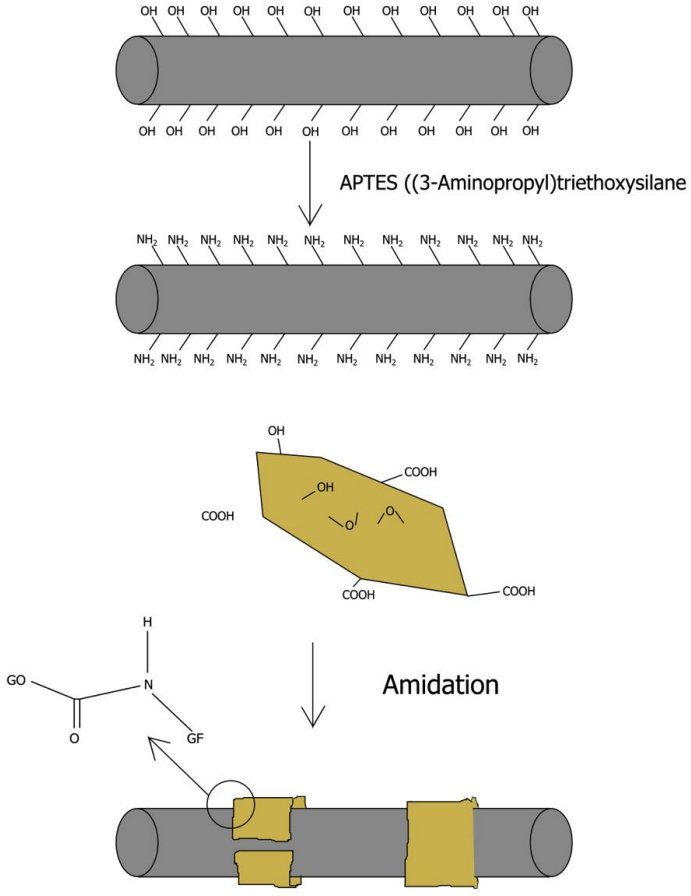

Figure 5. Grafting oxidized carbonaceous nanofillers onto GF surface (based on Ref. [52]).

By using the short-beam shear tests, Chen et al. [52] has shown that the ILSS of EP composite reinforced with graphene oxide (GO) grafted GF was by 20% higher those reinforced with GO coated GF, and almost by 50% higher than that containing unmodified GF.

Grafting of carbonaceous 1D (i.e. CNT, CNF) and 2D (i.e. graphene and other two-dimensional carbon materials [53]) nanofillers may be an acceptable way for GF, having inherent functionality (-OH) and relatively low thermal resistance. At the same time this is the major obstacle and the reason why CVD techniques can hardly be used for CNT/CNF growing onto GF.

3.2. CVD grafting (deposition) of nanofibers

Creation of "hairy" fibers by direct growing CNT or CNF onto the fiber surface has many benefits. The advantages include the enhancement of the fiber surface area, possibility of mechanical interlocking, capillary wetting by the matrix and local reinforcement of the interphase. All of the aforementioned aspects contribute to a better stress transfer from the matrix to the fibers. Major goal with composites containing hierarchical fibers is the improvement of the out-of-plane (transverse) properties without sacrificing the in-plane ones. It is obvious that radically grown CNT with suitable length and at a sufficiently high surface coverage (concentration) may work for transverse reinforcement. As a consequence, their effects appear in enhanced intraply (intralaminar) strength and interply (interlaminar) delamination resistance. Note that for improvement interlaminar delamination resistance, various strategies have been proposed at microscale level (e.g. z-pinning, stitching and needling in transverse direction, braiding), but all of them were associated with a depression of the in-plane mechanical performances.

CVD growing of nanotubes, nanofibers, and nanowires can be treated as a renewal of the whiskerization process from the mid-1970s [54]. Instead of generating silicon carbide or nitride single crystals at high temperatures (1300°-1800°C), CVD results in nanoscale fibrous structures at much lower temperatures (600-800°C). This temperature range is much too high for GF, and thus most results are achieved on carbon, silica, quartz and alumina fibers as shown next.

There are several different CVD variants. Nonetheless, the CVD is typically based on the following two steps: i) coating of the fiber or fiber assembly with a proper catalyst, and ii) growth of the nanofibers in a reactor using hydrocarbon sources. These two steps may be merged, as for example in injection CVD where deposition of a catalyst containing solution and pyrolysis of the hydrocarbon source take place simultaneously. The first report on CVD deposition of carbon nanofibers on CF is dated back to 1991 [55]. The deposited structure was herring bone/platelet like carbon. CNTs were first synthesized by Thostenson et. al [56] on CF by thermal CVD using predeposited metal catalysts on the CF surface. CNT-based hierarchical reinforcement in composites was already the specific subject of a review [57] in which the authors focused on the improvements of the composites performances. Depending on whether carbon nanofibers are produced on CF surface or on other fiber substrates we can speak about all-carbon hierarchical fibers or hybrid hierarchical fibers, respectively. The term "hybrid" is appropriate also when non-carbonaceous nanomaterials are deposited onto the CF surface.

3.2.1. Glass fibers

Although GF is not well suited for grafting with CNT, Wood et al. [58] reported about a successful case. In fact, MWCNT were grown on GF that was precoated with a Ni/Fe particle catalyst. GFs were plasma treated and drawn through a CVD chamber with carbon forming gas and nitrogen at T>600 °C. MWCNTs preferentially grown radially up to 7 µm and densely covered some portions of GF, while they were absent from other parts. Local twisting/kinking of the MWCNT appeared at 5-6 µm

distance for the fiber surface resulting in non-uniform morphology. Hybrid-fiber composites were prepared by suspending individual hybrid fibers in a DGEBA-based epoxy. Stiffness mapping through nanoindentation tests indicated 35% higher stiffness of the interphase compared to the bulk matrix. The growth of carbon nanomaterials on E-glass was also recently reported by Rahaman and Kar [59] who described an electroless plating method method for achieving a uniform coating of nickel catalyst on calcinated glass fiber. Carbon nanomaterials were grown over the GFs using thermal CVD technique. In particular, vertically aligned carbon nanofibers (CNFs) were obtained at 500 °C, while multiwalled carbon nanotubes (MWCNTs) were obtained over the GFs at 600 and 700 °C. Interestingly enough, the presence of carbon nanomaterials on the surface of GFs resulted to increase the electrical conductivity and dynamic mechanical storage modulus of epoxy/glass laminates.

3.2.2. Carbon fibers

Most of the works done so far addressed hierarchical CFs. Next the reader will be acquainted with relevant progress results in tabulated form.

Hierarchical fiber	**Deposition**		**Matrix**	**Interphase**		**Comments**	**Ref.**
CF/graft	**Technique**	**Conditions**	**Composites**	**Testing methods**	**Effects**		
CF/CNT	thermal CVD	Catalyst by magnetron sputtering followed by reduction to particles at T=660°C. CNT growth and 660°C for ½ h using C_2H_2	EP (amine) Microcomposites	SEM, BET, fragmentation	IFSS improvement	15% improvement in IFSS. Both catalyst deposition and CVD treatment of CF alone reduced the IFSS by 30%.	[56]
CF/MWCNT (aligned, random)	CVD	Aligned: pretreatment of CF in $MgSO_4$ in alcohol followed by exposure to Fe-phthalocyanine powder at 900°C for 15 min in Ar/H_2 Random: pretreatment of CF in $MgSO_4$ in alcohol followed by exposure to xylene and ferrocene catalysts at 800°C for 30 min in Ar/H_2	EP (amine) Microcomposites	SEM, single fiber tensile test, fragmentation	IFSS improvement	Nanotube deposition markedly reduced the tensile strength (30-37%), modulus of CF. Deterioration attributed to flaws due to thermal degradation/surface oxidation. MWCNT coated CF yielded higher IFSS than the unsized CF. Randomly grown MWCNT outperformed the aligned one.	[60]
CF/CNT, CNF	thermal CVD	Ni-based catalyst by dipping. Catalyst reduction at T=400°C. CNT production at 700°C using C_2H_2 for ½ hours	EP (amine) Tow impregnation	SEM, TEM, Raman	Improvement in tensile strength	Improvement in tensile strength due to CNT coating confirmed by fractography	[61]
CF/MWCNT (CF also sized)	thermal CVD	Carbon source/catalyst flow rate and CNT growth temperature (T=700-800°C) and time varied	-	SEM/TGA single fiber tensile tests	No significant reduction in tensile properties	Effects of CF sizing and CVD parameters studied	[62]
CF (PAN-based, pitch based)/CNT	thermal CVD	Catalyst: ferrocene; CNT growth: 700-750°C for 900s	-	SEM, TEM, X-ray, Raman thermal conductivity	Thermal conductivity increased	Thermal conductivity improvement assigned to a 3D CNT network	[63]
CF	thermal CVD	Fe-catalyst by immersion,	PMMA (from	SEM, BET contact	IFSS increased from	CNT grafting increased the BET surface area and	[64]

(oxidized)/CNT		carbon source: C_2H_2; CNT growth: 750°C, 1h	solution) Microcomposites	angle single fiber tensile, fragmentation	12.5 MPa (as received CF) to 13.1 MPa (oxidized) to 15.8 MPa (CNT-grafted)	decreased the CF tensile strength. This degradation attributed to the dissolution of iron particles into the CF surface.	
CF/MWCNT	Injection CVD	Feeding solution i.e. catalyst (ferrocene) and hydrocarbon (xylene,ethanol, ethylene diamine) injected to the furnace at T=850°C; CNT growth time: <2h. To produce aligned MWCNT, surface of CF coated with SiO_2 layer	EP (amine) Microcomposites	XPS, SEM, BET, contact angle, single fiber tensile test, fragmentation	IFSS improvement	CNTs with different orientation and length (up to 100μm) produced. Specific surface area enhanced by two orders of magnitude. IFSS dependence on MWCNT alignment and length, it was improved up to 175%. The tensile strength of the CF decreased with increasing growth time up to 33%.	[65]
CF/CNT	thermal CVD	Fe-Co bimetallic catalyst by wet impregnation. CNT growth at 750°C using Ar/C_2H_2 for ½ hr	EP (amine) Microcomposites	SEM, Raman, TGA, fragmentation supported by AE	IFSS improvement	IFSS enhanced from the 28 MPa (pristine) to 32 MPa (CNT grafted)	[66]
CF/CNT	aerosol-assisted CVD	Catalyst precursor: ferrocene; carbon source: C_2H_2; carrier gas: H_2/N_2. Aerosol from ferrocene/acetone mixture at T=700°C. CNT growth at 750°C for ½ hour	EP (anhydride) Microcomposites	SEM, BET, single fiber tensile and microbond test	IFSS doubled	CNT diameter at about 60 nm. CNT grafting caused a threefold increase in BET surface area. Moderate decrease (~10%) in CF tensile strength	[67]
CF substrates (tow, fabric, felt)/CN	injection CVD	Iron catalyst from ferrocene. Carbon source toluene. CNT growth at 750°C	Phenolic resin Compression molding	SEM, TEM, flexural tests	-	The flexural properties (strength, modulus) first decreased and above 5 wt% CNT content of the total composite weight increased monotonously.	[68]
CF fabric/CNT	thermal CVD	Ni catalyst: coating with Ni-nitrate solution followed by reduction to Ni powder (100nm) in the furnace. CNT growth at 700°C for 1h using CH_4.	EP Single fiber bundle impregnated	SEM, fiber bundle tensile test	-	Tensile strength and modulus increased. Analytical model proposed which considers the enlarged surface area	[69]
CF woven fabrics/CNT, CNF	thermal CVD	Catalysts: Ni, Fe-Co (immersion, into the catalyst precursor solutions followed by reduction (or	-	SEM, TEM, compression test	-	Compressibility of CNF/CNT-grafted woven fabrics of different structures studied. The fiber volume fraction of the compacted CNF/CNT-grafted textiles was markedly reduced compared to the ungrafted ones. This may affect	[50]

		without) CNT/CNF growth: 600 or 750°C for different times. Carbon source: C_2H_2				the production of advanced composites requiring high volume fraction reinforcements.	
CF fabric/CNT	thermal CVD	Catalyst: fabric coating in an acidic nickel sulphate containing bath. Reduction to Ni-P alloy at 500°C. CNT growth: 550°C using C_2H_2 carbon source	UP Microcomposites	SEM, DMA single fiber pull out	IFSS improvement	Effect of CNT growth time studied and an optimum value, based on IFSS and DMA data, concluded.	[70]
CF fabric/CNT	thermal CVD	CF Fabric was first coated by Al_2O_3. Catalyst precursor ($Fe(NO_3)_4$) in acetone. CNT growth at 750°C using C_2H_2 for ½ hour	EP (anhydride) Microcomposites	SEM, BET, contact angle, surface energy, single fiber tensile and microbond tests	IFSS doubled	Moderate decrease (10%) in the tensile strength of CF after CNT grafting. The alumina "buffer layer" had protective role and supported the normal alignment of CNTs. Wetting was markedly improved	[71]
CF fabric/MWCNT	Graphitic structures by design (GSD) + injection CVD (for comparison)	GSD: Fabric coated with SiO_2 and Ni films first. Breaking and reduction of the Ni film into nanometer sized Ni particles. CNT growth at 550°C using C_2H_4 as carbon source for 1h. CVD: Catalyst (ferrocene) dissolved in xylene formed the feed solution. CNT growth on the SiO_2 coated CF fabrics at 680°C for 1h.	EP Vacuum bagging	SEM, TEM, Raman, DMA, tensile test		Novel technique using reactive gas mixture proposed. The GSD-grown MWCNT is less crystalline than those grown by CVD. SiO_2 film protected the CF against catalyst diffusion. The thermal induced degradation effect was less for GSD than for CVD. Improvement in the performance with GSD-grown CNT demonstrated	[72]

Table 3: Carbon nanofiber grafting on CF: preparation and interphase effects. Notes: CF is unsized and PAN-based when not indicated in another way

The results in Table 3 clearly indicate that the creation of hierarchical CFs via CNT and CNF grafting through CVD is a very straightforward approach for interphase engineering. There are, however, several challenges with the catalytic CVD processes. The growth temperature of the nanofibers is quite high and thus should be reduced in order to minimize fiber damage. Some of the catalysts and carbon sources are toxic and thus should be replaced. The interaction of the CF with the catalysts (dissolution, eutectic formation) under the CNT growth conditions should be better understood and suitable circumventing strategies found. The GSD method (see Table 3. [72]) points into the right direction in this respect. Solving the above problems, the deterioration in the tensile properties of the parent CFs induced by the CVD treatment could be alleviated.

3.2.3. Other inorganic fibers

Because the growth of CNT and CNF in CVD processes takes place at high temperatures, fibers and fabrics of temperature resistant fibers, such as SiC, quartz, silica, alumina have been also considered for this kind of surface modification. Relevant results achieved with these fibers in the polymer composite field are listed in Table 4.

Hierarchical fiber type/graft	**Deposition**		**Matrix** **Composites**	**Interphase**		**Sensing**	**Comments**	**Ref.**
	Technique	**Conditions**		**Testing methods**	**Effects**			
SiC fabrics/CNT	Injection CVD	Catalyst + carbon source: ferrocene dissolved in xylene, CNT growth at 800°C for < 1h	EP (anhydrid) Fabrics infiltrated by resin, stacked and cured in autoclave	Interlaminar fracture toughness (G_{IC}), flexural test, damping, thermal conductivity	G_{IC} improved by 348%	-	G_{IC} improvement assigned to mechanical interlocking between SiC fibers and matrix due to the CNT "forest" grown. "Value added" use of CNT grafting also with respect to other transverse properties (thermal expansion, conductivity) and damping	[73]
Aluminum silicate, quartz/CNT	Injection CVD	Catalyst + carbon source: ferrocene dissolved in cyclohexane, CNT growth at 800°C for 1h	-	SEM, TEM, Raman	-	Electrical conductivity network found	Large difference in CNT characteristics found as a function of parent fiber type. Quartz fiber induced more homogenous growth of CNT (longer and more aligned) than aluminum silicate.	[74]

Alumina fiber fabric/CNT	CVD	$Fe(NO_3)_3$ catalyst from isopropanol solution applied. Its reduction to nanoparticle formation at 750°C.	EP Hand-lay-up and vacuum bag consolidation	SEM, TEM, OM, electrical conductivity, flexural strength	ILSS increased by 69%	Both in-plane and through thickness electrical conductivity increased with increasing CNT volume fraction (up to 3%)	Simultaneous enhancements of mechanical and electrical properties reported. Capillary driven wetting through the aligned CNT forest postulated	[75]
Quartz fiber fabric/MWCNT	CVD	Catalyst: fabric impregnated by aqueous $Ni(NO_3)_2$ solution; CNT growth at 650°C using C_2H_2 for up to 1h	EP (amine) Composites by VARTM	SEM, TEM, TGA, Raman, electrical conductivity, ILSS	ILSS increased by 15%	Electrical conductivity in both in and out-of-plane directions increased. The anisotropy diminished with increasing CNT growth time	Uniformly aligned MWCNT produced. Effects of catalyst concentration and CNT growth temperature studied.	[76]
Silica fiber (sized)/CNT	Injection CVD	Injection of catalyst precursor (ferrocene) and carbon source (toluene); CNT growth at T=760°C for up to 15 min	PMMA (from solution) Microcomposite	FE-SEM, BET, contact angle single fiber tensile test, fragmentation test	IFSS improved from 9.5 MPa (as-received) up to 24.3 MPa (CNT-grafted)	-	Dramatic increase in the BET surface area. Complete wetting of the CNT grafted fiber by PMMA. Strength of the silica fibers reduced by 30% after CNT growth possibly due to etching. By contrast, the modulus increased, that was assigned to densification of the network of silica (polycondensation)	[77]

Table 4: Carbon nanofiber grafting on various high temperature-resistant inorganic fibers: preparation and interphase effects

The main results achieved with the CNT grafting on high temperature resistant inorganic fibers, as listed in Table 4, might have inspired who pioneered the use of a protective silica or alumina layer on CFs before starting with the CVD treatment (see refs [71, 72]).

3.3. Grafting by non-carbon nanofibers

An increase in the surface area and an effective mechanical interlocking can be triggered by the grafting of non-carbon nanofibers or nanowires onto the reinforcing fibers. This approach has been followed by the group of Ehlert [78, 79]. These authors have created ZnO nanowire arrays on the surface of various reinforcing fibers, such as AF and CF. The idea followed was based on the fact that ZnO interacts strongly with carboxylic acid functional groups. The latter can be generated, however, on the surface of many reinforcing fibers by suitable techniques. In case of AF the amide bond is first cleaved by NaOH, then the Na^+ is exchanged by H^+ to create –COOH functional groups. This participates with Zn^{2+} ion in a coordination complex acting as seeding and anchoring size for the growth of the ZnO crystal (cf. Figure 6). The maximum temperature during the whole grafting, containing several steps, is 150°C (and that of the ZnO growth is even less, namely 90°C), which is far below of any of the CVD methods. The IFSS in an EP, determined by the fragmentation test, was enhanced by 51% when ZnO “nanowired” AF was tested instead of the as-received one. A further advantage of this approach was that the AF tensile strength was not negatively affected by the nanowires deposition process. Recall that a reduction in the fiber tensile strength is a common undesired "side-effect" of CVD treatments.

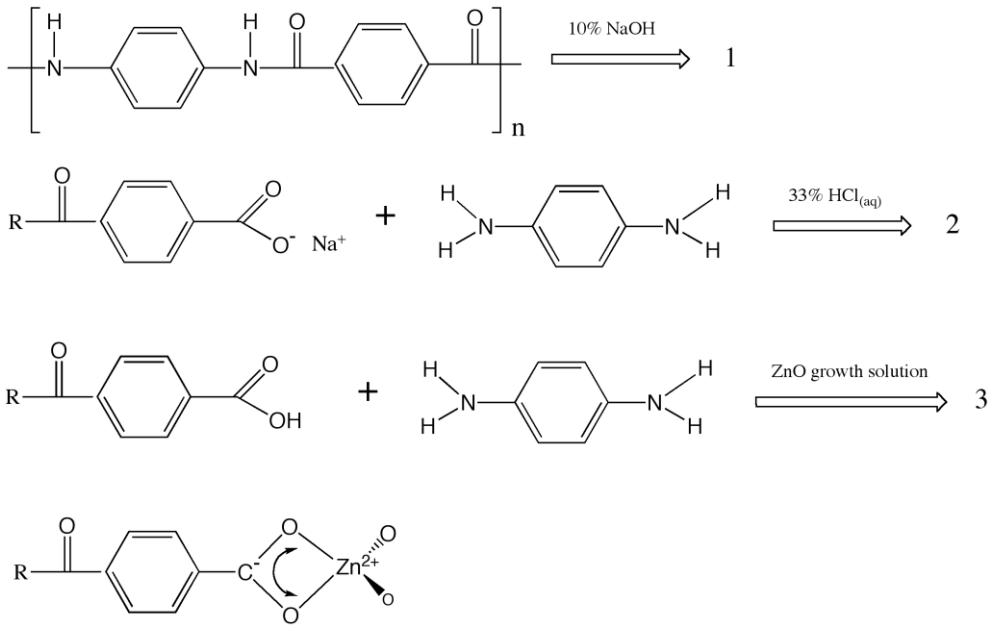

Figure 6. Reaction pathway of triggering ZnO growth on AF surface through cleavage of the amide bond [78].

This ZnO “nanowire whiskerization” was also adapted to CF [79]. The CFs were subjected to various surface treatments to produce functional groups, the presence of which was attested by XPS analysis. The IFSS strength, quantified by single-fiber fragmentation of EP-microcomposites, correlated with the

concentration of the surface ketone groups of CF, which participated in the coordination complexing with Zn^{2+}.

This kind of whiskerization from solution may be a very promising route of interphase nano-engineering. The major benefits are: no or less reduction of the substrate fiber tensile properties, growth at relatively low temperature, and possibility of achieving multifunctionality. In fact, ZnO display piezoelectric and semiconductor properties, which may be exploited in advanced composites for sensing applications [80].

4. Fiber surface modification by polymers

Various possibilities exist to modify the surface of reinforcing fibers by monomers, oligomers and polymers. Major targets of this strategy are: i) to enhance the cohesive interactions and ii) to tune the interphase properties upon request. The cohesive interactions between polymer-coated(grafted) fiber and the composite matrix may involve co-crystallization phenomena and the development of supramolecular structures. The modification of reinforcing fibers by polymer deposition is also aimed at creating an interphase with a gradient structure. In other words, the properties are gradually changing from the fiber surface toward the bulk matrix. In the next three paragraphs, recent developments in this field will be introduced on the basis of the following grouping: polymer grafting, plasma polymerization and self-assembly.

4.1. Polymer grafting

Feller and Grohens [81] used silane modified low molecular weight (10-60 kDa) polypropylene copolymers as novel coupling agents for GF (E-type) in isotactic polypropylene (PP). The silane function of such (co)polymers creates chemical bonds with the GF while the dangling chains participate in a co-crystallization process with the PP matrix. IFSS, deduced from microbond test, indicated that the grafting potential (owing to high silane content) should be compromised with the co-crystallization (supported by high molecular weight and long regular sequences) in order to get optimum bonding (IFSS ≈ 11MPa). Note that this value is still at about the half that was measured for PP-sized GF in a PP matrix containing maleic anhydride grafted PP (PP-g-MA) that might be considered as the state-of-the-art coupling agent [82]. Bismarck et al. [83] grafted polystyrene (PS) via bulk radical polymerization of styrene to CF surface. The contact angle and zeta-potential measurements confirmed that the surface of the grafted CF was PS-like. IFSS with the PS-grafted CF was threefold of the unsized, reference CF in PS according to pull-out tests. This was ascribed to the enhanced cohesion through massive entanglements. Trey et al [84] exploited the thiol-ene chemistry to produce a novel UV-curable thermoset matrix. Moreover, the interphase between GF and this resin was also involved in this thiol-ene click chemistry through a mercaptosilane in the GF sizing (Figure 7). Unexpectedly, the bonding between GF and the resin was not improved via the supposed reaction between –SH of the silane sizing and allyl groups of the “ene” compound of the resin.

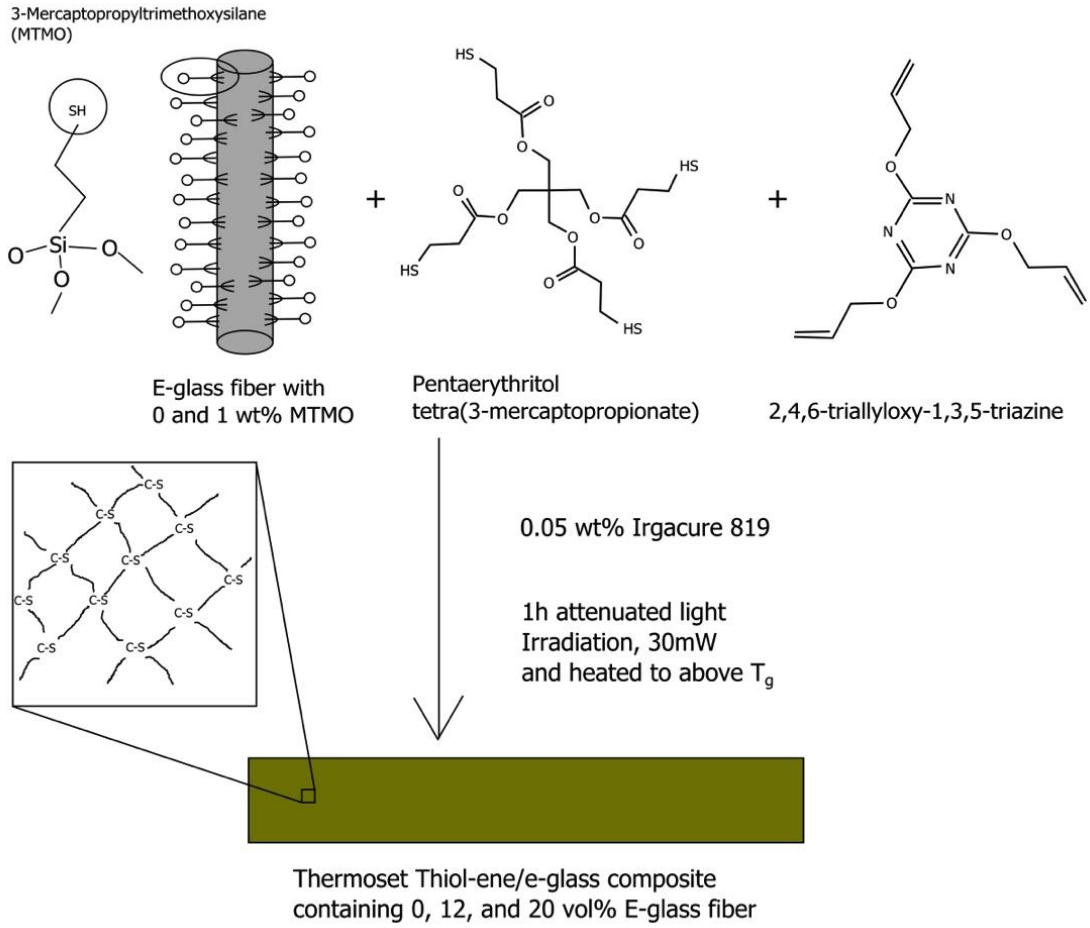

Figure 7. Thiol-ene chemistry for both the interphase modification and matrix curing (based on Ref. [84]).

Kuttner et al [85] adapted the thiol-ene reaction to produce a polymer coating via UV photo-polymerization. This was reached through the following steps:

Sulfhydrylation of the GF surface by a mercaptosilane is followed by coating with PS or PMMA via thiol-ene chemistry under UV irradiation. Note that the sulfhydrylation with 3-mercoptopropyl trimethoxysilane produces a polysiloxane layered network on the GF surface similar to that formed by a traditional silane containing sizing formulation. The thickness of the grafted polymer was up to 200 nm. The stiffness of the interphase was determined by AFM and found to be about the half of that of EP matrix. This was attributed to the swelling effect of EP exerted on the interphase.

Kuttner et al [86] explored the interphase modification possibilities via the thiol-ene chemistry through a “grafting from” and “grafting onto” strategy. These two techniques yielded different polymer thickness and grafting chain density values. In the “grafting from” approach the sulfhydrylated GF was coated by PS as described above. In the “grafting onto” approach presynthesized polybutadiene-block-polystyrene (PP-b-PS) was grafted onto the GF. IFSS was determined in single fiber pull-out tests from EP. It turned out that lower grafting densities are beneficial for IFSS enhancement in both approaches and the penetration of the grafted polymer chains into the matrix should not be hampered. Accordingly, optimization of the grafted chain density should be addressed instead of its maximization in future works.

Hyperbranched, dendrimeric, star-shaped polymers are promising interphase modifiers as well. They can be synthesized with varied functional groups capable of co-reactions with epoxy groups, double bonds of resins and chemically linkable at the same time to the surface functional groups of the reinforcing fibers. Although several papers are focused on the bulk modification of resins, mostly to improve their toughness by such dendritic polymers [87, 88], very few attempt were made to modify the interphase directly. Oréfice et al. [89] demonstrated that an interphase of hyperbranched structure may efficiently transfer the stress from the matrix to the fiber and improve the interfacial toughness at the same time. It is generally accepted that for the interfacial toughening, the interphase should be "soft". For that purpose, functional diblock copolymers were used which are covalently bonded to the fiber surface and sufficiently compatible on the other side with the matrix. Their stress transferring and toughening effects depend obviously on the molecular weight of the block segments (diffusion into and entangling with the bulk of the matrix molecules) [90].

4.2. Plasma polymerization

Plasma-chemical process is another way to improve the performance of composites via interphase engineering. Plasma surface treatment of fibers and use of the corresponding fibers in composites have been studied since the 1980s [15, 91, 92]. The plasma coating or polymerization seems to be one of the most effective methods to achieve both high strength and high toughness when suitable materials are selected for coating. Plasma polymerization deposits a homogeneous, pinhole free film to the fiber surface. Accordingly, the properties of the coating are not influenced by the underlying surface chemistry or topography of the fiber being coated. The polymerization conditions may yield coatings with different thickness, stiffness and even the fiber surface treatment for adhesion and sizing can be performed in a single step [93].

Cech [94] explored the plasma polymerization with various silanes in a mixture with oxygen gas to tailor the interphase between GF and unsaturated polyester (UP) resin. The author reported an up to 6.5 times increase in the ILSS measured by short beam shear test on UD aligned GF/polyester composites. This was achieved by a 0.1 µm thick plasma polymerized layer using tetravinylsilane/O_2 gas mixture. The above improvement in ILSS was 32% higher than that measured on composites prepared with industrially sized GFs specifically developed for UP resin-based composites. In follow up works of the Cech group [95, 96], tetravinylsilane was selected as monomer for plasma polymerization, the conditions of which have been varied. Using different plasma powers the chemical, physical and surface properties of the deposited films were varied in a broad range. IFSS increased by a factor of 2.3 whn the interphase thickness was rised from 50 nm to 5 µm.

The group of Jones [93] developed a continuous plasma polymerization coating process for GF using acrylic acid and/or 1,7 –octadiene monomers. The positive effect of the plasma coating on the IFSS was proven by the results of the single fiber fragmentation test performed as a function of the ratio of the monomers and coating thickness [93, 97]. The most important finding was linked to the thickness of the plasma polymerized coating, the layer thickness should be adjusted to the penetration (diffusion) depth of the matrix. As a consequence, the development of an IPN structured interphase is desired. It can be formed by swelling of the deposited cross-linked plasma polymerized layer by the resin prior to the curing of the latter. In case of EP/GF composites Liu et al. [98] estimated an optimum layer thickness in the range of some nm, when GF was coated by acrylic acid/1,7 –octadiene and allylamine/1,7 –octadiene monomer containing plasmas.

Needless to state that the polymer selected for plasma deposition should be “compatible” with the matrix resin of the composite material. Vautard et al. [99] adapted plasma polymerization to improve the adhesion of CF to vinylester resin (VE) cured by UV electron beam and also thermally. The steps followed by the authors were: i) plasma polymerization of maleic anhydride (MA) onto the CF surface, and ii) conversion of the MA into maleic imide with pendant allyl functionality. The allyl groups are co-reactive with the double bonds of the VE. Alternatively, the MA groups were converted to thiol functionalities, which can thus participate in thiol-ene (ene from the VE side) reactions. This concept, i.e. shielding of the CF surface by a plasma polymerized layer and providing it with functional groups being suitable to produce covalent bonding with the resin upon its curing, were the reasons behind the high adhesion between CF and matrix. According to our feeling, the future development with plasma polymerization techniques will address the covalent chemical bonding of the plasma deposited layer to the matrix.

4.3. Self-assembly

The term molecular self-assembly refers to those processes in which disordered molecules are converted into an organized supramolecular structure thereby using some specific, locally acting interactions between them. The local interactions may be of electrostatic nature, H-bonding, van der Waals forces, and π-π interactions.

Development of self-assembled monolayers (SAM), produced by suitable silane sizing on GF, was reported already in 1990. Holmes et al. [100] authored a review on this issue and quoted that 70-85% of the maximum IFSS of GF/EP can be obtained when 25-50% of the surface are covered with suitable functional groups. This finding was explained by steric hindrance due to the size of the EP molecules (and as a consequence not all functional groups are “accessible” for the EP molecules) and preferential absorption of the curable EP constituents on the surface.

He et al. [101] successfully triggered molecular self-assembly on CF surface. To develop the interphase, the CF surface was first Ag plated and then reacted with thiols of different chain length bearing various terminal functional groups. These thiols were grafted onto the Ag plated CF via Ag-S bonds. The structure of the SAMs depended on the molecular build-up (aliphatic, aromatic) of the thiols. -OH functionality of the thiols was more beneficial than $–NH_2$ one because the EP used was anhydride curable. According to microbond test results, the IFSS was enhanced from 30.7 MPa (untreated CF) to 32.1 MPa (Ag plating yielding surface roughness) and further to 33.2-36.0 MPa through SAM.

Self-assembly is a valuable tool to generate nanoscale polymer structures (monolayers). This strategy is widely used in biology, microelectronics, coating technology [101, 102] but not yet in the foremost of interest for polymer composites. This scenario may change in the near future because molecular self-assembly may turn into a further tool of interphase engineering. In a very recent work, Liu et al. [103] concluded that a self-assembled network of nucleating agent caused the transcrystallization of PP on PLLA fiber. Note that transcrystallization, and especially the structure of the transcrystalline layer, are key parameters for the successfull preparation of semicrystalline single polymer composites [104].

5. Interphase influenced by the matrix

It has been early recognized that the matrix composition and microstructure may strongly influence the fiber/matrix interphase and thus the performances of the corresponding composites [105]. It was widely accepted that the fiber interface is generally enriched of low molecular weight chains of the same polymer, though evidenced considerably later [106]. Better wetting of the reinforcing fibers by amorphous rather than by crystallizable microstructures of the same polymer was also reported [107, 108]. Use of polymeric coupling agents, such as maleated versions of the hosting thermoplastic matrix, is the state-of-the-art. NF-containing thermoplastics practically always contain polymeric coupling agents [109]. Their functional groups (generally anhydride) are co-reactive with those of the surface groups of NFs (-OH). Gamstedt et al. [110] observed that the IFSS between CF and UP resin depends on the chemical composition of the UP resin. UP with the highest degree of unsaturation yielded the best IFSS. This was assigned to the possible reaction between the surface functional groups of CF with the double bonds of the UP resin.

The above brief list of concepts makes intuitive that interphase tailoring may be designed also from the matrix side. In particular, according to the most recent trend manifested by the scientific community, the attention will be focused on interfacial effects caused by bulk modification of the matrices by nanofillers dispersion, and possible nano-structuring within the matrix.

5.1. Nanofillers in the bulk matrix

Zhang and coworkers [111] studied the effect of rigid spherical silica nanoparticles (up to 20 wt%) on the CF/EP adhesion as assessed by the transverse fiber bundle test. Finite element analysis was performed to determine the distribution and the effects of the thermal residual stresses. On the basis of the obtained results, the authors concluded that nano-silica particles in the EP did not noticeably affect the interfacial bonding. By contrast, improvements in the carbon/epoxy interfacial and interlaminar shear strength values were reported by Hossain at al. [112] when the matrix was modified with 1D (CNT) and 2D (clay, graphene) nanofillers. In fact, the ILSS of a CF woven fabric reinforced EP (cured by aromatic amine) was increased by at about 15% through incorporation of 0.3 wt% of amine-functionalized CNTs. This was attributed to possible reaction of the amine group CNT both with the epoxy group of the bulk EP and epoxy group of the silane sizing of the CF fabric . CNFs dispersed in UP after surfactant treatment enhanced the delamination fracture energy (G_{IC}) of GF fabric/UP composites when incorporated in less than 1 wt%. At higher CNF loading and without surfactant coating of CNF, the nanofillers were filtered off by the GF fabric [113]. It is worthwhile to underline that the effect of nanofillers in the last cited work is not really interphase-related. The positive effect observed is due to multiple crack deviation caused by CNF in the interlaminar layer. The group of Pegoretti has shown that clay [114] and graphite nanoplatelets (GNP) [115] incorporation in bulk EP may improve the IFSS to GF, in fact. The IFSS enhancement of about 30% was assigned to a better GF/EP wettability [114], and better mechanical properties of the EP matrix, and positive influence of GNP on the chemical affinity between GF and EP [115].

Positive effects of bulk matrix modifications with 0D (spherical), 1D and 2D nanofillers were also observed with thermoplastic resins. Pedrazzoli and Pegoretti [116] found that the IFSS, measured by the single-fiber fragmentation test of PP/GF microcomposites could be markedly enhanced by incorporating fumed silica up to 7 wt%. The best result was achieved when the matrix contained 5 wt% dimethyl dichlorosilane functionalized silica and 5 wt%. PP-g-MA coupling agent. For this nanocomposite, an IFSS value of about 25 MPa was found which is much higher than that one with the PP matrix (~3 MPa). The presence of both

fumed silica and PP-g-MA yielded a synergetic effect because the IFSS of the silica and PP-g-MA alone when added in 5 wt% each, laid at about 9 MPa. The observed effect was traced mostly to changes in the surface energetics. Arao et al. [117] demonstrated that the IFSS between PP and CF could be prominently enhanced by PP-g-MA (from 8.6 to 18.9 MPa) and even further with various types of nanofillers (silica and alumina nanoparticles, CNT, clay). According to single fiber pull-out tests, the IFSS data of the nanocomposites of composition PP/PP-g-MA/nanofillers = 95/4/1 wt% followed the ranking silica>alumina>CNT>clay. An improvement in the fiber/matrix adhesion has been found also with organoclay containing thermoplastic matrix composites and especially with PAs [118-120]. Vlasveld et al. [118] argued that the observed effect is related to the matrix stiffening induced by the organoclay because higher matrix modulus would give higher IFSS due to the improved stress transfer via the interphase. By contrast, Isitman et al. [120] ascribed this effect to the development of higher compressive residual stresses in presence of nanofillers at the fiber/matrix interface. According to a recent work by Pedrazzoli and Pegoretti [121], IFSS between GF and PP was enhanced by addition of GNP to the PP. The initial IFSS of about 3 MPa was increased up to about 14 MPa in presence of 7 wt% graphite nanoplatelets. A matrix with the ternary composition PP/PP-g-MA/GNP = 90/5/5 wt% yielded an IFSS value of almost 28 MPa. The work of adhesion between fiber and matrix correlated well with the IFSS data. Recall that similar effect was reported by the same group for EP-based composites [115].

It must be borne in mind that the effect of bulk modification on the fiber/matrix bonding is not trivial. Enrichment of the nanofillers in the interphase is most likely when they bear functional groups and may interact with those on the fiber surface. On the other hand, the wettability of the matrix should be affected via changes in the surface tension properties. Potential effect of thermal contractions cannot be disregarded either through nanofillers usually reduce the thermal expansion/contraction. So, further works should shed light on why the matrix modification influences the interphase properties.

5.2. Bulk matrix structuring

There are several possibilities of producing nanoscale phase separated thermoset and thermoplastic blends. In case of both thermosets and thermoplastics, the most promising strategy is to create a bi-continuous structure. Thermoplastics blends usually show a bi-continuous structure only in the early stage of mixing, afterwards thermodynamics driving forces generally induce the separation of one of the two phases and a segregated (dispersed) structure. Albeit some successful trials have been made with thermoplastic bends to preserve their bi-continuous morphology, especially with nanofillers as “phase stabilizers” [122], bi-continuity may be achieved with thermosetting resin based systems more easily. When both phases are cross-linked, the system exhibits interpenetrating network (IPN) structure, when one of them is linear, i.e. thermoplastic, then it is termed to as semi IPN. Such (semi) IPN systems are very promising matrices for composites even if their potential is not yet explored. It has to be mentioned that these systems quite often show a peculiar intermingled structure at a nanoscale level. For example, this feature has been clearly evidenced by AFM on VE/EP hybrid resins after physical etching [123].

In semi IPN structured systems the thickness of the characteristic ligament unit may be in the microscale range. Semi IPN can be generated by reaction induced phase separation (RISP) upon curing of resin containing high enough amount of thermoplastic polymer, which is initially dissolved in the resin. The IPN, semi IPN features may be well exploited to produce composites having high stiffness, strength and toughness at the same time. Atkins [124] proposed that intermittent bonding of fibers should result in such composites. Intermittent means that the fibers are only periodically sized to guarantee good adhesion to

the matrix. The sized/unsized pattern is periodically repeating along the fiber length. The unsized part may support crack blunting via mode-I debonding and crack deflection via mode-II debonding in UD composites. Local stress concentration can thus be effectively relieved and the layer damage zone is thus larger than for composites containing fully sized fiber (cf. Figure 8a). This yields per se enhanced toughness - so, why not to design this structure at the interphase level? For that purpose it is required that one phase of the (semi) IPN adheres well to the reinforcing fiber, whereas the other phase is more loosely bounded to the fiber (cf. Figure 8b). This concept was proposed by Karger-Kocsis and attempted with EP/VE = 1/1 blends. Note that the IPN structuring of the EP/VE hybrids was achieved in a one-pot synthesis, i.e., simultaneous curing of EP and VE. This concept was proved on reinforcing mats composed of ceramic fibers [125], basalt fibers [126] and flax fibers [127] . To trigger the good bonding of the inorganic fibers to either VE or EP, they were sized with vinyl or epoxysilanes, respectively. For selective adhesion to the flax fiber the interaction with its surface –OH and epoxy groups of the EP component was considered. However the authors not delivered direct evidence for the matrix structure caused intermittent bonding.

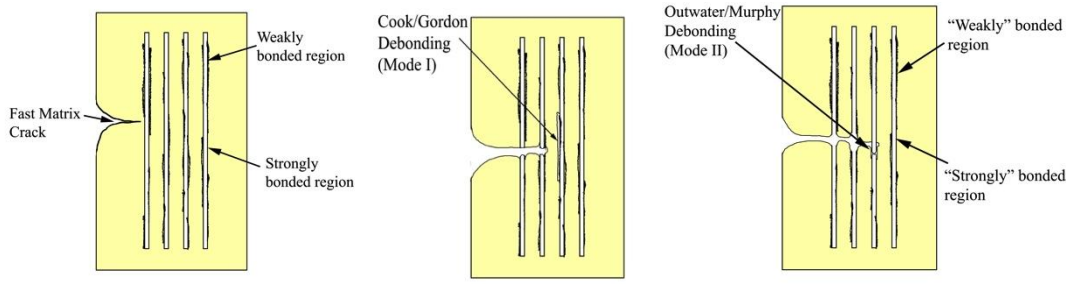

a)

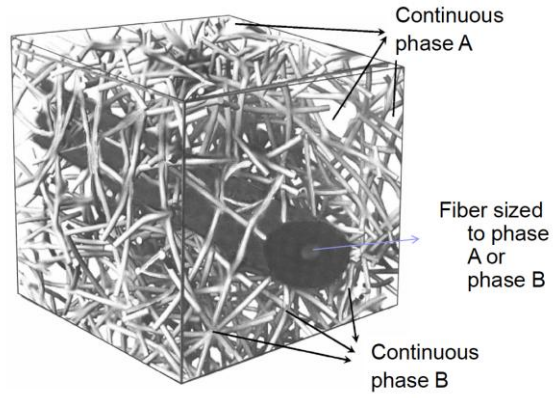

b)

Figure 8. (a) Effects of intermittent bonding in UD fiber reinforced composites (based on Ref. [124]) and (b) intermittent bonding achieved by matrix structuring (i.e. IPN).

The presence of semi IPN structure may be a nice tool for added functionality. A semi IPN structure can induce shape memory assisted self-healing, as proposed already in 2008 by Karger-Kocsis [128, 129]. Intermingling within the semi IPN units forms the net points needed for shape keeping, whereas T_g or T_m of the thermoplastic phase can be used as switch temperatures for setting the temporary shape. Healing is

ensured by molecular inter-diffusion of the thermoplastic phase. This concept may be adapted to the interphase region of composites, as well.

6. (Multi)functional/Smart Interphase

Current research and development activities are often focusing on (multi)functional interphase engineering and this aspect remains under spot of interest also in the near future. A (multi)functional interphase, apart from its traditional role, may overtake further tasks, such as sensing, healing, damping. Accordingly, (multi)functional materials typically have multiple roles: structural load bearing, energy absorption, sensing, vibration/damping control, energy absorption, etc.

(Multi)functional interphases can be created by different ways which were partly already introduced (see sizing in section 2). The relevance of this topic is the reason why a separate paragraph has been dedicated to it in this review. Next we summarize the achievements targeting sensing/damage detection, self-healing and other functional properties induced by a proper engineering of the interphase region.

6.1. Sensing/damage detection

Formation of an electrically conductive network of CNT, CNF or graphene in the polymer matrix surrounding the reinforcing fibers allows us for in situ sensing of deformation and damage. As Chou et al. [130] concluded, a nano-scale conductor is needed to sense the onset of micro-sized crack. This concept has been recently pushed forward by transferring the conductive network from the matrix to the interphase.

The group of Mäder explored the damage sensing possibilities of MWCNT networks deposited on the surface of various non-conductive reinforcing fibers, such as GF [25, 27, 29] and NF (jute) [45] by sizing/coating (cf. section 2). The authors demonstrated that the GF with MWCNT containing sizing had similar piezoresistivity (i.e. change in the electrical resistance upon load application) as CF thus allowing strain, and thus damage, sensing. The electrical properties of MWCNT coated GF in forms of single fibers in UD-composites changed as a function of stress/strain, temperature and humidity. This feature can be used to detect piezoresistive effects (damage onset cf. Figure 9) and the Tg in the interphase.

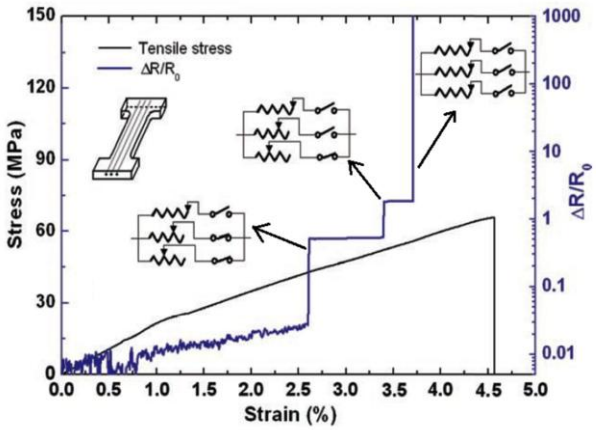

Figure 9. Simultaneous change of electrical resistance and stress as a function of tensile strain for triple GF/EP microcomposites Note: GF was sized with a MWCNT containing formulation (based on Ref. [29]).

The “bridging” of the MWCNTs between the crack flanks may work as “switch” (quoted as “junction-break” mechanism [29]) until the crack closure supports that reconnection of the pulled out and fractured MWCNTs.

The above results may open new routes for the in-situ structural health monitoring of polymer composites. In a recent paper Luo et al. [131] described the production of 1D fiber sensors. These sensors are composed of GF, AF and PET fiber substrates which were spray coated by single wall CNTs (SWCNT). During manufacturing the sensor may deliver information about the curing and cooling induced shrinkage through strain detection. The sensor built in the composite may be used for mapping the stress/strain state under various loading modes. As a consequence, the spray-coated “FibSen” fibers may replace Bragg grated optical fibers (FBG) used for both above tasks [132, 133]. Major benefit of the “Fibsen” 1D fibers is that their diameter is smaller or comparable with those of the reinforcing fibers of the composite unlike FBG fibers which are much thicker.

The next logical step in the development of functional reinforcing fibers is to check whether an electrical conductive polymer layer can be deposited onto the reinforcing fiber surface. For that purpose the most promising polymer is polyaniline (PANI). Hong et al. [134] showed in a recent paper that a PANI layer can be produced on the surface of UHMWPE fiber through in situ polymerization and doping. Though its sensing applications in suitable (cyclic) tests were not yet investigated, the above approach is very appealing for the future. Also natural fibers can be easily coated by PANI and used in sensing applications [135].

An interesting alternative is to produce a reinforcing fiber having piezoelectric coating. Lin and Sodano [136] predicted in a theoretical work that this is feasible and the related piezoelectrical structural fiber could be used for sensing/actuation and structural health monitoring.

6.2. Self-healing/repair

“Biological composites” in nature respond to damage through complex autonomic healing and representative mechanisms. Their adapting and mimicking are the driving forces of research also in the composites’ field. This development may be linked with problem of the damage detection: if we cannot detect the damage onset properly, why not to trigger autonomic (automatic) and intrinsic (stimulated) self-healing. About bio-inspired self-healing mechanisms, their terminology and adoption for polymer and (polymer) composites the reader may get valuable information from some excellent reviews [128, 137-140]. Development in the field started again with the bulk modification of polymers prior to focusing on the interface/interphase. As emphasized already several times, the interphase is most often the weakest region in composites where failure/damage start. Therefore, it is obvious that self-healing/repair actions should be preferentially located in the fiber/matrix interphase. In this respect two distinct research directions are generally followed:

i) Capsule-based healing systems (autonomous repair)
ii) Exploitation of reversible physical interactions and chemical reactions, which belong to intrinsic self-healing measures [43].

6.2.1. Capsule-based (autonomous)

In capsule-based self-healing systems the healing agent is confined in discrete capsules. Their rupture, caused by damage (typically by crack growth) releases the context of capsules that works for “healing”.

Recall that the fiber/matrix debonding prevents the load transfer between the “weak” matrix and “strong” reinforcement leading to stiffness and strength losses. Coalescence of the debonded area supports the onset of microscopic cracking and cause the ultimate failure of the composite. Accordingly, capsules should be located in the interphase and their size comparable or even lower than that of the fiber diameter.

There are different encapsulation techniques and strategies [139]. Not all of the encapsulation strategies developed for bulk materials are suitable for the interphase.

Jones et al [42, 43] adopted the solvent based healing chemistry for a single capsule approach. They encapsulated the healing epoxy along with a solvent (ethylphenyl cetate (EPA)) in a urea/formaldehyde resin-based (UF) shell. The latter was produced in situ by reacting urea with formaldehyde in oil (organic components) in water (aqueous solution) type emulsion. One of the major tasks was to produce sub-micrometer sized capsules. The healing process involves swelling of the matrix by the solvent thereby allowing the healing epoxy to reach locally the residual reactive amine groups of the matrix resin. The GF fibers were dip coated in an aqueous suspension containing the capsules [42], whereas for CF a binder formulation was necessary to stabilize the capsules on the CF surface [43]. As disclosed already in section 2 (Table 1), the healing efficiency, measured in repeated microbond tests, reached up to 80%. The beauty of this solvent based epoxy healing is that the stoichiometry is “disregarded”. This, however, should have been taken into account when both the healing resin and hardener would be encapsulated. In the latter case the stoichiometric ratio should be considered by different amount or sizes of the related capsules to be deposited, which is a quite hard task. Due to this reasons the single capsule technique has certainly more chance to a successful application since these capsules may be added through a carrier resins that could be in principle different from the composite matrix [141]. To trigger the polymerization of such “matrix dissimilar” resins additional treatments (heating, UV or electron beam indication) may be needed. This is associated, however, with a change from autonomous toward intrinsic healing.

6.2.2. Diels-Alder reaction (intrinsic)

Intrinsic self-healing materials do not have a sequestered healing agent but exhibits a self-healing capability that is triggered by the damaging itself or by an external stimulus (usually heat) [139]. The mechanisms involved are: molecular diffusion with entanglements, reversible polymerization, melting of a thermoplastic phase, hydrogen or ionic bonding. Multiple healing events are possible because all of the above processes and reactions are reversible.

Phenomena linked with molecular diffusion and/or melting may be at work for semi IPN structural systems as already discussed in section 5.2. Recall that semi IPN structuring may guarantee multifunctionality via the combination of shape memory and self-healing. The peculiar feature of ionomers is that they may undergo self-healing via re-aggregation of the ionic clusters upon the heat induced by the damage (typically impact) itself. This concept has been adopted for polymer composites in the bulk [142] but not yet for the interphase. Note that this approach is at the borderline of autonomous/intrinsic healing.

A widespread attention can be registered for healing through reversible chemical reactions; thereby special attention is paid to Diels-Alder type reactions. That was the reason of emphasizing this kind of reaction in the above subheading. The Diels-Alder (DA) reactions was discovered in the 1920s and used as crosslinking mechanism in mendable polymers for healing from 2002 [143]. For the DA cycloaddition as diene component furan whereas as dienophile component maleimide functionalities were selected from the beginning. The possible reason behind this fact is that the temperature range of the cycloaddition and the

break apart of the related adducts (retro DA reaction) is fitting well with the usual application temperatures of polymers. The recent developments in this field included also the issue of transferring the knowledge gained in bulk modification of resins, to the interphase region [143, 144].

Pioneering activity in this field should be attested to the group of Palmese [145-147]. The basic idea was to bring one of the required functional groups onto the fiber surface, whereas the counterpart groups are in the matrix resin. For example, maleimide functionalized GF was produced in two steps: i) grafting an amine functional silane coupling agent onto the GF, followed by ii) Michael addition reaction between the amine and a bismaleimide (BMI) compound – cf. Figure 10a.

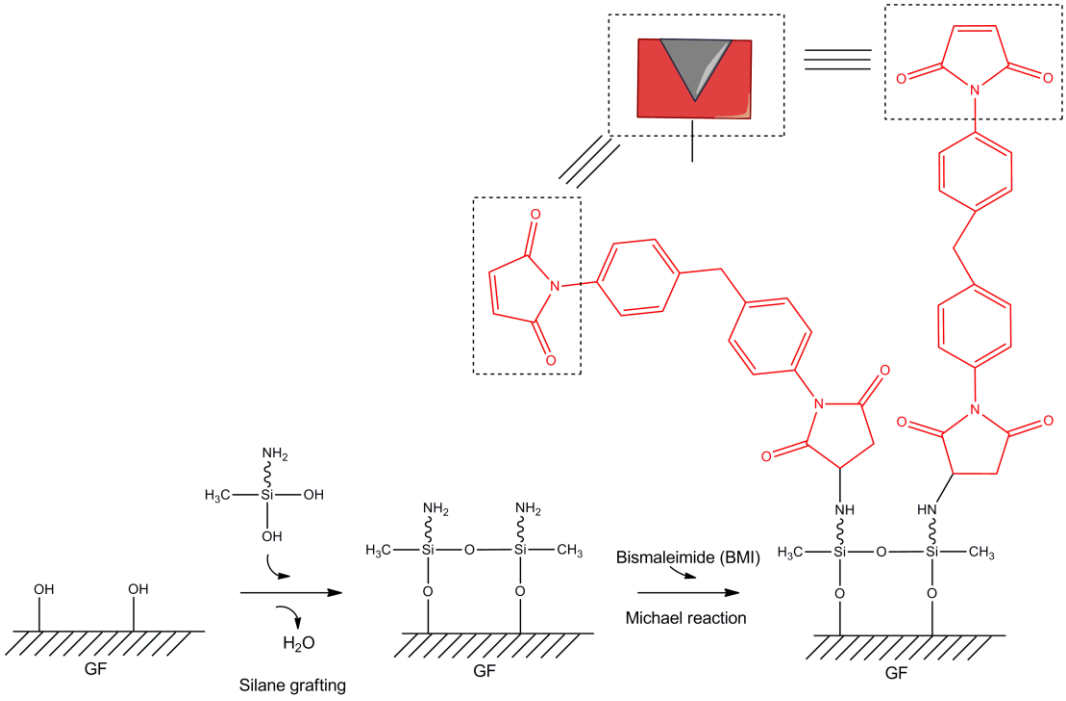

a)

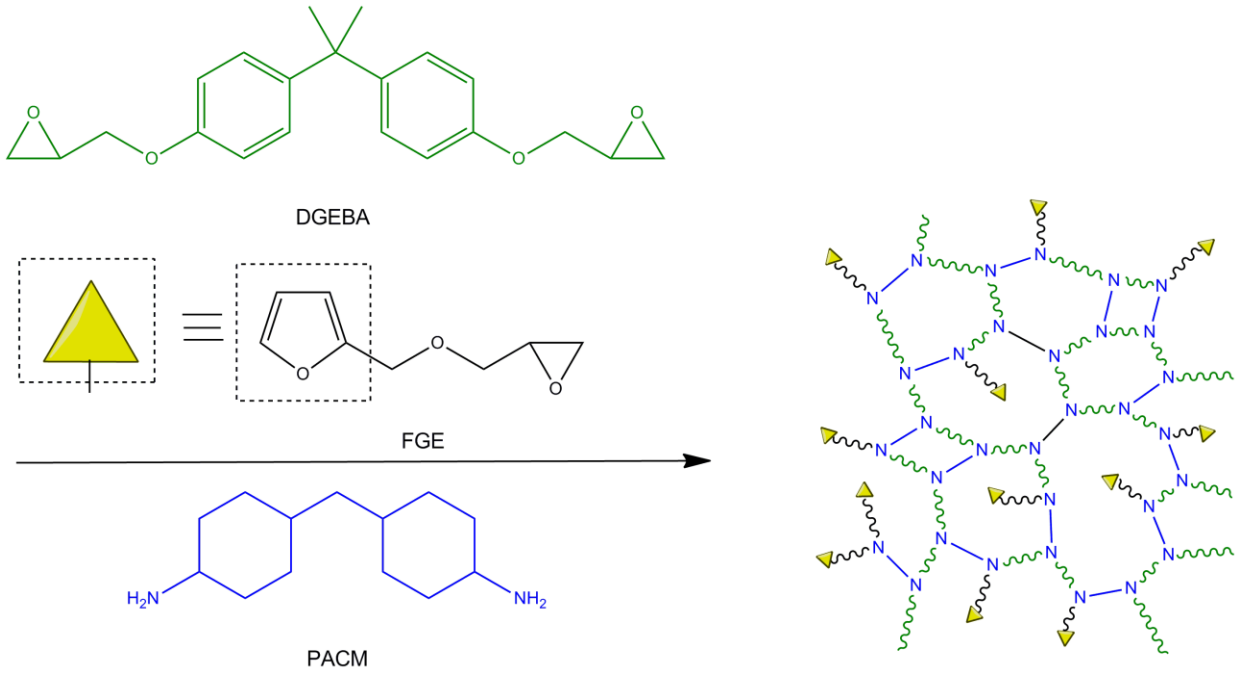

b)

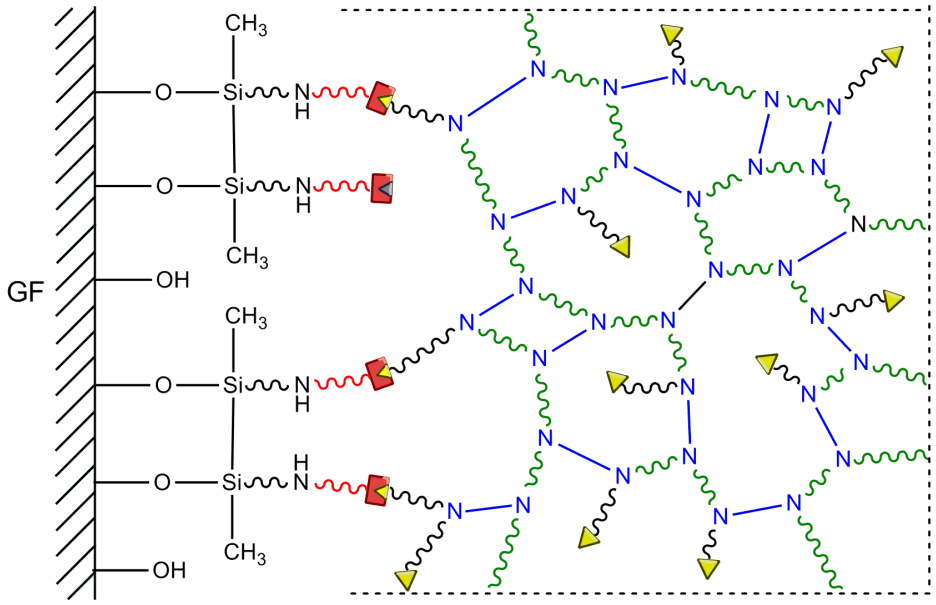

c)

Figure 10. Preparation of a maleimide-functionalized GF (based on ref. [145]) (a), possible composition of a furan-functionalized EP matrix (b) (based on Ref. [146]), and the final chemical network with reversible Diels-Alder bonding schematically (c). Note: because the Diels-Alder reaction belongs to click chemistry, the related bonding is marked by a key/lock symbol.

The EP matrix consisted of diglycidyl ether of bisphenol-A (DGEBA, bifunctional standard EP), a furfuryl glycidyl ether (FGE) and phenyl glycidyl ether (PGE). FGE and PGE are monofunctional EPs. For stoichiometric curing of the EP resin mixtures of different compositions a cycloaliphatic diamine (4,4' methylene biscyclohexanamine, PACM, was used – cf. Figure 10b). The healing efficiency was tested in

successive microdebond tests after a thermal treatment at T=90°C for 1h (retro DA) and T=22°C for 12 h (DA) [145]. The healing efficiency, initially at about 40%, was diminished after five healing cycles. In a companion work [146] it was found that the chain mobility, i.e. T_g of the EP matrix, has an important role in the DA cycloaddition. Complete recovery of the IFSS was reported for a resin system with a $T_g \approx 6$°C. A recent work of the Palmese group [147] addressed the room temperature healing of EP and EP/GF composites via DA reaction. Here the healing was achieved by a combination of solvent-induced swelling and covalent bonding through DA. The healing agent injected in the crack plane was BMI compound dissolved in dimethyl formamide (DMF). DA occurred between the mobile furans of the EP matrix and the BMI. The proposed mechanism is depicted in Figure 11.

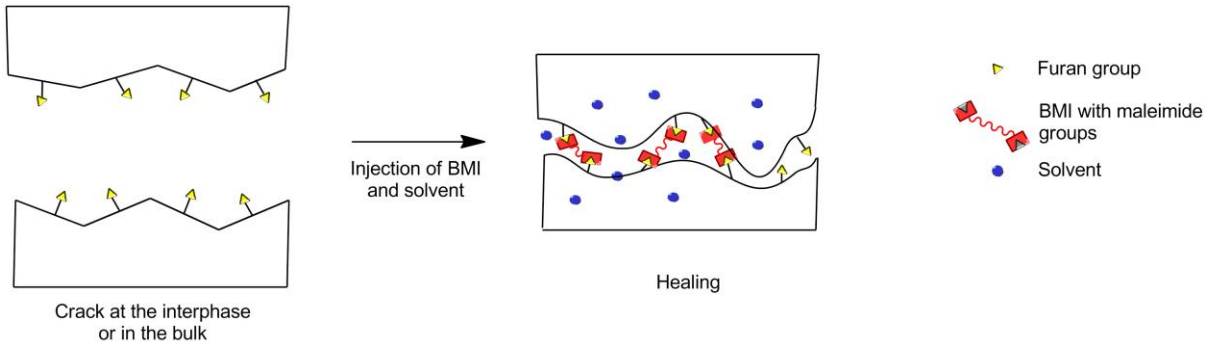

Figure 11. Proposed healing mechanism owing to physical (interlocking caused by solvent induced swelling) and chemical interactions (DA reaction between furan and maleimide functional groups) (based on ref. [147]). Symbols as in Figure 10.

Physical bonding alone resulted in ~28% recovery of the initial strength, whereas the covalent bonding through DA added a further ~42% contribute. So, the overall average healing efficiency was of about 70%, though in some cases even 100% recovery was measured. Recall that healing was achieved here at room temperature but via injecting a healing solution. In case of composites therefore holes should be drilled or other strategies should be found to inject the healing solution. Note that this solvent-assisted healing has some analogy to the encapsulated healing agent introduced before [42, 43].

A similar DA strategy, as shown above for GF, has been followed by Zhang et al. [148] for CF. Maleimide groups were grafted onto CF in a three-step treatment. This contained: i) oxidation in nitric acid resulting in –COOH, -CO and –OH functionalities, ii) converting the carboxyl groups into amine by tetraethylenepentamine amination, and iii) reacting the amine groups with BMI in Michael reaction. The related chemical pathway is given in Figure 12.

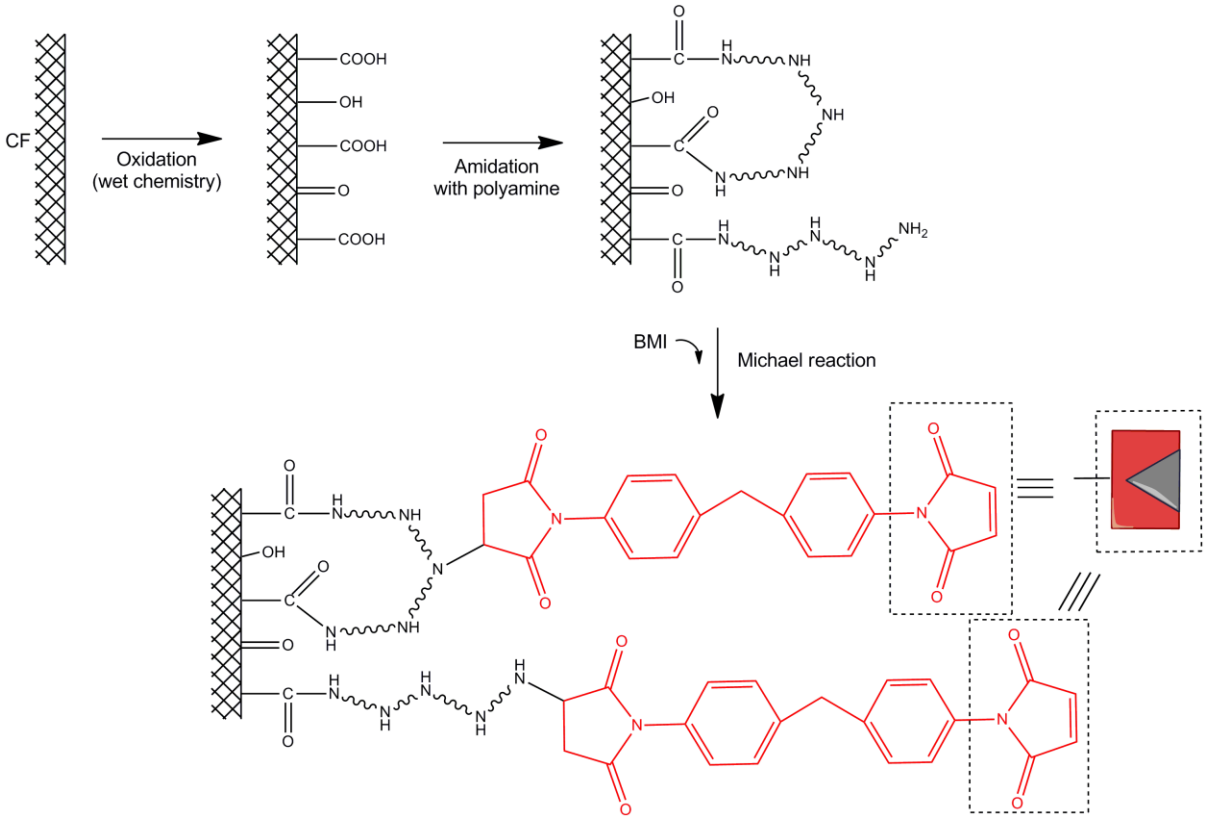

Figure 12. Scheme of grafting pathway of maleimide groups onto CF surface in order to trigger DA reactions (based on Ref. [148])

Similar to the approach of the group of Palmese [145-147], the EP was furan modified by adding FGE. The healing efficiency was checked by microbond tests. The single CF with the debonded microdroplet was kept at T=90°C for 1h (retro DA) followed by storing at room temperature for 24h prior to repeated microbond testing. The average self-healing efficiency after subtracting the frictional component from the test result was: 8% (untreated CF)<19% (CF oxidized for 30min)< 75% (CF oxidized for 60 min)>21% (CF oxidized for 90 min). The above ranking implies that not all functional groups can be functionalized with maleimide and/or only a part of them is accessible for the FGE. The healing efficiency in subsequent healing processes dropped also in this case (from 82% to 58% after the third healing). This was attributed to the formation of such DA adducts which do not break apart upon loading (irreversible DA bonds) – cf. Figure 13.

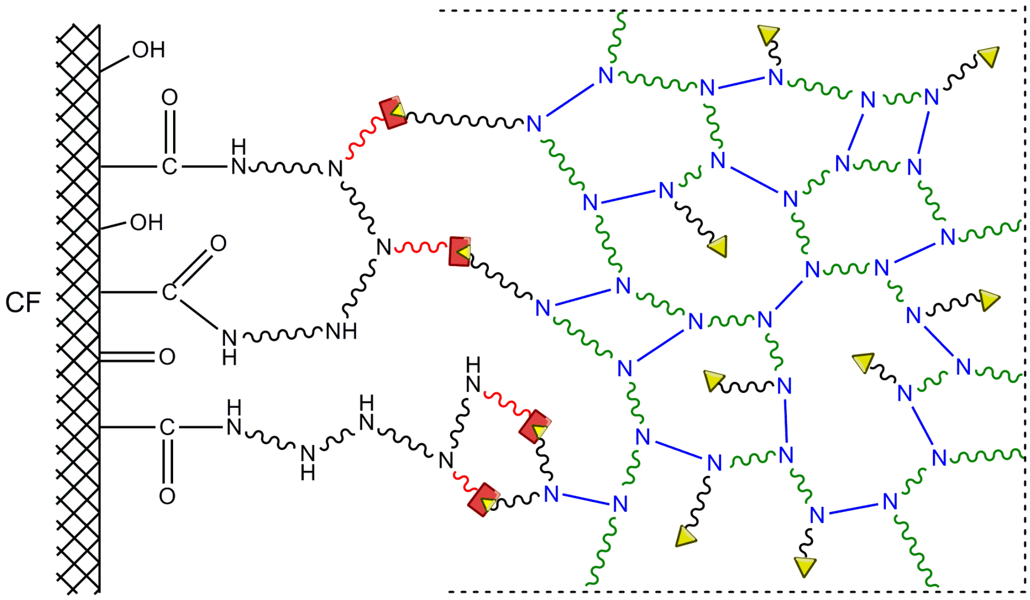

Figure 13. Interphase formation between maleimide functionalized CF and amine cured EP containing furan groups. Notes: mechanical debonding in microbond test splits the DA bonds, distorts the network and even some covalent bonds of the latter may break up. Self-healing through DA coupling is preceded by retro DA reaction. For symbols cf. Figure 10.

Apart from DA reactions there are some other possibilities, such as "dynamic urea bonds" [149] can be exploited for self-healing purpose.

6.3. Other properties

The vibration damping of composite materials is often too low for several applications. Vibration suppression can be attained by increasing the loss modulus. Several approaches were already followed to improve the damping capability of fiber reinforced composites, and some of them involves an engineering of the fiber/matrix interphase [150]. Since the vibration energy can be dissipated via frictional interaction, a certain slippage between the fiber and matrix could be beneficial and the related strategies involved coating of the fiber with highly viscoelastic polymers and with nanofillers. Note that for example CNT-CNT interactions and CNT-matrix frictional stick-slip effects may efficiently contribute to energy dissipation. These phenomena can be exploited in composites containing hierarchical fibers. The subject was explored by Tehrani et al. [72] who made use of the GSD technique. The GSD coated CF fabric reinforced EP showed considerably higher loss modulus in the studied frequency range (1-60 Hz) than all other reference composites (raw, heat treated, sputter coated and CVD coated). Accordingly, hierarchical structured reinforcing fibers may also improve the damping of the corresponding composites [73].

7. New insights in interphase

The recent developments in interphase engineering had an impact also on the characterization identification, testing techniques and modelling of the interphase in composites.

7.1. Experimental techniques

For the chemical analysis of the fiber surfaces several techniques have been well established. Their range covers X-ray photoelectron spectroscopy (XPS), Auger electron spectroscopy, time of flight secondary ion

mass spectrometry (ToF-SIMS), dynamic contact angle analysis and inverse gas chromatography (IGC, [2]) Jesson and Watts recently reviewed the main experimental techniques for the interface and interphase characterization [151]. To assess the surface functionality and heterogeneity, scanning probe microscopy (SPM) and its variants has been proven to be an useful technique [152].

Researchers have been always interested to get a deeper insight in the interphase properties. Our summary already introduced some new aspects and novel testing methodologies which will not be repeated here. Among the analytical techniques immobilizing of fluorescent dyes in the interphase may deliver new information on changes therein during curing [153]. Thermal AFM may be a further useful tool in this respect [154].

Testing of microcomposites is often coupled with other techniques, such as laser Raman microscopy. The experimental tests are nowadays often coupled with numerical analyses such as finite element modelling [155-157]. Apart from microbond and pull-out tests, nanoindentation is frequently used to determine the interphase thickness and assess the changes therein via mapping [158-160]. Results received with nanoindentation of composites with hierarchical fibers suggested that this technique may be problematic owing to the onset of locally arising stresses [161]. One can predict a break-through for tomography methods in interphase studies. Damage development and growth will likely be assessed in situ by suitable techniques, such as synchrotron X-ray tomography: the information coming from these tools may serve as valuable input parameters for modelling.

7.2. Modelling

Some attempts have been recently made to model the development of the interphase as a function of processing (curing) condition. In particular the concurrent processes of molecular diffusion and crosslinking were approached by numerical [162] and various multiscale simulation methods [163]. Outcome of the last cited work was that the crosslink density in the interphase is much lower than in the bulk matrix. This was traced to the simulation result that the amount of the hardener near to the fiber surface is not enough to react with the epoxy groups of the resin and sizing, respectively. This means that the interphase is formed at non-stoichiometric ratio.

To get a better understanding on the role of MWCNT grafted on CF under shear deformation in microbond and fragmentation tests a molecular dynamic model was developed [164]. The simulation predicted that MWCNT grafting enhanced the shear modulus and strength of the interphase compared to the matrix. Valuable information was received also on the shear force distribution within the representative unit cell. Romanov et al. [165] demonstrated in a 3D finite element model that CNTs grown on CF alter the stress distribution in composites, in fact. In this model a 3D unit cell of UD CF composite (volume fraction of CF = 0.6), with and without CNT forest on the CF surface was subjected to transverse tensile loading. The stress field was analyzed using the embedded regions technique. Figure 14 presents the counter plots of the maximum principal stress in the matrix for the composite with and without CNT overgrowth. In the former case the density of the CNT forest was varied (low, high).

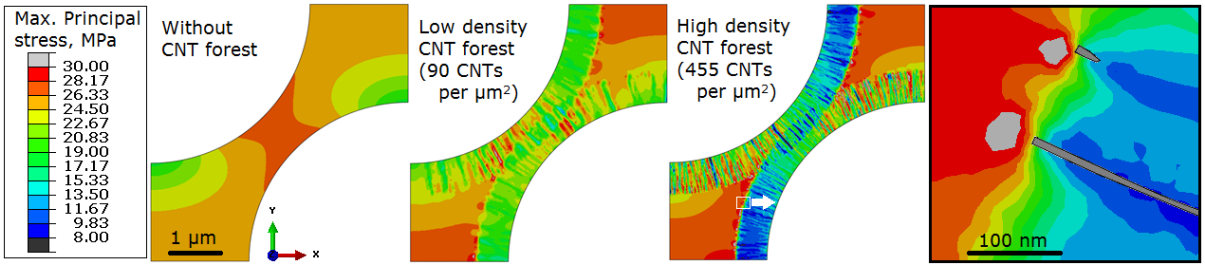

Figure 14. 2D contour plots of the maximum principal stress in a composite with UD aligned CFs without and with CNT forests on their surfaces. Notes: loading occurred in the x-direction. The density of the grown CNT on the hierarchical CF has been also considered. (adapted from Ref. [165]).

Figure 14 makes obvious that CNT grafting drastically changed the stress distribution. Two effects should be underlined:

i) CNTs introduces a local stress gradient with stress concentrations at their tips, and
ii) stress concentration of the CNT forest appears on microscale.

Accordingly, via CNT "foresting" the stress concentration at the fiber/matrix interface can be markedly suppressed. It can be predicted that further exhaustive modelling will be carried out to shed more light on interphase effects induced by novel nano-engineering techniques.

8. Outlook and future trends

Interphase engineering is profiting from the ongoing extensive research on nano-fillers and nano-composites. A large body of the main results has already been overtaken, adopted for the interphase, as shown in the review, and this tendency remains. The recent developments with polymers, marking a change from structural toward functional properties, transferred to the interphase. Attempts will be made to combine sensing with actuation function. Self-diagnostic options for structural health monitoring will also be addressed. For self-repair/healing novel approaches will be followed, thereby making use of the actual development of the click chemistry. Moreover, novel functions may be tackled, such as separation of the heat conduction from the electric one, thermal management by phase change material coating, electromagnetic interference shielding. A very promising field involving interphase engineering is related to the modification of conventional structural carbon fibres via activation (by steam, carbon dioxide, acid or potassium hydroxide) to create fibres which can be used simultaneously as electrode and reinforcement in structural composite supercapacitors [166, 167]. To support the mechanical interlocking, nano-patterning and -imprinting techniques [168] may be explored. Creation of novel functional properties in the interphase should not compromise, however its traditional load transfer role. Attempts will be made to enhance the resistance to fibrillation and buckling of AF and UHMWPE reinforcing fibers. For this purpose polymer coatings, produced by in situ polymerization from suitable monomers, such as pyrrole [169] are promising.

Interphase engineering will be supported by extensive modeling with more and more refined approaches of multiscale character. The input parameters of these models will be deduced from "optimized" tests. The latter implies "instrumented" tests meaning that the mechanical tests will be combined simultaneously with other analytical (e.g. Raman spectroscopy), structural (X-ray tomography, non-destructive tests, such as acoustic emission), and functional (conductivity-based methods) testing methods.

Acknowledgements

This work was partly supported by a grant of the Hungarian Research Funds (OTKA K 109409 and 114547).

References

[1] Papanicolaou GC, Paipetis AS, Theocaris PS. The concept of boundary interphase in composite mechanics. Colloid Polym Sci. 1978;256:625-30.

[2] Tze WTY, Gardner DJ, Tripp CP, O'Neill SC. Cellulose fiber/polymer adhesion: effects of fiber/matrix interfacial chemistry on the micromechanics of the interphase. J Adhes Sci Technol. 2006;20:1649-68.

[3] Keszei S, Matkó S, Bertalan G, Anna P, Marosi G, Tóth A. Progress in interface modifications: from compatibilization to adaptive and smart interphases. Eur Polym J. 2005;41:697-705.

[4] Zinck P, Mäder E, Gerard JF. Role of silane coupling agent and polymeric film former for tailoring glass fiber sizings from tensile strength measurements. J Mater Sci. 2001;36:5245-52.

[5] Jones FR. Interphase in Fiber-Reinforced Composites. In: Nicolais L, Borzacchiello A, editors. Wiley Encyclopedia of Composites. Second Edition ed. Hoboken, NJ, USA: John Wiley & Sons; 2012.

[6] Tanoglu M, Ziaee S, McKnight SH, Palmese GR, Gillespie JW, Jr. Investigation of properties of fiber/matrix interphase formed due to the glass fiber sizings. J Mater Sci. 2001;36:3041-53.

[7] Dey M, Deitzel JM, Gillespie JW, Schweiger S. Influence of sizing formulations on glass/epoxy interphase properties. Composites Part A. 2014;63:59-67.

[8] Herrera-Franco PJ, Drzal LT. COMPARISON OF METHODS FOR THE MEASUREMENT OF FIBER MATRIX ADHESION IN COMPOSITES. Composites. 1992;23:2-27.

[9] Kim J-K, Mai Y-M. Engineered interfaces in fiber reinforced composites. Amsterdam, The Netherlands: Elsevier; 1998.

[10] Zinck P, Gerard J. Thermo-hydrolytic resistance of polyepoxide–glass fibres interfaces by the microbond test. Compos Sci Technol. 2008;68:2028-33.

[11] Chee Ho KK, Qian H, Bismarck A. Carbon Fiber: Surface Properties. In: Nicolais L, Borzacchiello A, editors. Wiley Encyclopedia of Composites. Second Edition ed. Hoboken, NJ, USA: John Wiley & Sons; 2012.

[12] Hoecker F, Karger-Kocsis J. Surface energetics of carbon fibers and its effects on the mechanical performance of CF/EP composites. J Appl Polym Sci. 1996;59:139-53.

[13] Grishchuk S, Gryshchuk O, Weber M, Karger-Kocsis J. Structure and toughness of polyethersulfone (PESU)-modified anhydride-cured tetrafunctional epoxy resin: Effect of PESU molecular mass. J Appl Polym Sci. 2012;123:1193-200.

[14] Liu W, Zhang S, Li B, Yang F, Jiao W, Hao L, et al. Improvement in interfacial shear strength and fracture toughness for carbon fiber reinforced epoxy composite by fiber sizing. Polym Compos. 2014;35:482-8.

[15] Netravali AN, Mittal KL. Fiber Surface Treatment: Relevance to Interfacial Characteristics. In: Nicolais L, Borzacchiello A, editors. Wiley Encyclopedia of Composites. Second Edition ed. Hoboken, NJ, USA: John Wiley & Sons; 2012.

[16] Fuqua MA, Huo S, Ulven CA. Natural Fiber Reinforced Composites. Polym Rev. 2012;52:259-320.

[17] Aguilar-Rios A, Herrera-Franco PJ, Martinez-Gomez AD, Valadez-Gonzalez A. Improving the bonding between henequen fibers and high density polyethylene using atmospheric pressure ethylene-plasma treatments. Exp Pol Lett. 2014;8:491-504.

[18] Medina L, Schledjewski R. Water glass as hydrophobic and flame retardant additive for natural fibre reinforced composites. J Nanostr Pol Comp. 2009;5:107-14.

[19] Khoathane MC, Sadiku ER, Wambua PM. Effect of water glass treatment on the mechanical and thermooxidative properties of kenaf and sisal fibres. J Reinf Plast Compos. 2012;31:1261-9.

[20] Grishchuk S, Castellà N, Karger-Kocsis J. Hybrid resins from polyisocyanate/vinyl ester/water glass systems: Structure and properties. Eur Polym J. 2007;43:1245-57.

[21] Karger-Kocsis J. Water glass – an alternative precursor for sol-gel derived silica nanofiller in polymer composites? Exp Pol Lett. 2014;8:880.

[22] Fiedler B, Gojny F, Wichmann M, Bauhofer W, Schulte K. Can carbon nanotubes be used to sense damage in composites? Eur J Control. 2004;29:81-94.

[23] Lubineau G, Rahaman A. A review of strategies for improving the degradation properties of laminated continuous-fiber/epoxy composites with carbon-based nanoreinforcements. Carbon. 2012;50:2377–95.

[24] Barber AH, Zhao Q, Wagner HD, Baillie CA. Characterization of E-glass–polypropylene interfaces using carbon nanotubes as strain sensors. Compos Sci Technol. 2004;64:1915-9.

[25] Gao S-l, Zhuang R-C, Zhang J, Liu J-W, Mäder E. Glass Fibers with Carbon Nanotube Networks as Multifunctional Sensors. Adv Funct Mater. 2010;20:1885-93.

[26] Warrier A, Godara A, Rochez O, Mezzo L, Luizi F, Gorbatikh L, et al. The effect of adding carbon nanotubes to glass/epoxy composites in the fibre sizing and/or the matrix. Composites Part A. 2010;41:532-8.

[27] Zhang J, Zhuang R, Liu J, Mäder E, Heinrich G, Gao S. Functional interphases with multi-walled carbon nanotubes in glass fibre/epoxy composites. Carbon. 2010;48:2273-81.

[28] Liao L, Wang X, Fang P, Liew KM, Pan C. Interface enhancement of glass fiber reinforced vinyl ester composites with flame-synthesized carbon nanotubes and its enhancing mechanism. ACS Appl Mater Interfaces. 2011;3:534-8.

[29] Zhang J, Liu J, Zhuang R, Mader E, Heinrich G, Gao S. Single MWNT-glass fiber as strain sensor and switch. Adv Mater. 2011;23:3392-7.

[30] An Q, Rider AN, Thostenson ET. Hierarchical composite structures prepared by electrophoretic deposition of carbon nanotubes onto glass fibers. ACS Appl Mater Interfaces. 2013;5:2022-32.

[31] Bekyarova E, Thostenson ET, Yu A, Kim H, Gao J, Tang J, et al. Multiscale Carbon Nanotube−Carbon Fiber Reinforcement for Advanced Epoxy Composites. Langmuir. 2007;23:3970-4.

[32] Laachachi A, Vivet A, Nouet G, Ben Doudou B, Poilâne C, Chen J, et al. A chemical method to graft carbon nanotubes onto a carbon fiber. Mater Lett. 2008;62:394-7.

[33] Tang G, Zang Z, Chang D, Wei G, Wang D, Mi W, et al. Study on the Interfacial Behavior of Clay-Coated Carbon Fiber-Reinforced PEI Composites. Polym-Plast Technol. 2012;51:861-5.

[34] Rodriguez AJ, Guzman ME, Lim C-S, Minaie B. Mechanical properties of carbon nanofiber/fiber-reinforced hierarchical polymer composites manufactured with multiscale-reinforcement fabrics. Carbon. 2011;49:937-48.

[35] Rodriguez AJ, Guzman ME, Lim C-S, Minaie B. Synthesis of multiscale reinforcement fabric by electrophoretic deposition of amine-functionalized carbon nanofibers onto carbon fiber layers. Carbon. 2010;48:3256-9.

[36] Schaefer JD, Rodriguez AJ, Guzman ME, Lim C-S, Minaie B. Effects of electrophoretically deposited carbon nanofibers on the interface of single carbon fibers embedded in epoxy matrix. Carbon. 2011;49:2750-9.

[37] Liao WH, Tien HW, Hsiao ST, Li SM, Wang YS, Huang YL, et al. Effects of multiwalled carbon nanotubes functionalization on the morphology and mechanical and thermal properties of carbon fiber/vinyl ester composites. ACS Appl Mater Interfaces. 2013;5:3975-82.

[38] Battisti A, Esqué-de los Ojos D, Ghisleni R, Brunner AJ. Single fiber push-out characterization of interfacial properties of hierarchical CNT-carbon fiber composites prepared by electrophoretic deposition. Compos Sci Technol. 2014;95:121-7.

[39] Jin SY, Young RJ, Eichhorn SJ. Hybrid carbon fibre–carbon nanotube composite interfaces. Compos Sci Technol. 2014;95:114-20.

[40] Zhang S, Liu W, Wang J, Li B, Hao L, Wang R. Improvement of interfacial properties of carbon fiber-reinforced poly(phthalazinone ether ketone) composites by introducing carbon nanotube to the interphase. Polym Compos. 2014:n/a-n/a.

[41] Chen L, Jin H, Xu Z, Shan M, Tian X, Yang C, et al. A design of gradient interphase reinforced by silanized graphene oxide and its effect on carbon fiber/epoxy interface. Mater Chem Phys. 2014;145:186-96.

[42] Jones AR, Blaiszik BJ, White SR, Sottos NR. Full recovery of fiber/matrix interfacial bond strength using a microencapsulated solvent-based healing system. Compos Sci Technol. 2013;79:1-7.

[43] Jones AR, Cintora A, White SR, Sottos NR. Autonomic healing of carbon fiber/epoxy interfaces. ACS Appl Mater Interfaces. 2014;6:6033-9.

[44] Sharma M, Gao S, Mäder E, Sharma H, Wei LY, Bijwe J. Carbon fiber surfaces and composite interphases. Compos Sci Technol. 2014;102:35-50.

[45] Zhuang R-C, Doan TTL, Liu J-W, Zhang J, Gao S-L, Mäder E. Multi-functional multi-walled carbon nanotube-jute fibres and composites. Carbon. 2011;49:2683-92.

[46] Zhang R, Deng H, Valenca R, Jin J, Fu Q, Bilotti E, et al. Carbon nanotube polymer coatings for textile yarns with good strain sensing capability. Sensor Actuat A: Phys. 2012;179:83-91.

[47] Pommet M, Juntaro J, Heng JYY, Mantalaris A, Lee AF, Wilson K, et al. Surface Modification of Natural Fibers Using Bacteria: Depositing Bacterial Cellulose onto Natural Fibers To Create Hierarchical Fiber Reinforced Nanocomposites. Biomacromolecules. 2008;9:1643-51.

[48] Juntaro J, Pommet M, Kalinka G, Mantalaris A, Shaffer MSP, Bismarck A. Creating Hierarchical Structures in Renewable Composites by Attaching Bacterial Cellulose onto Sisal Fibers. Adv Mater. 2008;20:3122-6.

[49] Zhang G, Rasheva Z, Karger-Kocsis J, Burkhart T. Synergetic role of nanoparticles and micro-scale short carbon fibers on the mechanical profiles of epoxy resin. Exp Pol Lett. 2011;5:859-72.

[50] Lomov SV, Gorbatikh L, Kotanjac Ž, Koissin V, Houlle M, Rochez O, et al. Compressibility of carbon woven fabrics with carbon nanotubes/nanofibres grown on the fibres. Compos Sci Technol. 2011;71:315-25.

[51] Fang M, Zhang Z, Li J, Zhang H, Lu H, Yang Y. Constructing hierarchically structured interphases for strong and tough epoxy nanocomposites by amine-rich graphene surfaces. J Mater Chem. 2010;20:9635.

[52] Chen J, Zhao D, Jin X, Wang C, Wang D, Ge H. Modifying glass fibers with graphene oxide: Towards high-performance polymer composites. Compos Sci Technol. 2014;97:41-5.

[53] Bianco A, Cheng HM, Enoki T, Gogotsi Y, Hurt RH, Koratkar N, et al. All in the graphene family - A recommended nomenclature for two-dimensional carbon materials. Carbon. 2013;65:1-6.

[54] Rabotnov J, Perov B, Lutsan V, Ssorina T, Stepanitsov E. Carbon Fibers—Their Place in Modern Technology. Proc 2nd Carbon Fibre Conf, The Plastics Institute, London 1974. p. 65.

[55] Downs WB, Baker RTK. Novel carbon fiber-carbon filament structures. Carbon. 1991;29:1173-9.

[56] Thostenson ET, Li WZ, Wang DZ, Ren ZF, Chou TW. Carbon nanotube/carbon fiber hybrid multiscale composites. J Appl Phys. 2002;91:6034-7.

[57] Qian H, Greenhalgh ES, Shaffer MSP, Bismarck A. Carbon nanotube-based hierarchical composites: a review. J Mater Chem. 2010;20:4751-62.

[58] Wood CD, Palmeri MJ, Putz KW, Ho G, Barto R, Catherine Brinson L. Nanoscale structure and local mechanical properties of fiber-reinforced composites containing MWCNT-grafted hybrid glass fibers. Compos Sci Technol. 2012;72:1705-10.

[59] Rahaman A, Kar KK. Carbon nanomaterials grown on E-glass fibers and their application in composite. Compos Sci Technol. 2014;101:1-10.

[60] Sager RJ, Klein PJ, Lagoudas DC, Zhang Q, Liu J, Dai L, et al. Effect of carbon nanotubes on the interfacial shear strength of T650 carbon fiber in an epoxy matrix. Compos Sci Technol. 2009;69:898-904.

[61] Sharma SP, Lakkad SC. Effect of CNTs growth on carbon fibers on the tensile strength of CNTs grown carbon fiber-reinforced polymer matrix composites. Composites Part A. 2011;42:8-15.

[62] Zhang Q, Liu J, Sager R, Dai L, Baur J. Hierarchical composites of carbon nanotubes on carbon fiber: Influence of growth condition on fiber tensile properties. Compos Sci Technol. 2009;69:594-601.

[63] Naito K, Yang J-M, Xu Y, Kagawa Y. Enhancing the thermal conductivity of polyacrylonitrile- and pitch-based carbon fibers by grafting carbon nanotubes on them. Carbon. 2010;48:1849-57.

[64] Qian H, Bismarck A, Greenhalgh ES, Shaffer MSP. Carbon nanotube grafted carbon fibres: A study of wetting and fibre fragmentation. Composites Part A. 2010;41:1107-14.

[65] Lv P, Feng Y-y, Zhang P, Chen H-m, Zhao N, Feng W. Increasing the interfacial strength in carbon fiber/epoxy composites by controlling the orientation and length of carbon nanotubes grown on the fibers. Carbon. 2011;49:4665-73.

[66] Boura O, Diamanti EK, Grammatikos SA, Gournis D, Paipetis AS. Carbon nanotube growth on high modulus carbon fibres: Morphological and interfacial characterization. Surf Interface Anal. 2013;45:1372-81.

[67] An F, Lu C, Li Y, Guo J, Lu X, Lu H, et al. Preparation and characterization of carbon nanotube-hybridized carbon fiber to reinforce epoxy composite. Mater Des. 2012;33:197-202.

[68] Mathur RB, Chatterjee S, Singh BP. Growth of carbon nanotubes on carbon fibre substrates to produce hybrid/phenolic composites with improved mechanical properties. Compos Sci Technol. 2008;68:1608-15.

[69] Hung KH, Kuo WS, Ko TH, Tzeng SS, Yan CF. Processing and tensile characterization of composites composed of carbon nanotube-grown carbon fibers. Composites Part A. 2009;40:1299-304.

[70] Agnihotri P, Basu S, Kar KK. Effect of carbon nanotube length and density on the properties of carbon nanotube-coated carbon fiber/polyester composites. Carbon. 2011;49:3098-106.

[71] An F, Lu C, Guo J, He S, Lu H, Yang Y. Preparation of vertically aligned carbon nanotube arrays grown onto carbon fiber fabric and evaluating its wettability on effect of composite. Appl Surf Sci. 2011;258:1069-76.

[72] Tehrani M, Safdari M, Boroujeni AY, Razavi Z, Case SW, Dahmen K, et al. Hybrid carbon fiber/carbon nanotube composites for structural damping applications. Nanotechnology. 2013;24:155704.

[73] Veedu VP, Cao A, Li X, Ma K, Soldano C, Kar S, et al. Multifunctional composites using reinforced laminae with carbon-nanotube forests. Nat Mater. 2006;5:457-62.

[74] Zhang Q, Qian W, Xiang R, Yang Z, Luo G, Wang Y, et al. In situ growth of carbon nanotubes on inorganic fibers with different surface properties. Mater Chem Phys. 2008;107:317-21.

[75] Garcia EJ, Wardle BL, John Hart A, Yamamoto N. Fabrication and multifunctional properties of a hybrid laminate with aligned carbon nanotubes grown In Situ. Compos Sci Technol. 2008;68:2034-41.

[76] Jin L, Zhang L, Su D, Li C. Direct Growth of Aligned Carbon Nanotubes on Quartz Fibers for Structural Epoxy Composites. Ind Eng Chem Res. 2012;51:4927-33.

[77] Qian H, Bismarck A, Greenhalgh ES, Shaffer MSP. Carbon nanotube grafted silica fibres: Characterising the interface at the single fibre level. Compos Sci Technol. 2010;70:393-9.

[78] Ehlert GJ, Sodano HA. Zinc oxide nanowire interphase for enhanced interfacial strength in lightweight polymer fiber composites. ACS Appl Mater Interfaces. 2009;1:1827-33.

[79] Ehlert GJ, Galan U, Sodano HA. Role of surface chemistry in adhesion between ZnO nanowires and carbon fibers in hybrid composites. ACS Appl Mater Interfaces. 2013;5:635-45.

[80] Lin Y, Ehlert G, Sodano HA. Increased Interface Strength in Carbon Fiber Composites through a ZnO Nanowire Interphase. Adv Funct Mater. 2009;19:2654-60.

[81] Feller JF, Grohens Y. Coupling ability of silane grafted poly(propene) at glass fibers/poly(propene) interface. Composites Part A. 2004;35:1-10.

[82] Karger-Kocsis J, Czigány T. Effects of interphase on the fracture and failure behavior of knitted fabric reinforced composites produced from commingled GF/PP yarn. Composites Part A. 1998;29:1319-30.

[83] Bismarck A, Pfaffernoschke M, Springer J, Schulz E. Polystyrene-grafted Carbon Fibers: Surface Properties and Adhesion to Polystyrene. J Thermoplast Compos Mater. 2005;18:307-31.

[84] Trey SM, Kristofer Gamstedt E, Mäder E, Jönsson S, Johansson M. Glass fiber reinforced high glass transition temperature thiol–ene networks. Composites Part A. 2011;42:1800-8.

[85] Kuttner C, Tebbe M, Schlaad H, Burgert I, Fery A. Photochemical synthesis of polymeric fiber coatings and their embedding in matrix material: morphology and nanomechanical properties at the fiber-matrix interface. ACS Appl Mater Interfaces. 2012;4:3484-92.

[86] Kuttner C, Hanisch A, Schmalz H, Eder M, Schlaad H, Burgert I, et al. Influence of the polymeric interphase design on the interfacial properties of (fiber-reinforced) composites. ACS Appl Mater Interfaces. 2013;5:2469-78.

[87] Nguyen FN, Saks AM, Berg JC. Use of polyethyleneimine dendrimer as a novel graded-modulus interphase material in polymeric composites. J Adhes Sci Technol. 2007;21:1375-93.

[88] Karger-Kocsis J, Fröhlich J, Gryshchuk O, Kautz H, Frey H, Mülhaupt R. Synthesis of reactive hyperbranched and star-like polyethers and their use for toughening of vinylester–urethane hybrid resins. Polymer. 2004;45:1185-95.

[89] Oréfice RL, Clark AE, Brennan AB. Bioactive composites with designed interphases based on hyperbranched macromers. J Appl Polym Sci. 2006;99:1153-66.

[90] Deng SH, Zhou XD, Zhu MQ, Fan CJ, Lin QF. Interfacial toughening and consequent improvement in fracture toughness of carbon fiber reinforced epoxy resin composites: induced by diblock copolymers. Exp Pol Lett. 2013;7:925-35.

[91] Li R, Ye L, Mai Y-W. Application of plasma technologies in fibre-reinforced polymer composites: a review of recent developments. Composites Part A. 1997;28:73-86.

[92] Donnet JB, Brendle M, Dhami TL, Bahl OP. Plasma treatment effect on the surface energy of carbon and carbon fibers. Carbon. 1986;24:757-70.

[93] Marks DJ, Jones FR. Plasma polymerised coatings for engineered interfaces for enhanced composite performance. Composites Part A. 2002;33:1293-302.

[94] Cech V. Plasma-polymerized organosilicones as engineered interlayers in glass fiber/polyester composites. Compos Interfaces. 2007;14:321-34.

[95] Cech V, Palesch E, Lukes J. The glass fiber–polymer matrix interface/interphase characterized by nanoscale imaging techniques. Compos Sci Technol. 2013;83:22-6.

[96] Cech V, Knob A, Hosein HA, Babik A, Lepcio P, Ondreas F, et al. Enhanced interfacial adhesion of glass fibers by tetravinylsilane plasma modification. Composites Part A. 2014;58:84-9.

[97] Photjanataree P, Liu Z, Jones FR. The Role of a Nanoscale Interphase from Plasma Polymers on the Micromechanics of Fiber Composites. Macromol Mater Eng. 2012;297:523-31.

[98] Liu Z, Zhao F, Jones FR. Optimising the interfacial response of glass fibre composites with a functional nanoscale plasma polymer coating. Compos Sci Technol. 2008;68:3161-70.

[99] Vautard F, Fioux P, Vidal L, Siffer F, Roucoules V, Schultz J, et al. Use of plasma polymerization to improve adhesion strength in carbon fiber composites cured by electron beam. ACS Appl Mater Interfaces. 2014;6:1662-74.

[100] Holmes G, Feresenbet E, Raghavan D. Using self-assembled monolayer technology to probe the mechanical response of the fiber interphase-matrix interphase interface. Compos Interfaces. 2003;10:515-46.

[101] He J, Huang Y, Liu L, Cao H. Controlled interface between carbon fiber and epoxy by molecular self-assembly method. Mater Chem Phys. 2006;99:388-93.

[102] Puzari A, Borah JP. Ionic self-assembly and hierarchies of polymeric structures generating nanoscale architecture: opportunities ahead from industrial perspective. Rev Adv Mater Sci. 2013;34:88-106.

[103] Liu K, Jin M, La R, Zhang J, Wang T, Zhang X. Transcrystallization of isotactic polypropylene containing a self-assembled nucleating agent nanonetwork. Mater Lett. 2014;125:209-12.

[104] Karger-Kocsis J, Bárány T. Single-polymer composites (SPCs): Status and future trends. Compos Sci Technol. 2014;92:77-94.

[105] Drzal LT. The interphase in epoxy composites. Adv Polym Sci. 1986;75:1-32.

[106] Carlier V, Sclavons M, Jonas AM, Jérôme R, Legras R. Probing Thermoplastic Matrix−Carbon Fiber Interphases. 1. Preferential Segregation of Low Molar Mass Chains to the Interface. Macromolecules. 2001;34:3725-9.

[107] Hoecker F, Karger-Kocsis J. Effects of crystallinity and supermolecular formations on the interfacial shear strength and adhesion in GF/PP composites. Polym Bull. 1993;31:707-14.

[108] Hoecker F, KargerKocsis J. On the effects of processing conditions and interphase of modification on the fiber/matrix load transfer in single fiber polypropylene composites. J Adhes. 1995;52:81-100.

[109] Graupner N, Rößler J, Ziegmann G, Müssig J. Fibre/matrix adhesion of cellulose fibres in PLA, PP and MAPP: A critical review of pull-out test, microbond test and single fibre fragmentation test results. Composites Part A. 2014;63:133-48.

[110] Gamstedt EK, Skrifvars M, Jacobsen TK, Pyrz R. Synthesis of unsaturated polyesters for improved interfacial strength in carbon fibre composites. Composites Part A. 2002;33:1239-52.

[111] Zhang J, Deng S, Wang Y, Ye L, Zhou L, Zhang Z. Effect of nanoparticles on interfacial properties of carbon fibre–epoxy composites. Composites Part A. 2013;55:35-44.

[112] Hossain MK, Chowdhury MMR, Salam MB, Malone J, Hosur MV, Jeelani S, et al. Improved thermomechanical properties of carbon fiber reinforced epoxy composite using amino functionalized XDCNT. J Appl Polym Sci. 2014:n/a-n/a.

[113] Sadeghian R, Gangireddy S, Minaie B, Hsiao K-T. Manufacturing carbon nanofibers toughened polyester/glass fiber composites using vacuum assisted resin transfer molding for enhancing the mode-I delamination resistance. Composites Part A. 2006;37:1787-95.

[114] Dorigato A, Morandi S, Pegoretti A. Effect of nanoclay addition on the fiber/matrix adhesion in epoxy/glass composites. J Compos Mater. 2012;46:1439-51.

[115] Pedrazzoli D, Pegoretti A, Kalaitzidou K. Synergistic effect of exfoliated graphite nanoplatelets and short glass fiber on the mechanical and interfacial properties of epoxy composites. Compos Sci Technol. 2014;98:15-21.

[116] Pedrazzoli D, Pegoretti A. Silica nanoparticles as coupling agents for polypropylene/glass composites. Compos Sci Technol. 2013;76:77-83.

[117] Arao Y, Yumitori S, Suzuki H, Tanaka T, Tanaka K, Katayama T. Mechanical properties of injection-molded carbon fiber/polypropylene composites hybridized with nanofillers. Composites Part A. 2013;55:19-26.

[118] Vlasveld DPN, Parlevliet PP, Bersee HEN, Picken SJ. Fibre–matrix adhesion in glass-fibre reinforced polyamide-6 silicate nanocomposites. Composites Part A. 2005;36:1-11.

[119] Daud W, Bersee HEN, Picken SJ, Beukers A. Layered silicates nanocomposite matrix for improved fiber reinforced composites properties. Compos Sci Technol. 2009;69:2285-92.

[120] Isitman NA, Aykol M, Kaynak C. Nanoclay assisted strengthening of the fiber/matrix interface in functionally filled polyamide 6 composites. Compos Struct. 2010;92:2181-6.

[121] Pedrazzoli D, Pegoretti A. Expanded graphite nanoplatelets as coupling agents in glass fiber reinforced polypropylene composites. Composites Part A. 2014;66:25-34.

[122] Cercle C, Favis BD. Generalizing interfacial modification in polymer blends. Polymer. 2012;53:4338-43.

[123] Gryshchuk O, Karger-Kocsis J. Influence of the type of epoxy hardener on the structure and properties of interpenetrated vinyl ester/epoxy resins. J Polym Sci, Part A: Polym Chem. 2004;42:5471-81.

[124] Atkins AG. Intermittent bonding for high toughness/ high strength composites. J Mater Sci. 1975;10:819-32.

[125] Szabó JS, Karger-Kocsis J, Gryshchuk O, Czigány T. Effect of fibre surface treatment on the mechanical response of ceramic fibre mat-reinforced interpenetrating vinylester/epoxy resins. Compos Sci Technol. 2004;64:1717-23.

[126] Czigány T, Pölöskei K, Karger-Kocsis J. Fracture and failure behavior of basalt fiber mat-reinforced vinylester/epoxy hybrid resins as a function of resin composition and fiber surface treatment. J Mater Sci. 2005;40:5609-18.

[127] Szabó J, Romhány G, Czigány T, Karger-Kocsis J. Interpenetrating vinylester/epoxy resins reinforced by flax fiber mat. Adv Compos Letter. 2003;12:115-20.

[128] Yuan YC, Yin T, Rong MZ, Zhang MQ. Self healing in polymers and polymer composites. Concepts, realization and outlook: A review. Exp Pol Lett. 2008;2:238-50.

[129] Karger-Kocsis J, Kéki S. Biodegradable polyester-based shape memory polymers: Concepts of (supra)molecular architecturing. Exp Pol Lett. 2014;8:397-412.

[130] Chou T-W, Gao L, Thostenson ET, Zhang Z, Byun J-H. An assessment of the science and technology of carbon nanotube-based fibers and composites. Compos Sci Technol. 2010;70:1-19.

[131] Luo S, Obitayo W, Liu T. SWCNT-thin-film-enabled fiber sensors for lifelong structural health monitoring of polymeric composites - From manufacturing to utilization to failure. Carbon. 2014;76:321-9.

[132] Harsch M, Karger-Kocsis J, Herzog F. Influence of Cure Regime on the Strain Development in an Epoxy Resin as Monitored by a Fiber Bragg Grating Sensor. Macromol Mater Eng. 2007;292:474-83.

[133] Nielsen MW, Schmidt JW, Hogh JH, Waldbjorn JP, Hattel JH, Andersen TL, et al. Life cycle strain monitoring in glass fibre reinforced polymer laminates using embedded fibre Bragg grating sensors from manufacturing to failure. J Compos Mater. 2013;48:365-81.

[134] Hong J, Pan Z, Yao M, Zhang X. Preparation and properties of continuously produced conductive UHMWPE/PANI composite yarns based on in-situ polymerization. Synthetic Metals. 2014;193:117-24.

[135] Merlini C, Barra GMO, Schmitz DP, Ramoa SDAS, Silveira A, Araujo TM, et al. Polyaniline-coated coconut fibers: Structure, properties and their use as conductive additives in matrix of polyurethane derived from castor oil. Polym Test. 2014;38:18-25.

[136] Lin Y, Sodano HA. Concept and model of a piezoelectric structural fiber for multifunctional composites. Compos Sci Technol. 2008;68:1911-8.

[137] Trask RS, Williams GJ, Bond IP. Bioinspired self-healing of advanced composite structures using hollow glass fibres. J Royal Soc Interf. 2007;4:363-71.

[138] Fischer H. Self-repairing material systems—a dream or a reality? Nat Sci. 2010;02:873-901.

[139] Blaiszik BJ, Kramer SLB, Olugebefola SC, Moore JS, Sottos NR, White SR. Self-Healing Polymers and Composites. Annual Rev Mat Res. 2010;40:179-211.

[140] Syrett JA, Becer CR, Haddleton DM. Self-healing and self-mendable polymers. Polym Chem. 2010;1:978.

[141] Kling S, Czigány T. Damage detection and self-repair in hollow glass fiber fabric-reinforced epoxy composites via fiber filling. Compos Sci Technol. 2014;99:82-8.

[142] Sundaresan VB, Morgan A, Castellucci M. Self-Healing of Ionomeric Polymers with Carbon Fibers from Medium-Velocity Impact and Resistive Heating. Smart Mat Res. 2013;2013:ID 271546, 12 pages.

[143] Chen X, Dam MA, Ono K, Mal A, Shen H, Nutt SR, et al. A Thermally Re-mendable Cross-Linked Polymeric Material. Science. 2002;295:1698-702.

[144] Chen X, Wudl F, Mal AK, Shen H, Nutt SR. New Thermally Remendable Highly Cross-Linked Polymeric Materials. Macromolecules. 2003;36:1802-7.

[145] Peterson AM, Jensen RE, Palmese GR. Thermoreversible and remendable glass–polymer interface for fiber-reinforced composites. Compos Sci Technol. 2011;71:586-92.

[146] Peterson AM, Jensen RE, Palmese GR. Kinetic considerations for strength recovery at the fiber-matrix interface based on the Diels-Alder reaction. ACS Appl Mater Interfaces. 2013;5:815-21.

[147] Peterson AM, Jensen RE, Palmese GR. Room-temperature healing of a thermosetting polymer using the Diels-Alder reaction. ACS Appl Mater Interfaces. 2010;2:1141-9.

[148] Zhang W, Duchet J, Gerards J. Self-healable interfaces based on thermo-reversible Diels–Alder reactions in carbon fiber reinforced composites. J Colloid Interface Sci. 2014;430:61-8.

[149] Ying H, Zhang Y, Cheng J. Dynamic urea bond for the design of reversible and self-healing polymers. Nat Commun. 2014;5:3218.

[150] Chandra R, Singh SP, Gupta K. A study of damping in fiber-reinforced composites. J Sound Vibr. 2003;262:475-96.

[151] Jesson DA, Watts JF. The Interface and Interphase in Polymer Matrix Composites: Effect on Mechanical Properties and Methods for Identification. Polym Rev. 2012;52:321-54.

[152] Kafi A, Huson M, Creighton C, Khoo J, Mazzola L, Gengenbach T, et al. Effect of surface functionality of PAN-based carbon fibres on the mechanical performance of carbon/epoxy composites. Compos Sci Technol. 2014;94:89-95.

[153] Lenhart JL, van Zanten JH, Dunkers JP, Zimba CG, James CA, Pollack SK, et al. Immobilizing a Fluorescent Dye Offers Potential to Investigate the Glass/Resin Interface. J Colloid Interface Sci. 2000;221:75-86.

[154] Tillman MS, Hayes BS, Seferis JC. Analysis of polymeric composite interphase regions with thermal atomic force microscopy. J Appl Polym Sci. 2001;80:1643-9.

[155] Hodzic A, Kalyanasundaram S, Kim JK, Lowe AE, Stachurski ZH. Application of nano-indentation, nano-scratch and single fibre tests in investigation of interphases in composite materials. Micron. 2001;32:765-75.

[156] Lee S-H, Wang S, Pharr GM, Xu H. Evaluation of interphase properties in a cellulose fiber-reinforced polypropylene composite by nanoindentation and finite element analysis. Composites Part A. 2007;38:1517-24.

[157] Sockalingam S, Nilakantan G. Fiber-Matrix Interface Characterization through the Microbond Test. Int J Aeron Space Sci. 2012;13:282-95.

[158] Díez-Pascual AM, Gómez-Fatou MA, Ania F, Flores A. Nanoindentation Assessment of the Interphase in Carbon Nanotube-Based Hierarchical Composites. J Phys Chem C. 2012;116:24193-200.

[159] Li Y, Li M, Gu Y, Zhang Z, Guan P. Investigation of the nanoscale mechanical properties of carbon fiber/epoxy resin interphase. I. analysis of fiber-stiffening effect during the nanoindentation process based on numerical simulation. Polym Compos. 2012;33:1387-94.

[160] Qian H, Kalinka G, Chan KLA, Kazarian SG, Greenhalgh ES, Bismarck A, et al. Mapping local microstructure and mechanical performance around carbon nanotube grafted silica fibres: Methodologies for hierarchical composites. Nanoscale. 2011;3:4759-67.

[161] Qian H, Bismarck A, Greenhalgh ES, Kalinka G, Shaffer MSP. Hierarchical composites reinforced with carbon nanotube grafted fibers: The potential assessed at the single fiber level. Chem Mater. 2008;20:1862-9.

[162] Yang F, Pitchumani R. Processing-interphase-property relationship in fiber-reinforced thermosetting-matrix composites. Polym Compos. 2005;26:193-208.

[163] Li M, Gu Y-Z, Liu H, Li Y-X, Wang S-K, Wu Q, et al. Investigation the interphase formation process of carbon fiber/epoxy composites using a multiscale simulation method. Compos Sci Technol. 2013;86:117-21.

[164] Yang L, He X, Mei L, Tong L, Wang R, Li Y. Interfacial shear behavior of 3D composites reinforced with CNT-grafted carbon fibers. Composites Part A. 2012;43:1410-8.

[165] Romanov VS, Lomov SV, Verpoest I, Gorbatikh L. Can carbon nanotubes grown on fibers fundamentally change stress distribution in a composite? Composites Part A. 2014;63:32-4.

[166] Javaid A, Ho KKC, Bismarck A, Shaffer MSP, Steinke JHG, Greenhalgh ES. Multifunctional structural supercapacitors for electrical energy storage applications. J Compos Mater. 2014;48:1409-16.

[167] Shirshova N, Qian H, Shaffer MSP, Steinke JHG, Greenhalgh ES, Curtis PT, et al. Structural composite supercapacitors. Composites Part A. 2013;46:96-107.

[168] Ding X, Heiden PA. Recent Developments in Molecularly Imprinted Nanoparticles by Surface Imprinting Techniques. Macromol Mater Eng. 2014;299:268-82.

[169] Ruan F, Bao L. Mechanical Enhancement of UHMWPE Fibers by Coating with Carbon Nanoparticles. Fib and Pol. 2014;15:723-8.

Table 1

Table 1: Interphases produced by nanofiller containing sizing/coating on inorganic fibers, their characteristics and effects

Fiber type	**Nanofiller type, amount in sizing medium**	**Sizing/Coating formulation**	**Matrix** **Composites**	**Sizing/Coating technique**	**Interphase**		**Sensing**	**Comments**	**Ref.**
					Testing methods	**Effects**			
GF (E-glass)	SWCNT 0.5 wt% (solution)	Low MW EVA, PMMA, Poly(styrene-methyl-methacrylate)	PP Microcomposites	Solution coating	Single fiber fragmentation test	Variation in critical fiber length (l_c)	Strain sensor effect calibrated by Raman spectroscopy	Strain sensing proved. Adhesion improvement also due to SWCNT	[24]
GF (alkali resistant, ARG)	MWCNT with –COOH functionality 0.5 wt% (dispersion)	Aqueous dispersions with surfactants, sonicated MWCNT/surfactant = 2/3	EP (amine) Microcomposites	Dip coating	FE-ESEM, EFM, nanoindentation	Interphase region, 20-500 nm	Semiconductive interphase resulting from MWCNT network; piezoresistivity checked for sensing. The electrical conductivity depended also on temperature and humidity	First report on non GF-based composite. Conductive network capable to detect the T_g in the interphase.	[25]
GF (E-glass)	MWCNT 0.5 wt% (dispersion)	Aqueous EP-compatible phenoxy sizing with MWCNT applied for the as-received GF sizing	EP (amine) UD composites from prepregs	Dip coating	SEM TMA	T_g increase	-	Crack initiation energy (G_{Ic}) slightly increased, while propagation energy decreased in mode I interlaminar fracture test. Effect of CNT in the bulk matrix higher than in the sizing	[26]
GF (ARG)	MWCNT with –COOH functionality, 0.5 wt% (dispersion)	Aqueous dispersion with non-ionic surfactant and epoxy functional silane (coupling agent), sonicated	EP (Amine) Microcomposites	Dip coating, electrophoretic deposition (EPD). Sizing amount: 1-2 wt%	Single fiber tensile test, single fiber fragmentation test	l_c was smaller (IFSS higher) for EPD than for dip coated fibers	Electrical resistance of single fiber composite measured under tensile loading	EPD coating is more beneficial than dip coating and yields a more homogenous interphase. Changes in the electrical resistivity of the interphase assigned	[27]

								to elastic and plastic deformations of the interphase	
GF (ECR)	F-CNT, SWCNT 0.021 wt%	Ethanol dispersion (0.5 mg/mL) sonicated	Vinyl ester (VE) UD composites	Spraying	SEM, TEM	Impact resistance (transverse to fiber direction) improved by 15%.	-	F-CNT out performed SWCNT having more defects and functional groups at the side-wall than SWCNT. This resulted in better dispersion and better interphase reinforcement	[28]
GF (ARG)	MWCNT with –COOH functionality, 0.05 wt% (dispersion)	Aqueous dispersion with non-ionic surfactant	EP (amine) Single and triple fiber microcomposites	EPD	-	-	Change in electrical resistance under tensile load measured, also as a function of temperature	Interphase probed as strain sensor and switch	[29]
GF fabric (E-glass)	MWCNT, also ozone treated and subsequently functionalized by polyethyleneimine, 1g/L (dispersion)	Dispersion, also containing epoxysilane	EP (amine) fabric Reinforced composite through VARTM	EPD	In-plane shear tests	In-plane shear strength doubled with MWCNT at 14 vol%	Change in the electrical resistivity as a function of MWCNT content and shear loading measured	EPD adapted for GF fabrics. Polyethyleneimine, linking the epoxy sized GF and the brittle EP matrix proved to be the right additive	[30]
GF (fabric)	SWCNT, MWCNT with –COOH functionality	Aqueous dispersion	EP (amine) Fabric-reinforced composites by VARTM	EPD	SEM, ILSS	ILSS improved by 27% due to 0.25% MWCNT in the composite	In-plane and out-of-plane electrical conductivity measured	Electrophoresis is efficient to produce “multiscale hybrid composites” with enhanced ILSS and out-of-plane (transverse) mechanical and electrical properties	[31]
CF (unsized then	MWCNT with –COOH functionality	Solvent dispersion, 100mg/L (dispersion)	-	Chemichal grafting	SEM, TEM, FTIR	-	-	Chemical reactions (ester, anhydride and amide	[32]

oxidized in air)				Dispersion deposition in several steps				formation) supposed between the functional groups of MWCNT and oxidized CF, but not proved	
CF	Clay	Aqueous ammonia solution	PEI Hand lay-up of prepregs and hot pressing	Immersion	Single fiber pull-out, SEM, XPS	ILSS and flexural strength increased	-	Improvements in ILSS and flexural strength attributed to surface roughening of CF (mechanical interlocking)	[33]
CF (woven fabric)	Carbon nanofiber (CNF) also with –COOH and $–NH_2$ functionalities	Aqueous dispersion	EP (amine) Composites by VARTM	EPD	Optical Microscopy (OM), SEM	ILSS enhanced	-	"Multiscale-reinforced" fabrics were used to produce "hierarchical composites". Panels with amine functionalized CNF showed the highest property improvements (ILSS=12%, compressive strength = 13%) compared to the composites without CNF.	[34]
CF (woven fabric)	CNF with $–NH_2$ functionality	Aqueous dispersion after sonication	-	EPD, two step EPD with potential change	OM, SEM	-	-	CNFs wrapped around the CF. Covalent bonding toward EP surmized through the $–NH_2$ of CNF. Enhancement in ILSS, compressive stress and delamination resistance predicted	[35]
CF (unsized, sized)	CNF, with –COOH functionality	Aqueous dispersion	EP (amine) Microcomposite	EPD	FE-SEM, fragmentation	Changes in IFSS detected.	-	Best IFSS achieved with sized CF coated with	[36]

						Single fiber tensile tests performed and analyzed by the Weibull approach		carboxyl functionalized CNF. Unsizing of CF reduced IFSS which was enhanced by CNF coating	
CF (woven fabric)	MWCNT, also with carboxyl and acryl functionalities	Dispersion in matrix resin <1phr nanofiller (phr – part per hundred parts resin)	VE (bisphenol A-based) Hand lay-up and hot pressing	Dipping	TEM, XPS, SEM	Flexural strength, modulus and T_g increased	-	Improvements in the mechanical properties according to ranking MWCNT<carboxyl modified MWCNT<acryl grafted MWCNT. The acryl functional groups of the latter participated in the radical crosslinking. Properties improvements also with increasing MWCNT content.	[37]
CF (unsized)	MWCNT with carboxyl functionality	Aqueous dispersion with surfactant	EP (amine) UD laminates by VARTM	EPD continuous line	SEM, ILSS, single fiber push out	ILSS improved by 40%	-	EPD conditions on the MWCNT deposition studied. Improvement in ILSS did not correlate with MWCNT amount deposited (<1 wt%). According to single fiber push out (monotonic, cylic) the fiber/matrix bonding was not affected	[38]
CF (low and high modulus)	SWCNT with carboxyl functionality	Ethanol dispersion (0.1 wt% dispersion) + silane solution	EP (amine)	Immersion	Single fiber composite, SEM, Raman spectroscopy	IFSS is markedly improved (>50%)	-	IFSS determined by calibration of the Raman shift of the 2D band in the	[39]

								model composite. IFSS improvement due to enhanced interfacial surface (SWCNT effect) and chemical bonding of the latter via –COOH to the epoxy groups of EP	
CF (unsized)	MWCNT also with amine functionality	PAEK containing sizing MWCNT content: 1wt%	PAEK Microcomposites	Impregnation of CF tow	SEM, BET surface, wetting microbond test	IFSS enhanced by 60%	-	BET surface area of the MWCNT containing sizing was six times higher than without MWCNT. Presence of MWCNT improved both wetting of CF and IFSS	[40]
CF (unsized)	Graphene oxide (GO) also silanized	Aqueous dispersion, sonicated (3mg/ml, dispersion)	EP (anhydride) UD composite via RTM Microcomposites	Dipping (carbon nanoparticle content <1 wt%)	OM, AFM, XPS, SEM, FTIR microbond test	IFSS enhanced by <60%	-	A gradient interphase concluded. Its stiffness was lower than CF but higher than EP. The hierarchical composite with 0.5 wt% silanized GO showed the highest improvement (IFSS = 60%, ILSS = 19%, flexural strength, modulus and tensile strength by ca. 15% each)	[41]
GF (E-glass)	Capsules containing reactive EP and solvent	Aqueous dispersion of UF-walled capsules	EP (amine) Microcomposites	Dip coating	Repeated microbond tests after full debonding	Healing efficiency of the IFSS	-	Almost complete autonomic healing found. The mean capsule size was at about 2 and 0.6 µm, respectively, in the series	[42]
CF	Capsules	Aqueous dispersion	EP (amine)	Dip coating	Repeated	Healing	-	Autonomic healing	[43]

	containing reactive EP and solvent	UF-walled capsules combined with binder in different ways	Microcomposites		microbond tests after full debonding	efficiency of the IFSS		demonstrated. The resin/solvent combination yielded up to 80% recovery of the IFSS as a function capsule coverage and binder method	

Table 2

Table 2: Interphases produced by nanofiller containing sizing/coating on organic fibers, their characteristics and effects

Fiber type	**Nanofiller type, amount in sizing medium**	**Sizing/Coating formulation**	**Matrix** **Composites**	**Sizing/Coating technique**	**Interphase**		**Sensing**	**Comments**	**Ref.**
					Testing methods	**Effects**			
NF (jute) Single fiber fabric	MWCNT with carboxyl functionality	Aqueous dispersion with non-ionic surfactant	EP (amine) Microcomposites, Fabric-reinforced composite via VAP	Dip coating	FE-SEM, EFM, DMA	-	Sensing behavior of the MWCNT coated jute fibers for temperature, humidity and stress/strain response checked	Interconnected MWCNT network in the interphase proved for multifunctional sensing. Single MWCNT coated jute fiber exhibited high humidity sensitivity. Controllable anisotropic dielectric properties noticed for MWCNT coated fabric reinforced composite	[45]
TPU (yarn)	MWCNT with amine functionality	MWCNT dispersion in solvent, sonicated and "thickened" by TPU solution	-	Roll coating	SEM	-	Relative electrical resistance as a function of strain, applied also cyclically, measured	The elastic TPU yarn showed good strain sensing ability at an equivalent MWCNT concentration of as low as 0.015 wt%.	[46]
NF (hemp, sisal)	Nanocellulose, cellulose nanofibrils	Cellulose producing bacteria	PLLA, CAB	Bacterial deposition via static culture, fermentation	OM, SEM, XPS, single fiber pull-out test	IFSS improvement depended on NF type	-	"Green" method to modify the surface of NFs presented. Adhesion of nanocellulose (5-6%) to NF is via H-bonding. NF type and fermentation process conditions should be properly selected. Change in the surface energy of the modified NF with "hierarchical structure" may serve for improved wetting.	[47, 48]

Table 3

Table 3: Carbon nanofiber grafting on CF: preparation and interphase effects. Notes: CF is unsized and PAN-based when not indicated in another way

Hierarchical fiber **CF/graft**	**Deposition**		**Matrix** **Composites**	**Interphase**		**Comments**	**Ref.**
	Technique	**Conditions**		**Testing methods**	**Effects**		
CF/CNT	thermal CVD	Catalyst by magnetron sputtering followed by reduction to particles at T=660°C. CNT growth and 660°C for ½ h using C_2H_2	EP (amine) Microcomposites	SEM, BET, fragmentation	IFSS improvement	15% improvement in IFSS. Both catalyst deposition and CVD treatment of CF alone reduced the IFSS by 30%.	[56]
CF/MWCNT (aligned, random)	CVD	Aligned: pretreatment of CF in $MgSO_4$ in alcohol followed by exposure to Fe-phthalocyanine powder at 900°C for 15 min in Ar/H_2 Random: pretreatment of CF in $MgSO_4$ in alcohol followed by exposure to xylene and ferrocene catalysts at 800°C for 30 min in Ar/H_2	EP (amine) Microcomposites	SEM, single fiber tensile test, fragmentation	IFSS improvement	Nanotube deposition markedly reduced the tensile strength (30-37%), modulus of CF. Deterioration attributed to flaws due to thermal degradation/surface oxidation. MWCNT coated CF yielded higher IFSS than the unsized CF. Randomly grown MWCNT outperformed the aligned one.	[60]
CF/CNT, CNF	thermal CVD	Ni-based catalyst by dipping. Catalyst reduction at T=400°C. CNT production at 700°C using C_2H_2 for ½ hours	EP (amine) Tow impregnation	SEM, TEM, Raman	Improvement in tensile strength	Improvement in tensile strength due to CNT coating confirmed by fractography	[61]
CF/MWCNT (CF also sized)	thermal CVD	Carbon source/catalyst flow rate and CNT growth temperature (T=700-800°C) and time varied	-	SEM/TGA single fiber tensile tests	No significant reduction in tensile properties	Effects of CF sizing and CVD parameters studied	[62]
CF (PAN-based, pitch based)/CNT	thermal CVD	Catalyst: ferrocene; CNT growth: 700-750°C for 900s	-	SEM, TEM, X-ray, Raman thermal conductivity	Thermal conductivity increased	Thermal conductivity improvement assigned to a 3D CNT network	[63]
CF (oxidized)/CNT	thermal CVD	Fe-catalyst by immersion, carbon source: C_2H_2; CNT growth: 750°C, 1h	PMMA (from solution) Microcomposites	SEM, BET contact angle single fiber tensile, fragmentation	IFSS increased from 12.5 MPa (as received CF) to 13.1 MPa (oxidized) to 15.8 MPa (CNT-grafted)	CNT grafting increased the BET surface area and decreased the CF tensile strength. This degradation attributed to the dissolution of iron particles into the CF surface.	[64]

CF/MWCNT	Injection CVD	Feeding solution i.e. catalyst (ferrocene) and hydrocarbon (xylene,ethanol, ethylene diamine) injected to the furnace at T=850°C; CNT growth time: <2h. To produce aligned MWCNT, surface of CF coated with SiO_2 layer	EP (amine) Microcomposites	XPS, SEM, BET, contact angle, single fiber tensile test, fragmentation	IFSS improvement	CNTs with different orientation and length (up to 100μm) produced. Specific surface area enhanced by two orders of magnitude. IFSS dependence on MWCNT alignment and length, it was improved up to 175%. The tensile strength of the CF decreased with increasing growth time up to 33%.	[65]
CF/CNT	thermal CVD	Fe-Co bimetallic catalyst by wet impregnation. CNT growth at 750°C using Ar/C_2H_2 for ½ hr	EP (amine) Microcomposites	SEM, Raman, TGA, fragmentation supported by AE	IFSS improvement	IFSS enhanced from the 28 MPa (pristine) to 32 MPa (CNT grafted)	[66]
CF/CNT	aerosol-assisted CVD	Catalyst precursor: ferrocene; carbon source: C_2H_2; carrier gas: H_2/N_2. Aerosol from ferrocene/acetone mixture at T=700°C. CNT growth at 750°C for ½ hour	EP (anhydride) Microcomposites	SEM, BET, single fiber tensile and microbond test	IFSS doubled	CNT diameter at about 60 nm. CNT grafting caused a threefold increase in BET surface area. Moderate decrease (~10%) in CF tensile strength	[67]
CF substrates (tow, fabric, felt)/CN	injection CVD	Iron catalyst from ferrocene. Carbon source toluene. CNT growth at 750°C	Phenolic resin Compression molding	SEM, TEM, flexural tests	-	The flexural properties (strength, modulus) first decreased and above 5 wt% CNT content of the total composite weight increased monotonously.	[68]
CF fabric/CNT	thermal CVD	Ni catalyst: coating with Ni-nitrate solution followed by reduction to Ni powder (100nm) in the furnace. CNT growth at 700°C for 1h using CH_4.	EP Single fiber bundle impregnated	SEM, fiber bundle tensile test	-	Tensile strength and modulus increased. Analytical model proposed which considers the enlarged surface area	[69]
CF woven fabrics/CNT, CNF	thermal CVD	Catalysts: Ni, Fe-Co (immersion, into the catalyst precursor solutions followed by reduction (or without) CNT/CNF growth: 600 or 750°C for different times. Carbon source: C_2H_2	-	SEM, TEM, compression test	-	Compressibility of CNF/CNT-grafted woven fabrics of different structures studied. The fiber volume fraction of the compacted CNF/CNT-grafted textiles was markedly reduced compared to the ungrafted ones. This may affect the production of advanced composites requiring high volume fraction reinforcements.	[50]
CF fabric/CNT	thermal CVD	Catalyst: fabric coating in an acidic nickel sulphate containing bath. Reduction to Ni-P alloy at 500°C. CNT	UP Microcomposites	SEM, DMA single fiber pull out	IFSS improvement	Effect of CNT growth time studied and an optimum value, based on IFSS and DMA data, concluded.	[70]

		growth: 550°C using C_2H_2 carbon source					
CF fabric/CNT	thermal CVD	CF Fabric was first coated by Al_2O_3. Catalyst precursor ($Fe(NO_3)_4$) in acetone. CNT growth at 750°C using C_2H_2 for ½ hour	EP (anhydride) Microcomposites	SEM, BET, contact angle, surface energy, single fiber tensile and microbond tests	IFSS doubled	Moderate decrease (10%) in the tensile strength of CF after CNT grafting. The alumina "buffer layer" had protective role and supported the normal alignment of CNTs. Wetting was markedly improved	[71]
CF fabric/MWCNT	Graphitic structures by design (GSD) + injection CVD (for comparison)	GSD: Fabric coated with SiO_2 and Ni films first. Breaking and reduction of the Ni film into nanometer sized Ni particles. CNT growth at 550°C using C_2H_4 as carbon source for 1h. CVD: Catalyst (ferrocene) dissolved in xylene formed the feed solution. CNT growth on the SiO_2 coated CF fabrics at 680°C for 1h.	EP Vacuum bagging	SEM, TEM, Raman, DMA, tensile test		Novel technique using reactive gas mixture proposed. The GSD-grown MWCNT is less crystalline than those grown by CVD. SiO_2 film protected the CF against catalyst diffusion. The thermal induced degradation effect was less for GSD than for CVD. Improvement in the performance with GSD-grown CNT demonstrated	[72]

Table 4

Table 4: Carbon nanofiber grafting on various high temperature-resistant inorganic fibers: preparation and interphase effects

Hierarchical fiber type/graft	Deposition		Matrix Composites	Interphase		Sensing	Comments	Ref.
	Technique	Conditions		Testing methods	Effects			
SiC fabrics/CNT	Injection CVD	Catalyst + carbon source: ferrocene dissolved in xylene, CNT growth at 800°C for < 1h	EP (anhydrid) Fabrics infiltrated by resin, stacked and cured in autoclave	Interlaminar fracture toughness (G_{IC}), flexural test, damping, thermal conductivity	G_{IC} improved by 348%	-	G_{IC} improvement assigned to mechanical interlocking between SiC fibers and matrix due to the CNT "forest" grown. "Value added" use of CNT grafting also with respect to other transverse properties (thermal expansion, conductivity) and damping	[73]
Aluminum silicate, quartz/CNT	Injection CVD	Catalyst + carbon source: ferrocene dissolved in cyclohexane, CNT growth at 800°C for 1h	-	SEM, TEM, Raman	-	Electrical conductivity network found	Large difference in CNT characteristics found as a function of parent fiber type. Quartz fiber induced more homogenous growth of CNT (longer and more aligned) than aluminum silicate.	[74]
Alumina fiber fabric/CNT	CVD	$Fe(NO_3)_3$ catalyst from isopropanol solution applied. Its reduction to nanoparticle formation at 750°C.	EP Hand-lay-up and vacuum bag consolidation	SEM, TEM, OM, electrical conductivity, flexural strength	ILSS increased by 69%	Both in-plane and through thickness electrical conductivity increased with increasing CNT volume fraction (up to 3%)	Simultaneous enhancements of mechanical and electrical properties reported. Capillary driven wetting through the aligned CNT forest postulated	[75]

Quartz fiber fabric/MWCNT	CVD	Catalyst: fabric impregnated by aqueous $Ni(NO_3)_2$ solution; CNT growth at 650°C using C_2H_2 for up to 1h	EP (amine) Composites by VARTM	SEM, TEM, TGA, Raman, electrical conductivity, ILSS	ILSS increased by 15%	Electrical conductivity in both in and out-of-plane directions increased. The anisotropy diminished with increasing CNT growth time	Uniformly aligned MWCNT produced. Effects of catalyst concentration and CNT growth temperature studied.	[76]
Silica fiber (sized)/CNT	Injection CVD	Injection of catalyst precursor (ferrocene) and carbon source (toluene); CNT growth at T=760°C for up to 15 min	PMMA (from solution) Microcomposite	FE-SEM, BET, contact angle single fiber tensile test, fragmentation test	IFSS improved from 9.5 MPa (as-received) up to 24.3 MPa (CNT-grafted)	-	Dramatic increase in the BET surface area. Complete wetting of the CNT grafted fiber by PMMA. Strength of the silica fibers reduced by 30% after CNT growth possibly due to etching. By contrast, the modulus increased, that was assigned to densification of the network of silica (polycondensation)	[77]

Figure 1

Click here to download high resolution image

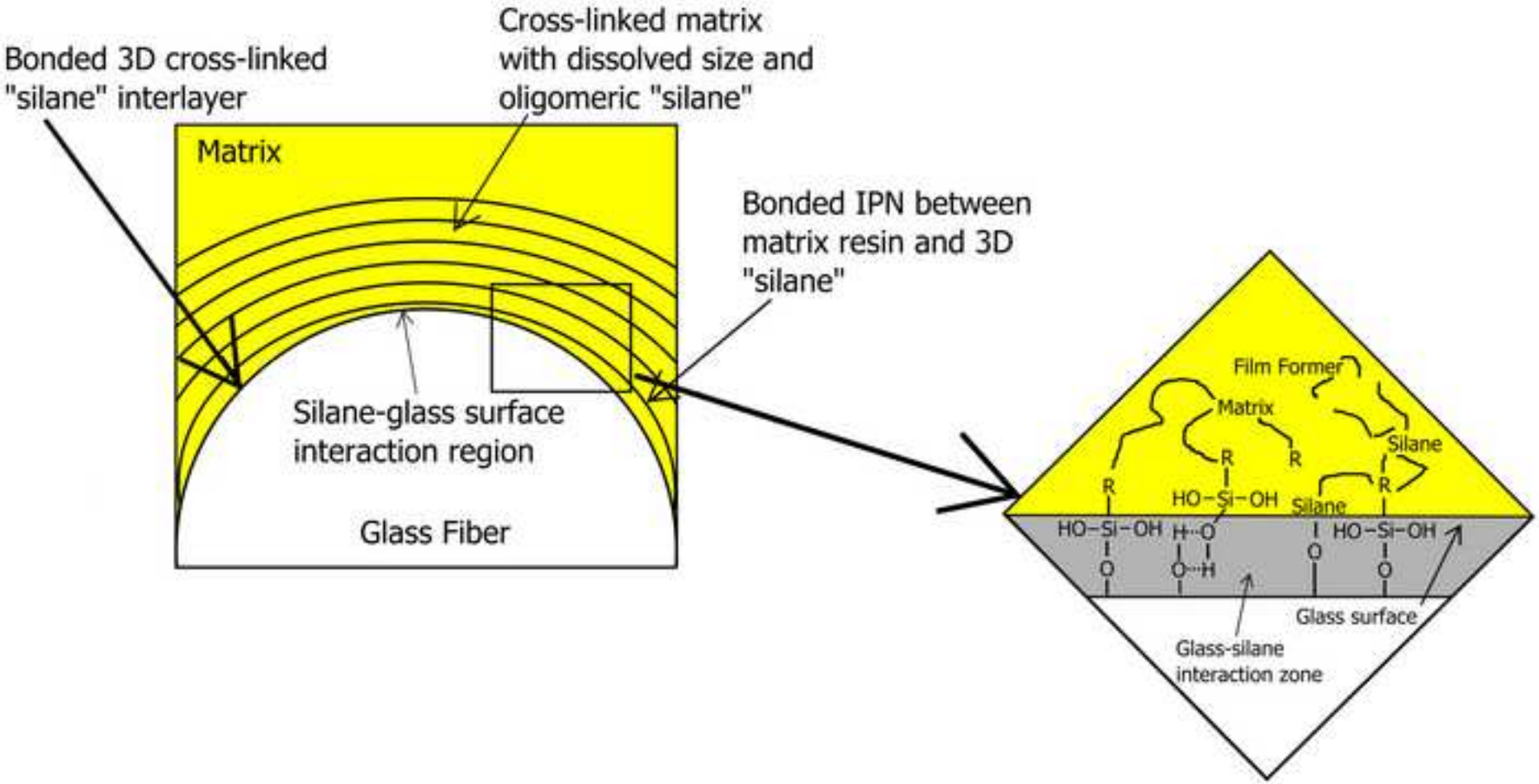

Figure 2a

Click here to download high resolution image

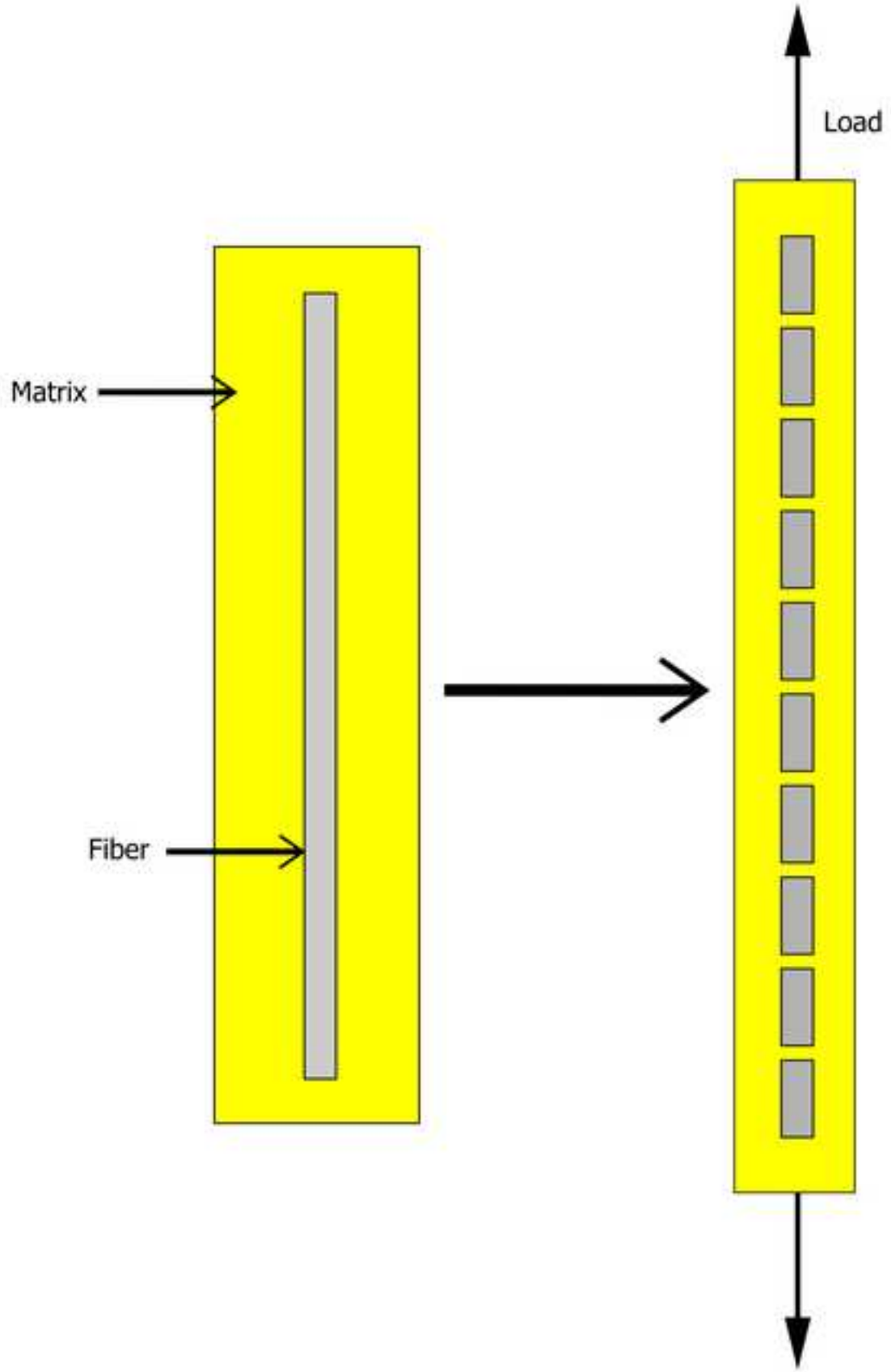

Figure 2b

Click here to download high resolution image

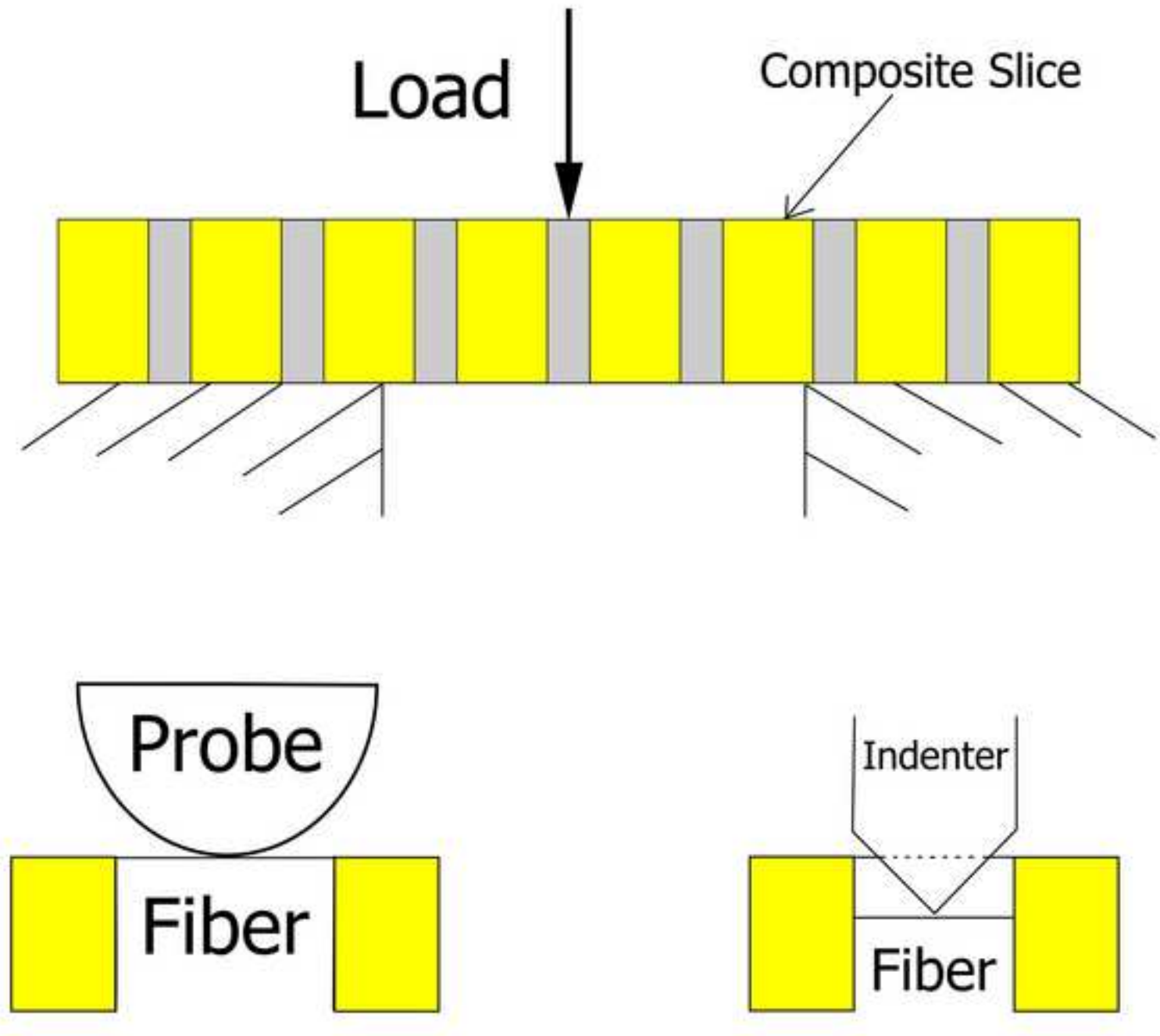

Figure 2c

Click here to download high resolution image

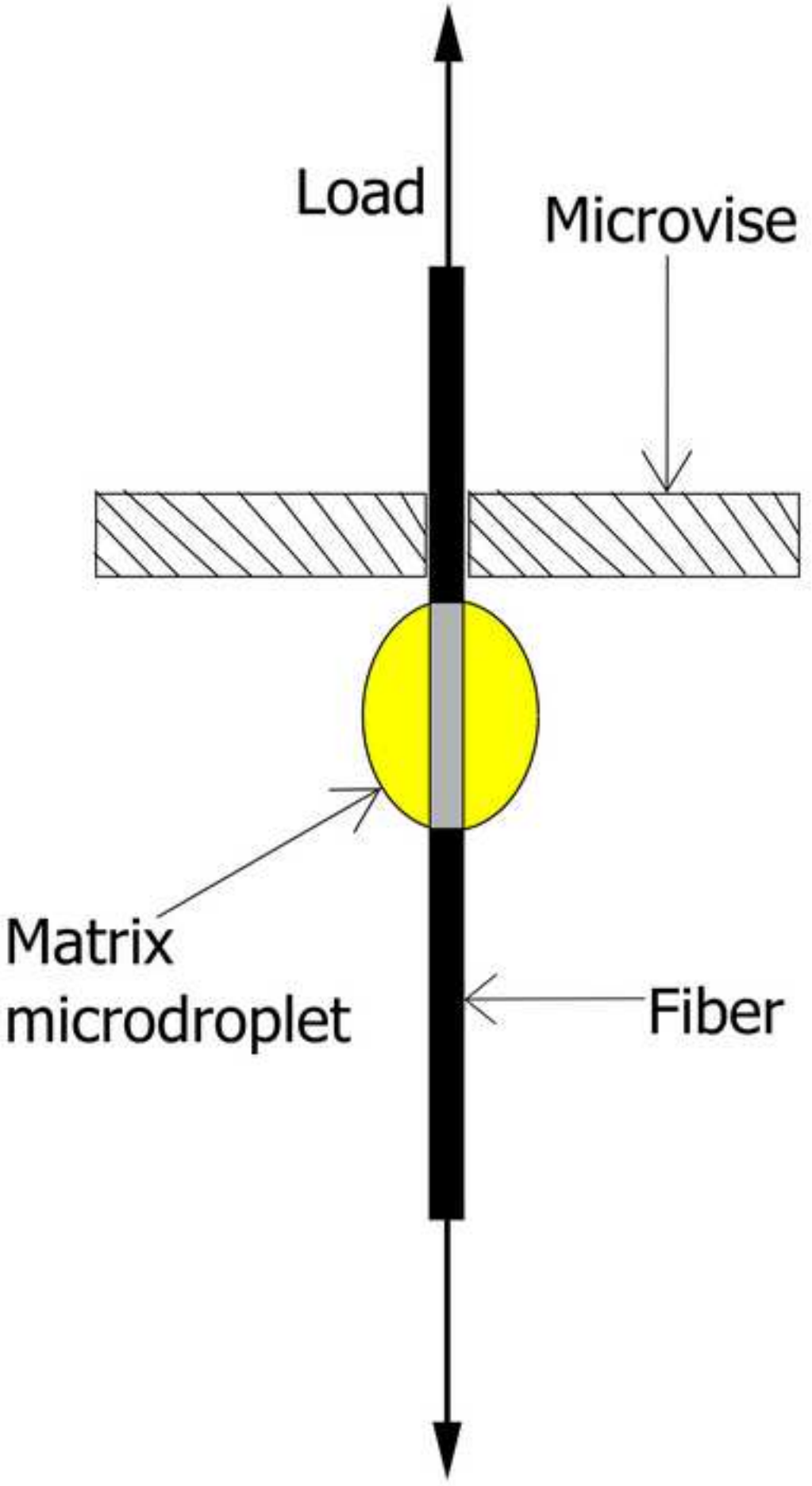

Figure 2d

Click here to download high resolution image

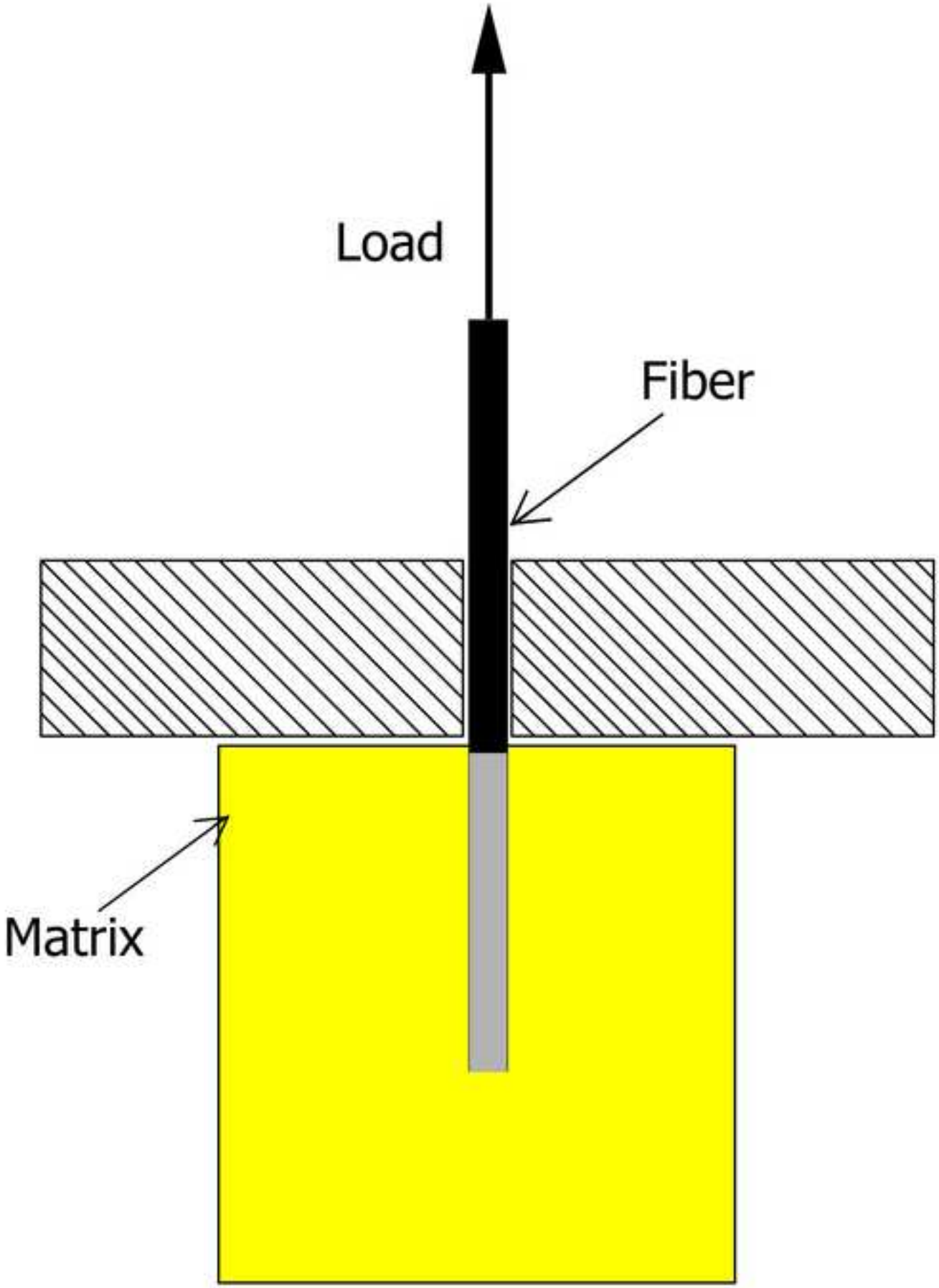

Figure 2e

Click here to download high resolution image

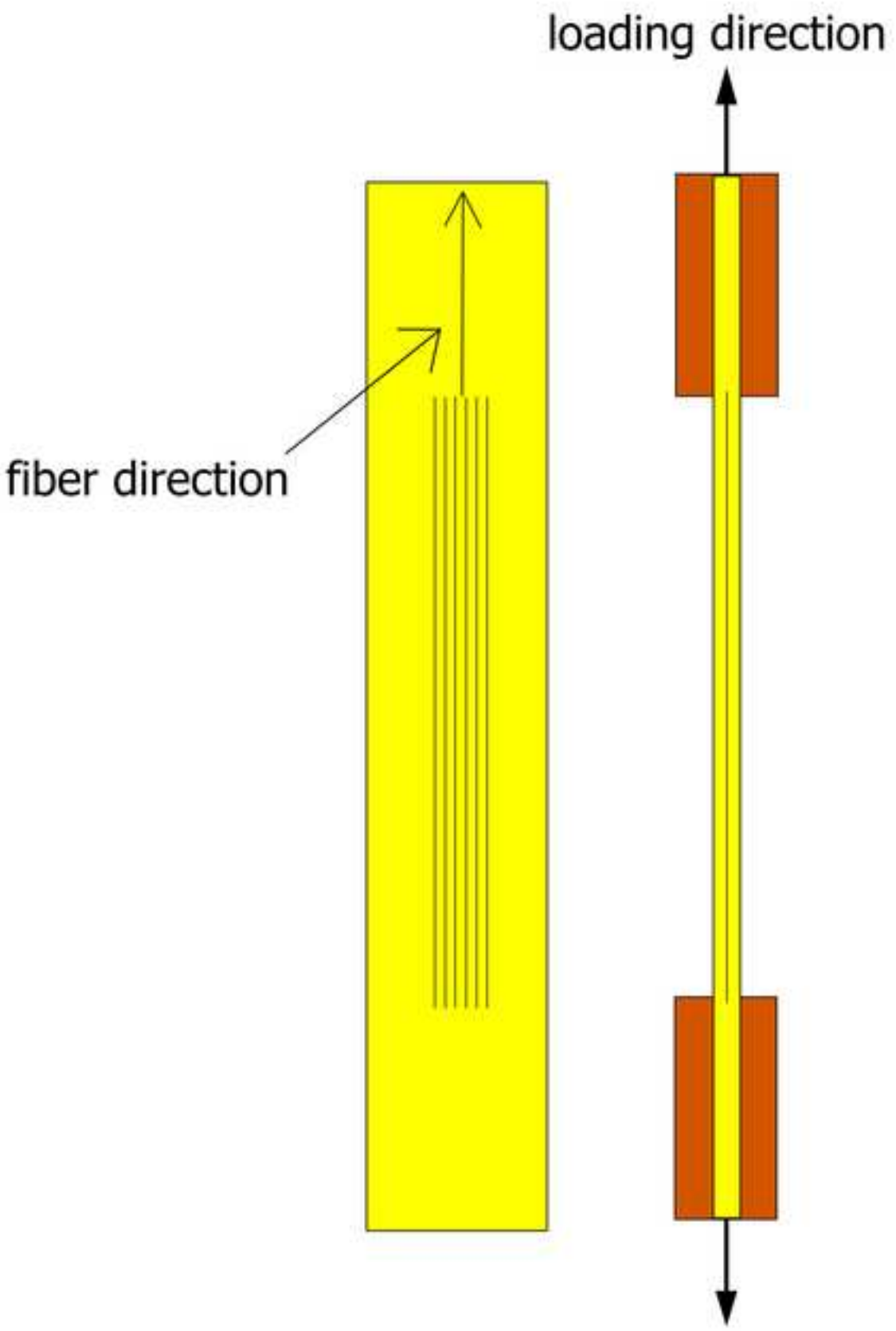

Figure 2f

Click here to download high resolution image

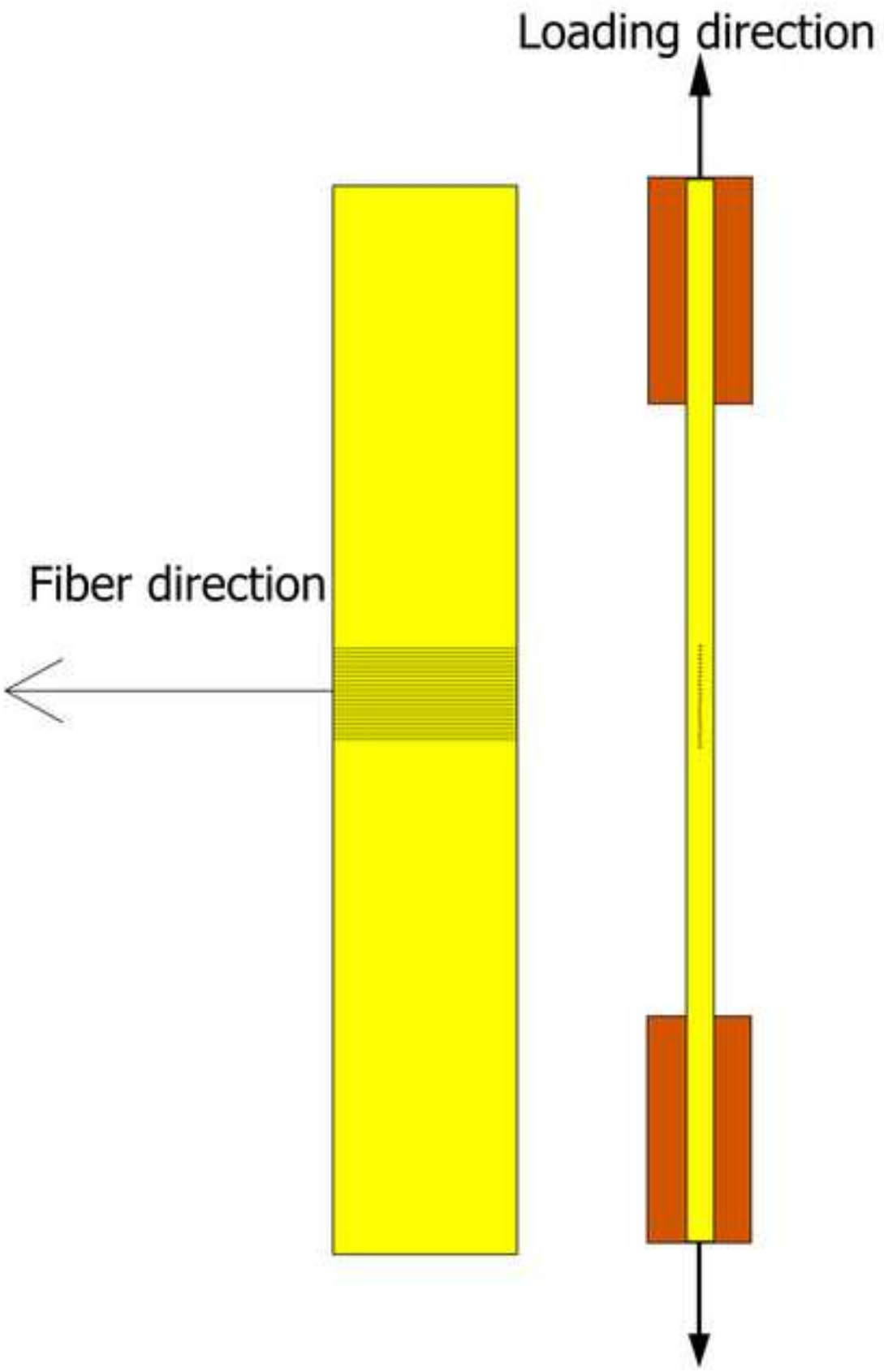

Figure 2g

Click here to download high resolution image

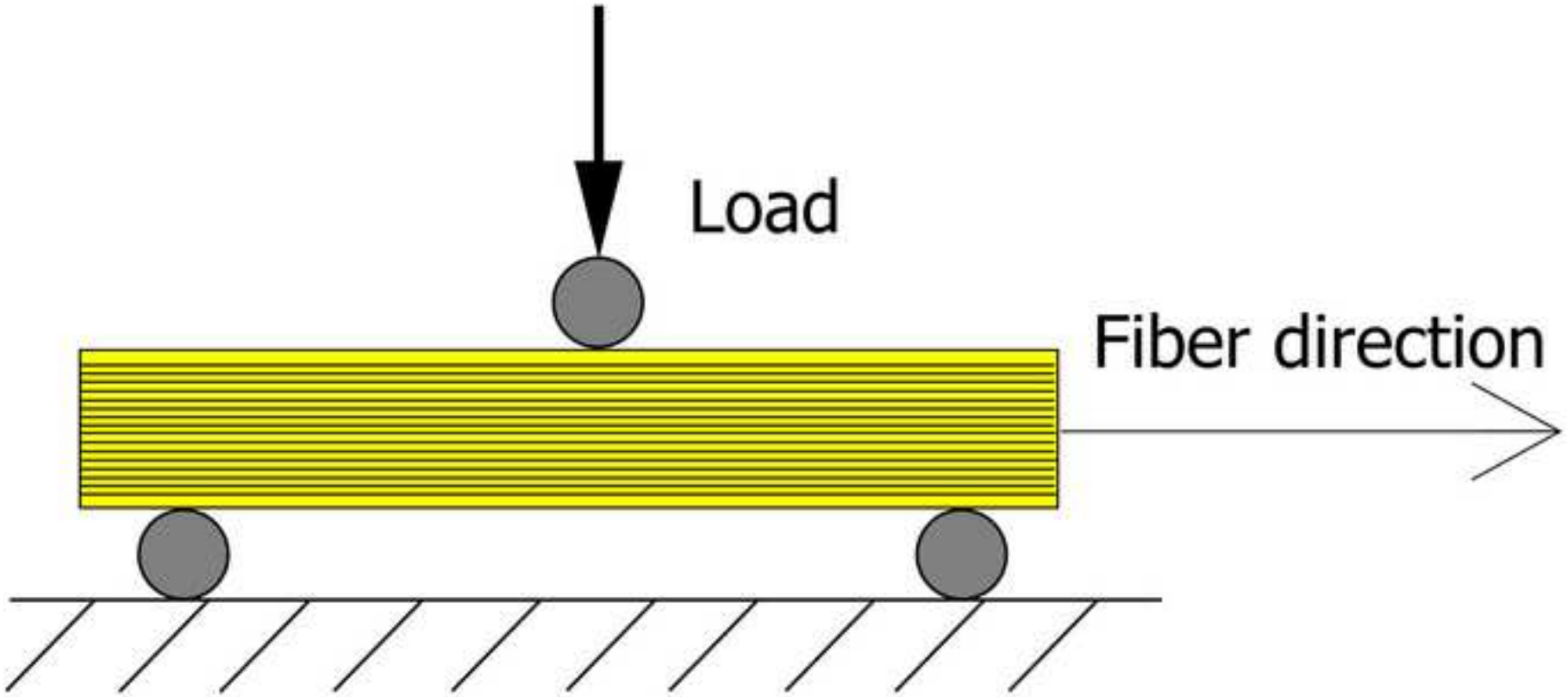

Figure 2h

Click here to download high resolution image

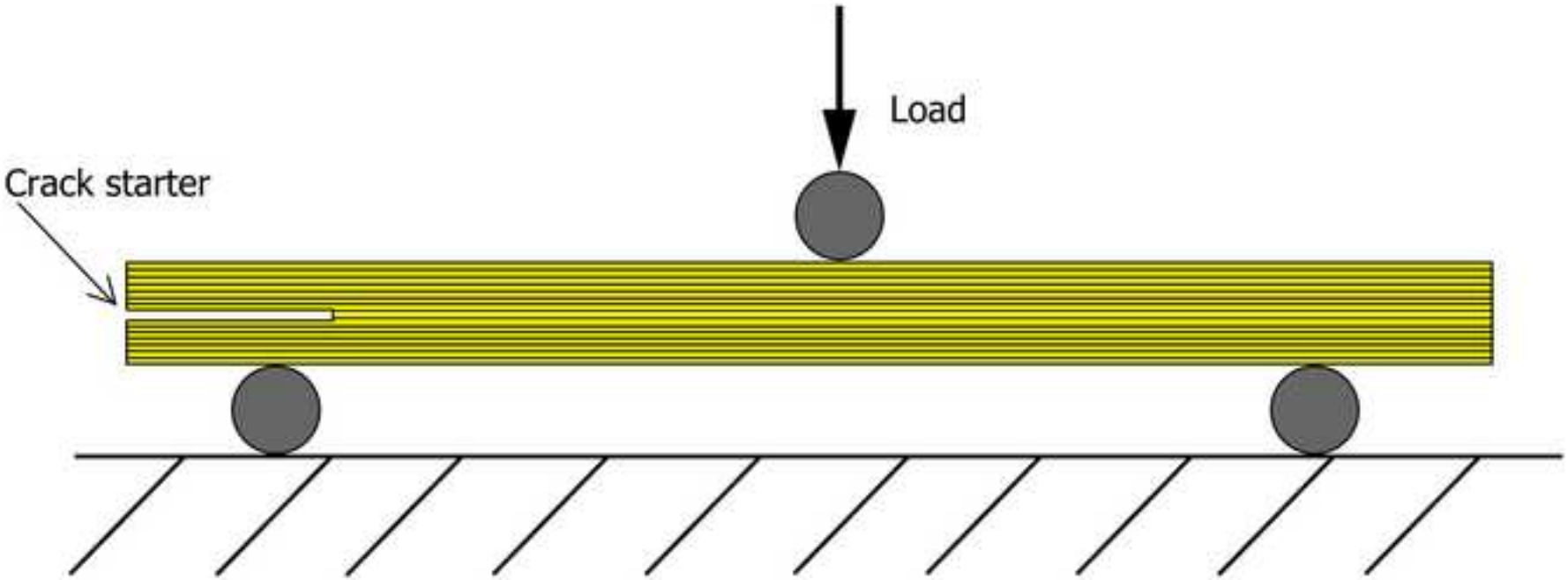

Figure 2i

Click here to download high resolution image

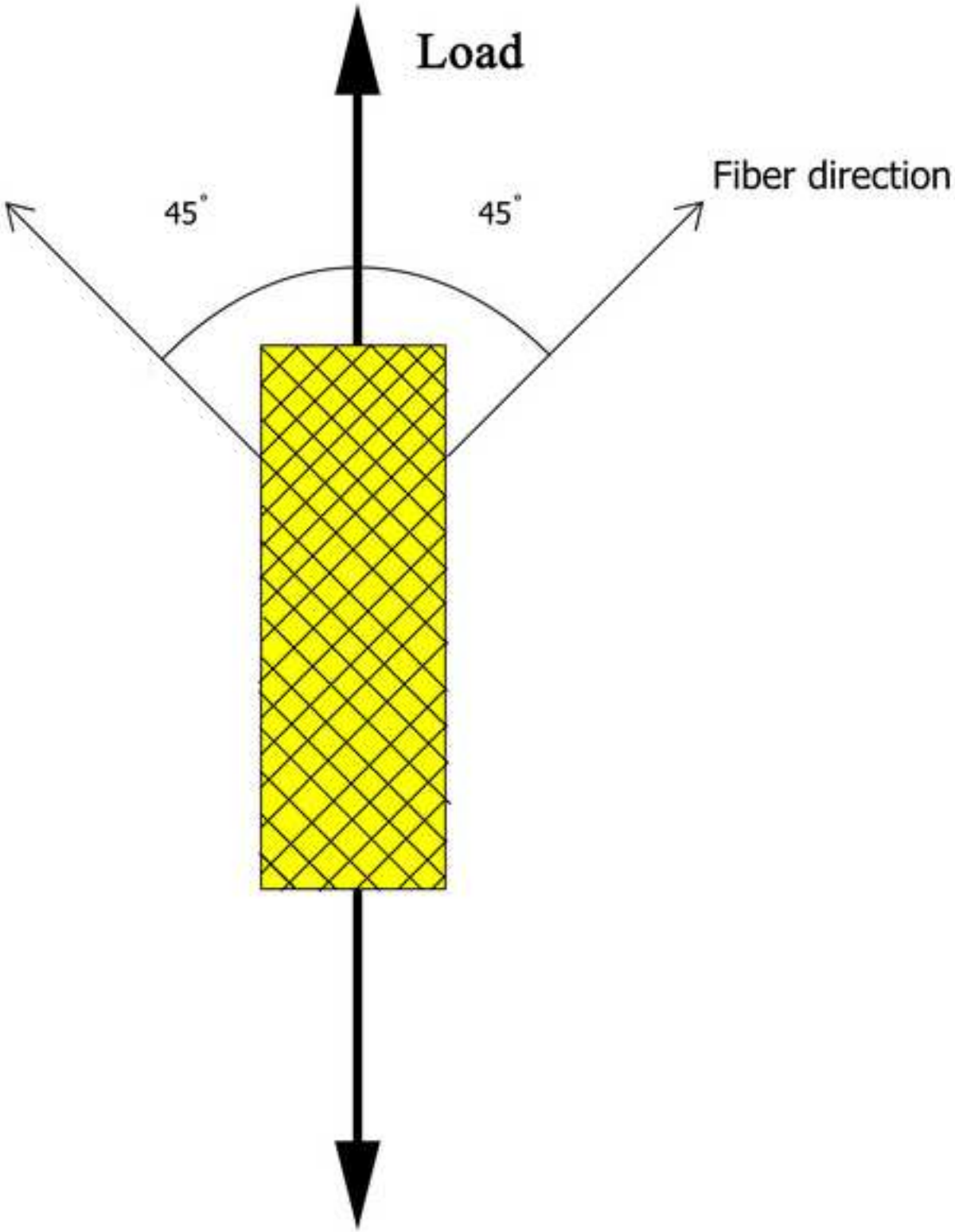

Figure 2l

Click here to download high resolution image

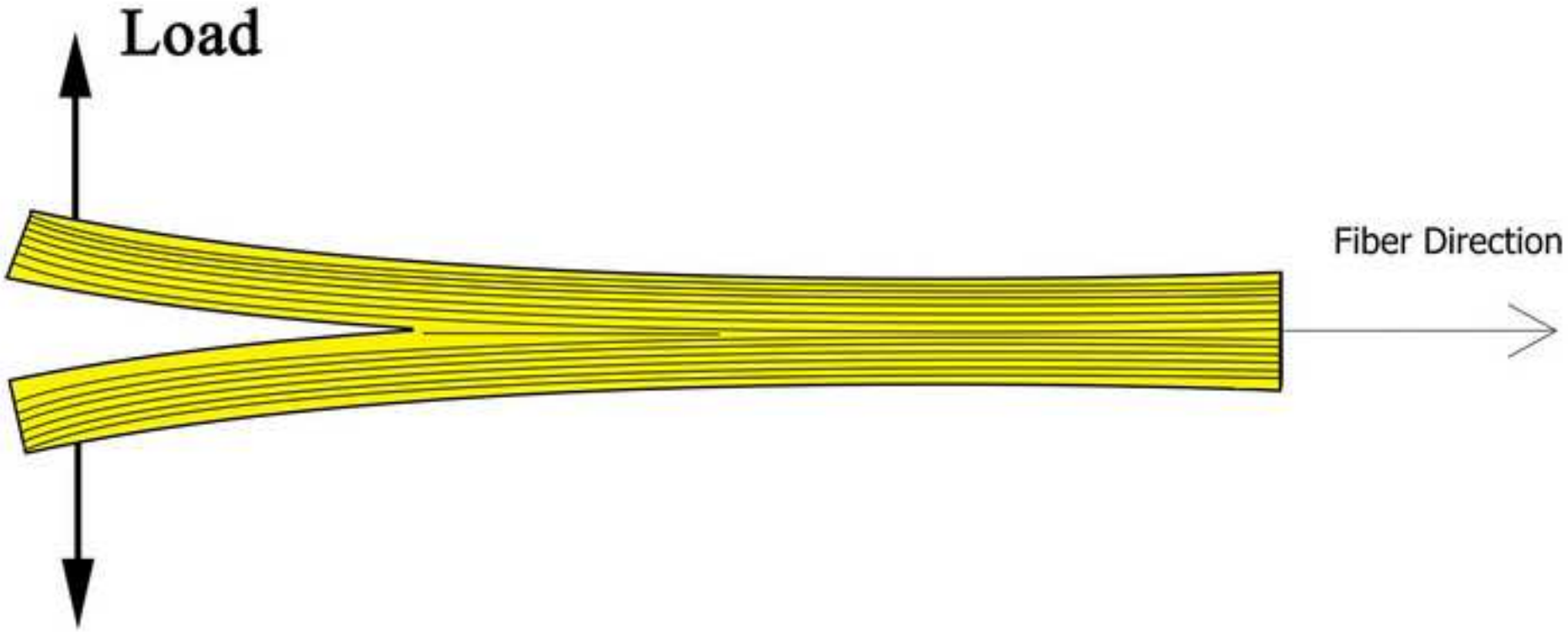

Figure 2m

Click here to download high resolution image

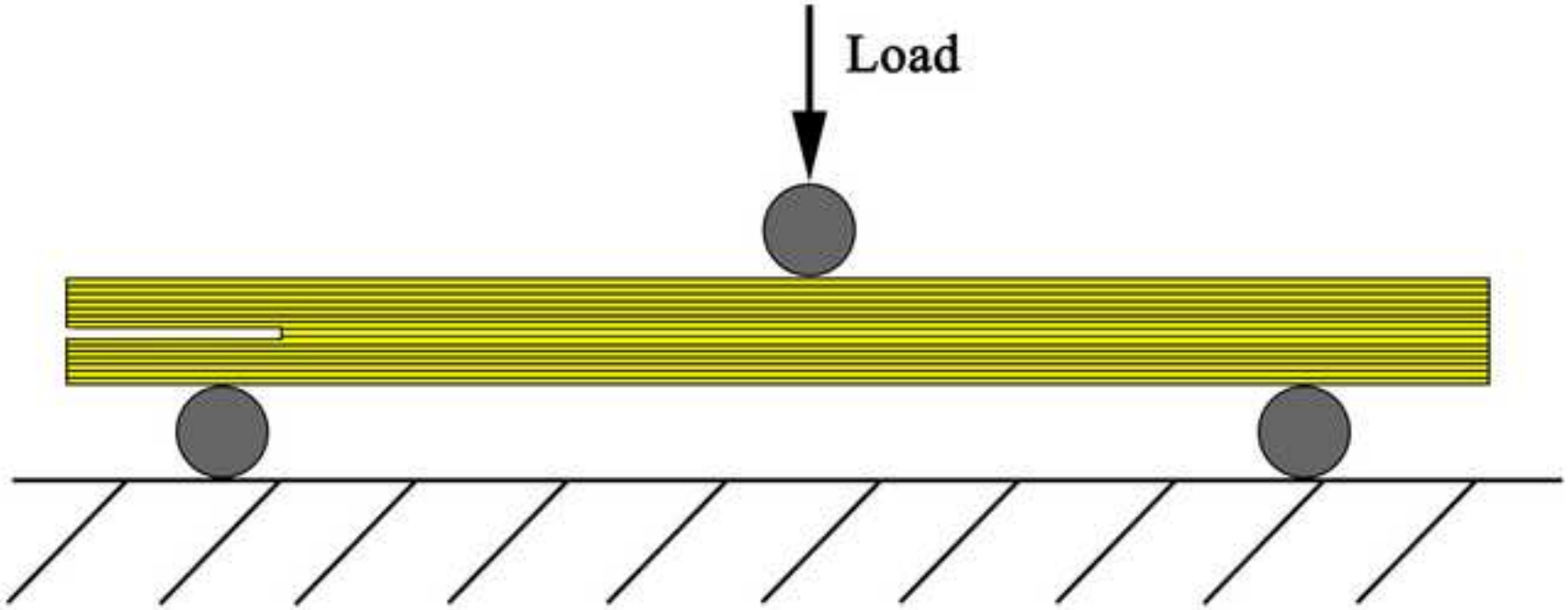

Figure 3

Click here to download high resolution image

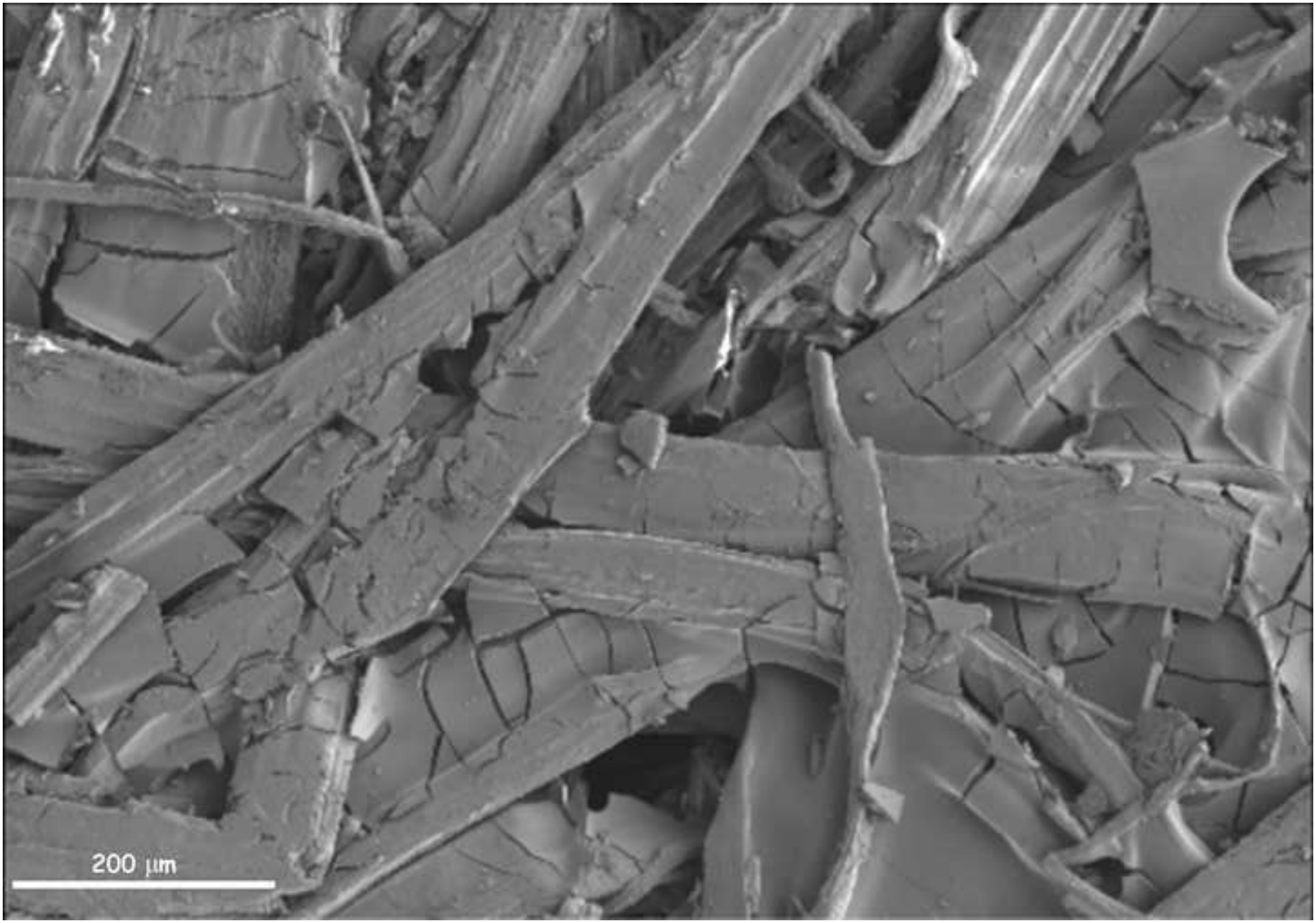

Figure 4 a,b,c

Click here to download high resolution image

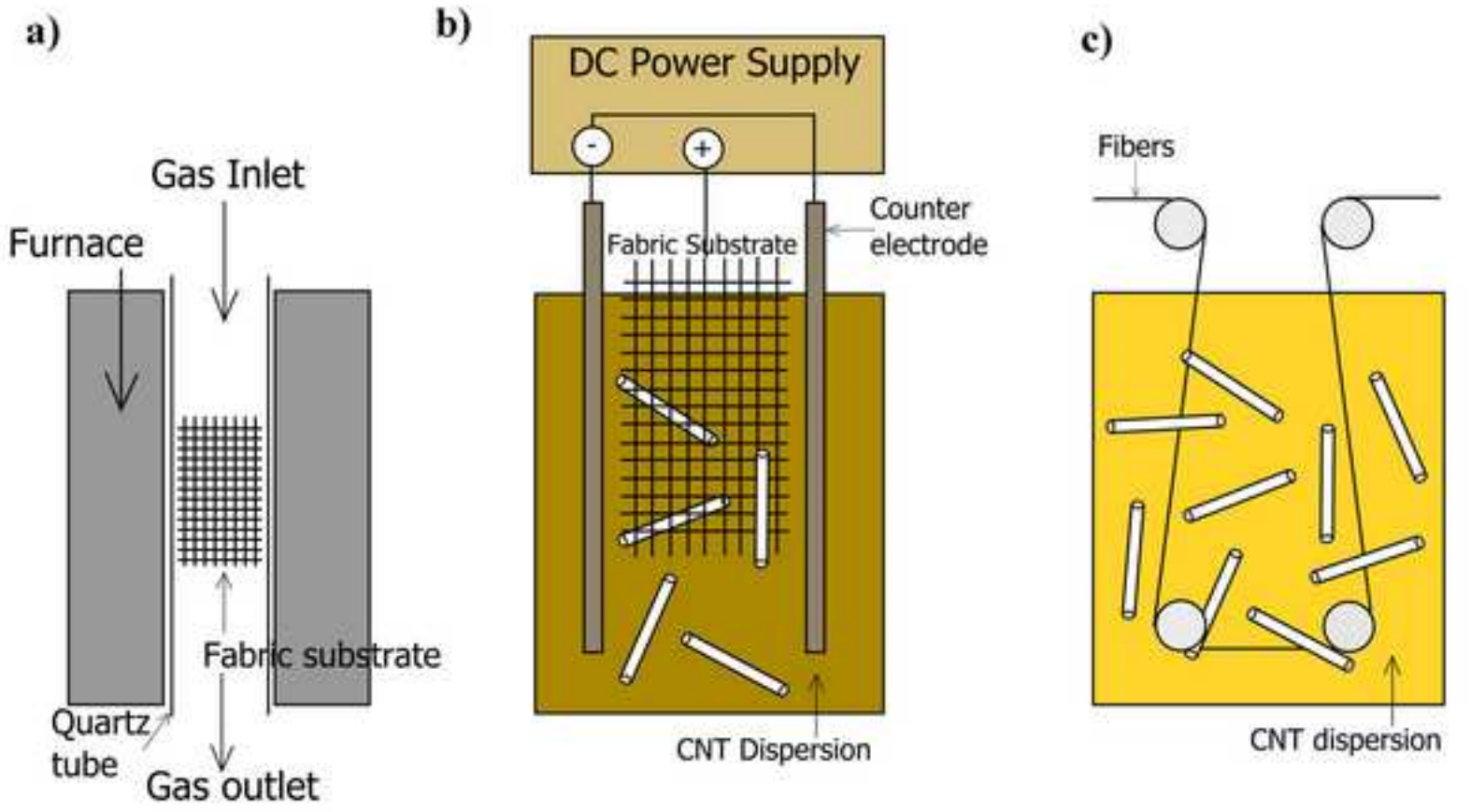

Figure 4d
Click here to download high resolution image

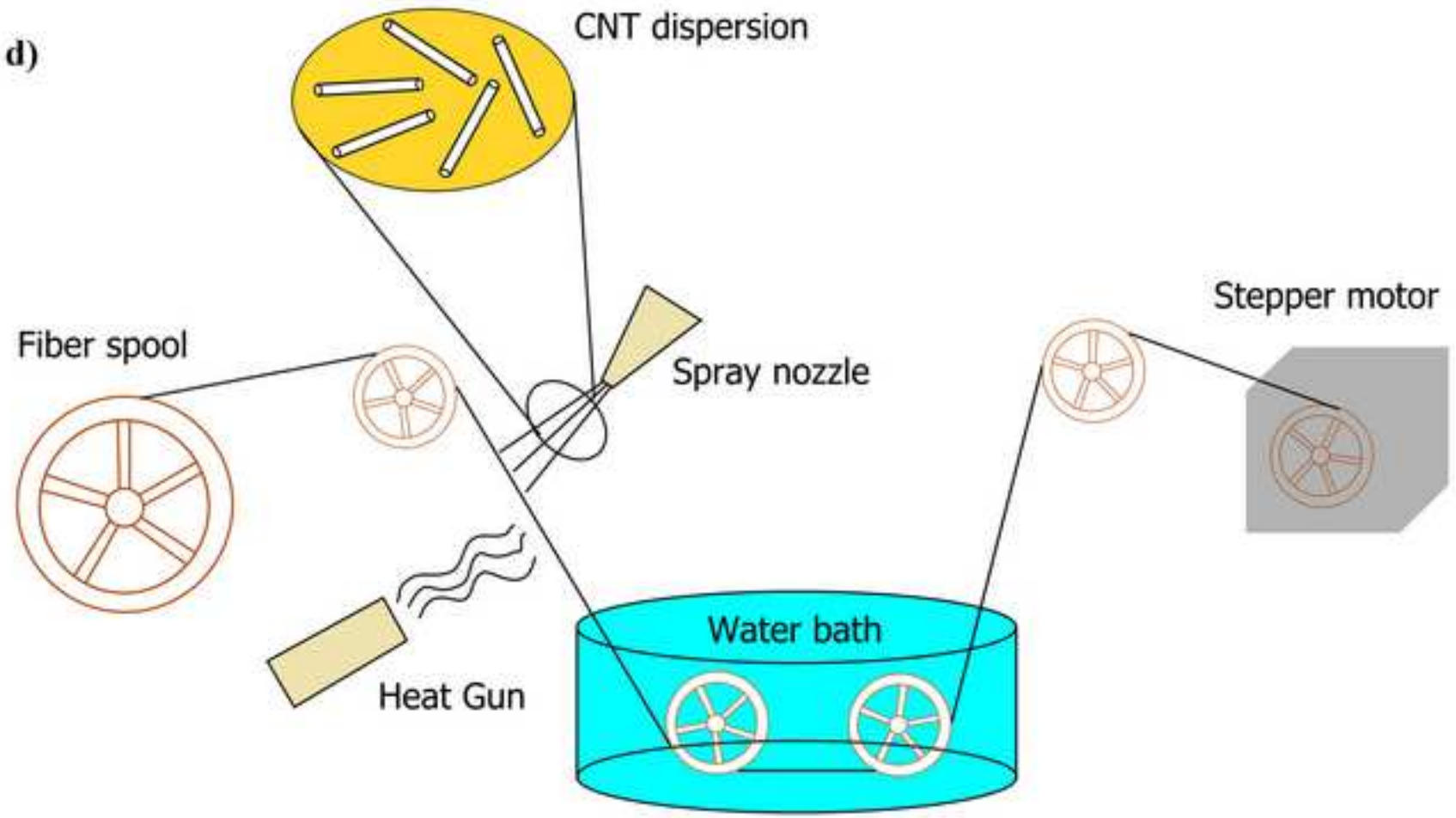

Figure 5

Click here to download high resolution image

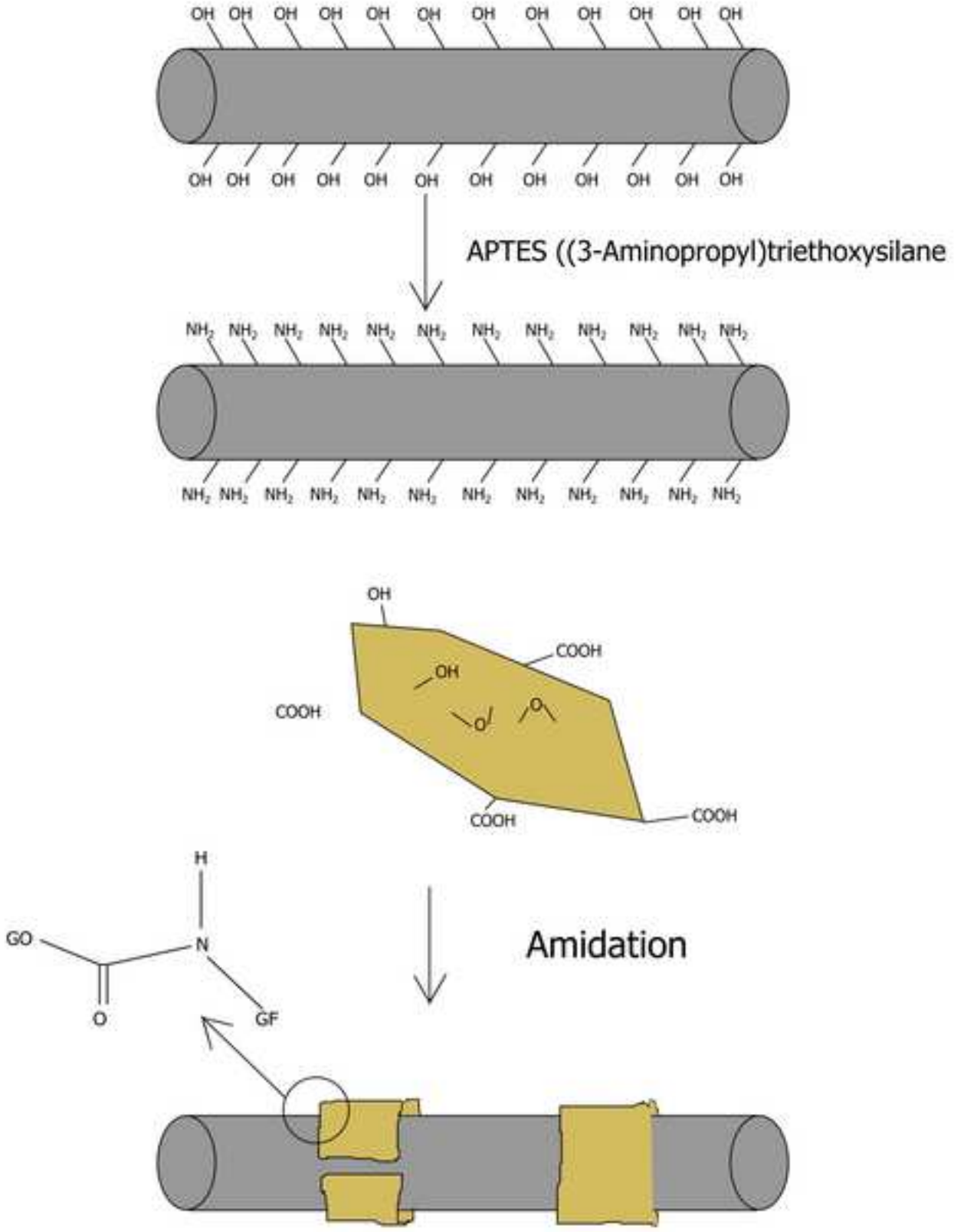

Figure 6

Click here to download high resolution image

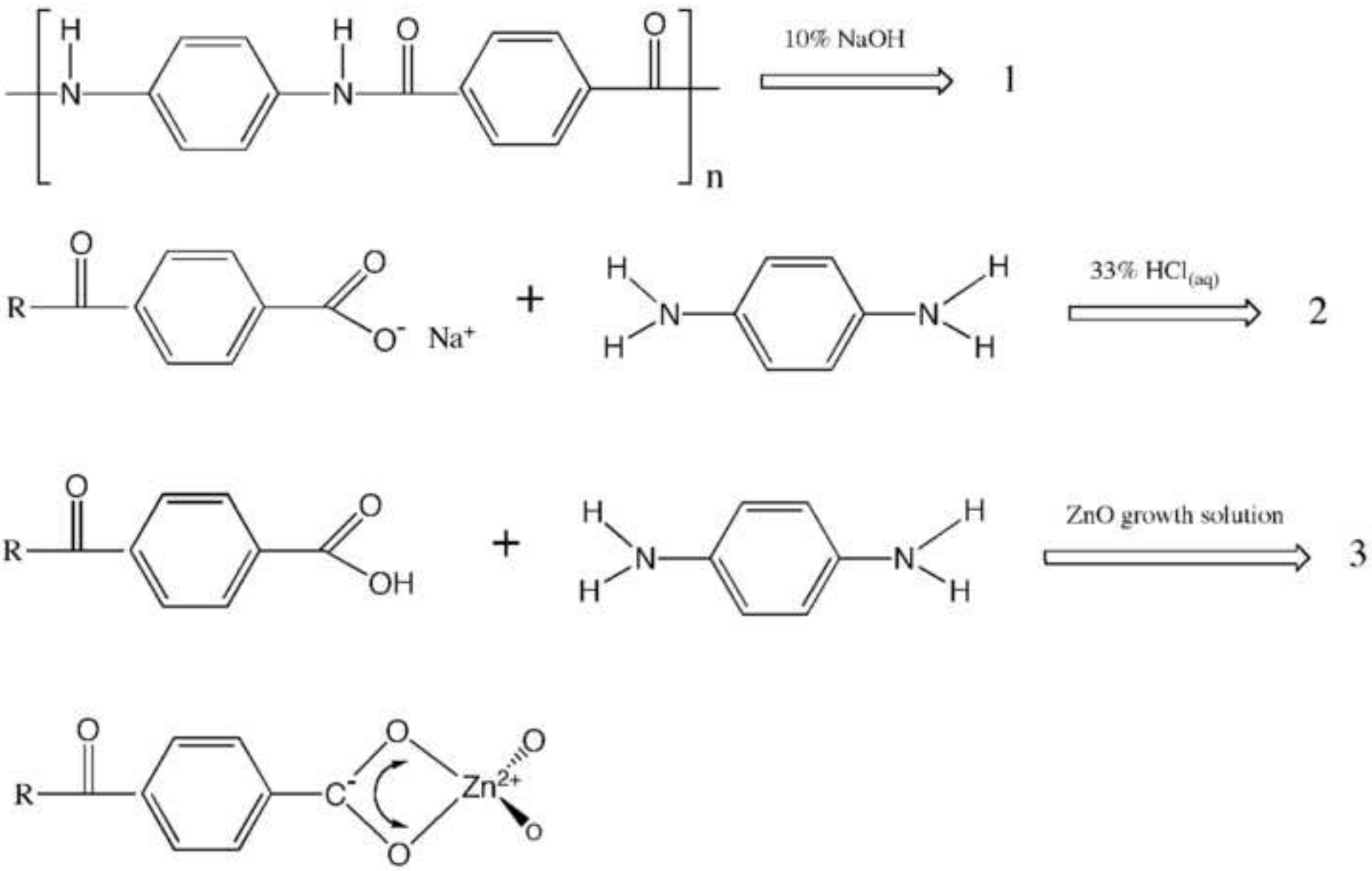

Figure 7

Click here to download high resolution image

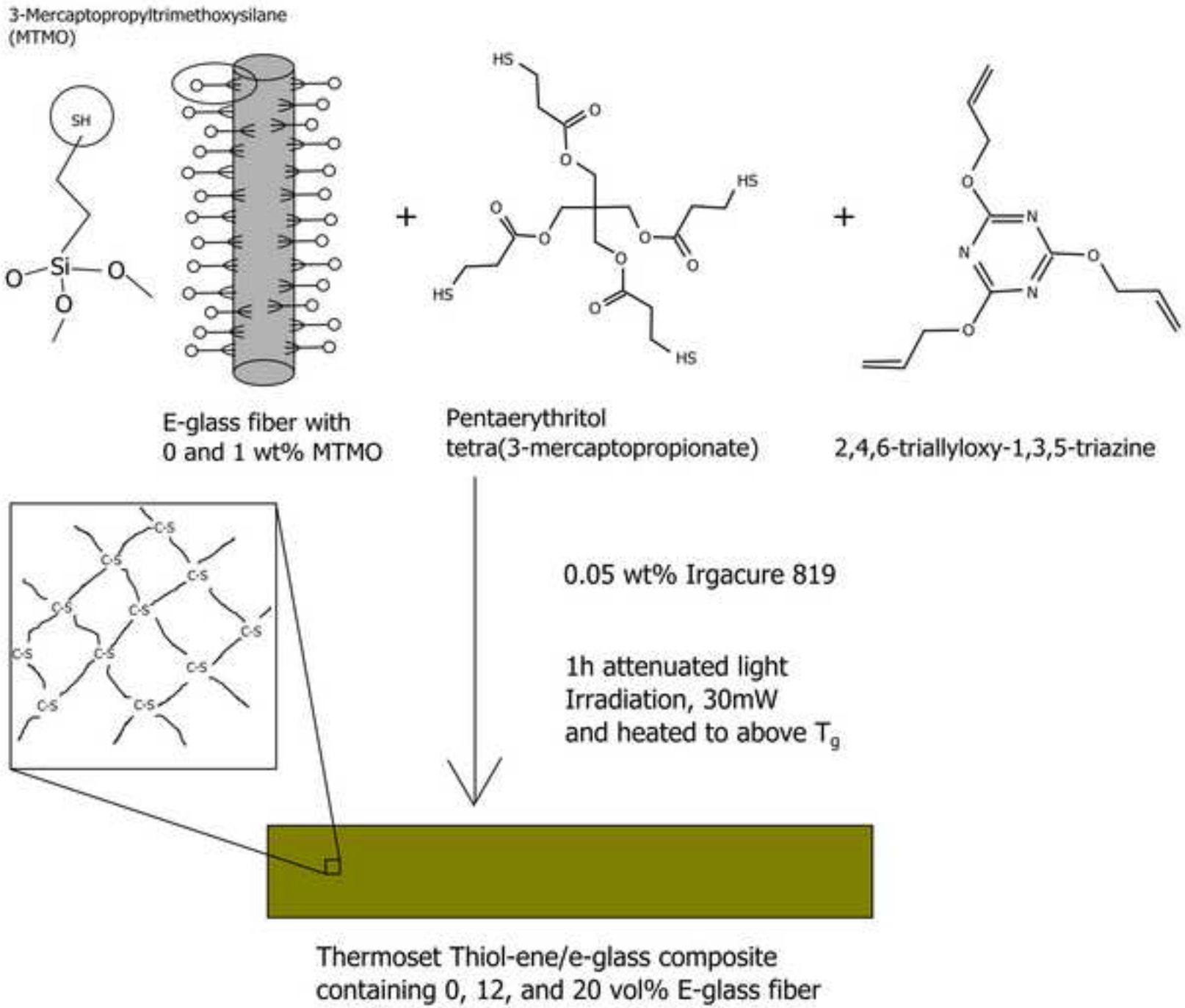

Figure 8a-1
Click here to download high resolution image

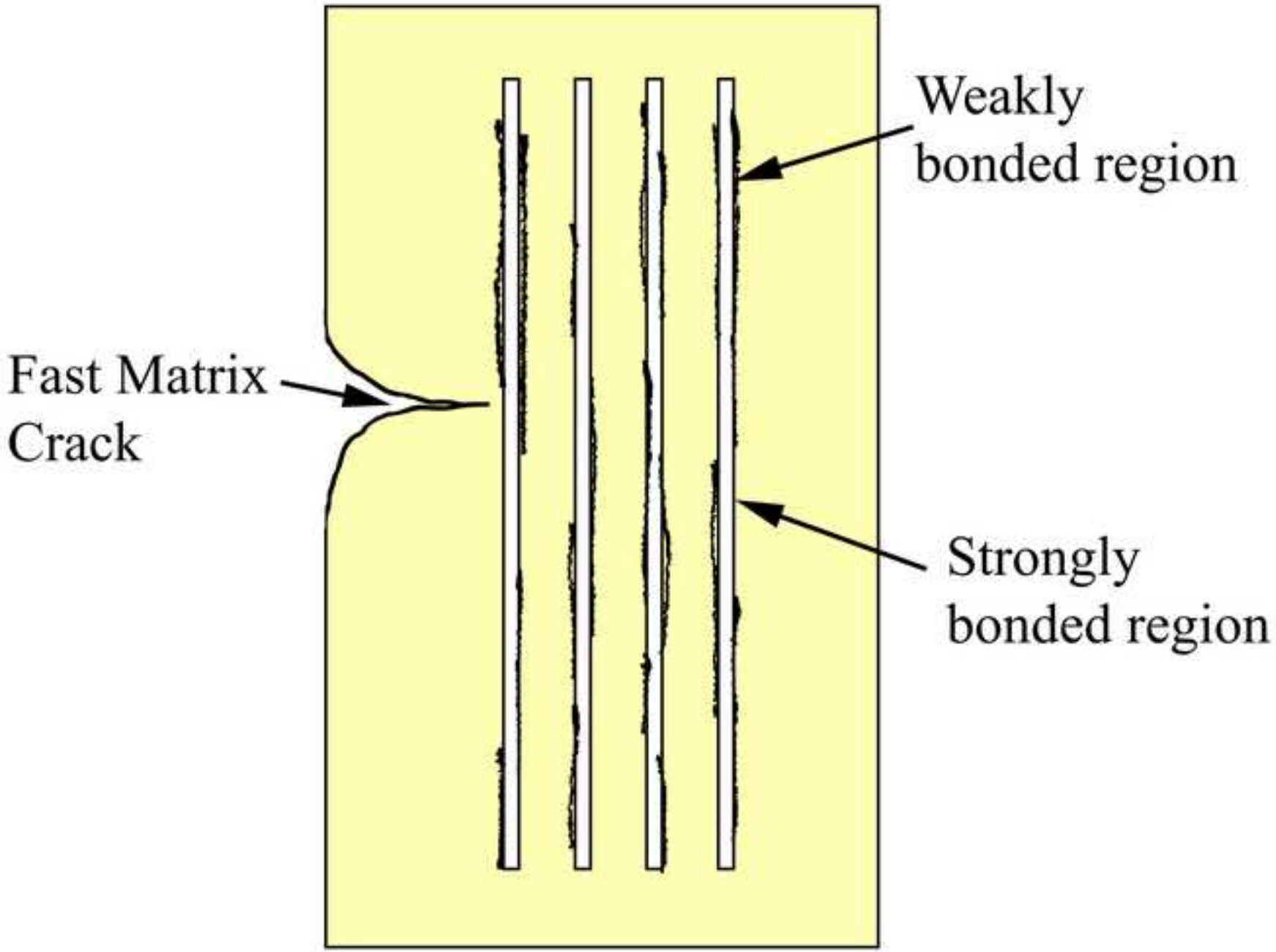

Figure 8a-2
Click here to download high resolution image

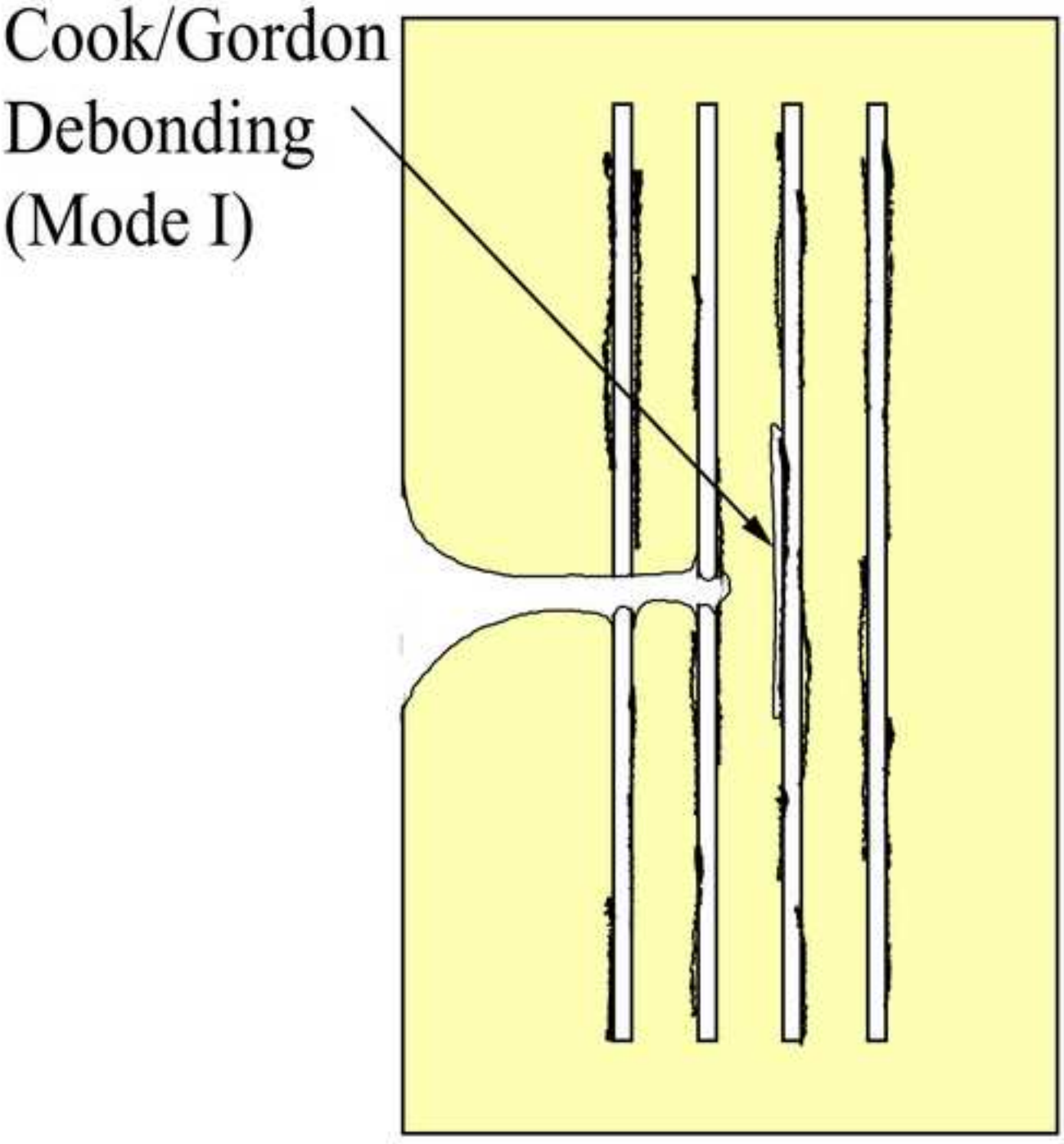

Figure 8a-3
Click here to download high resolution image

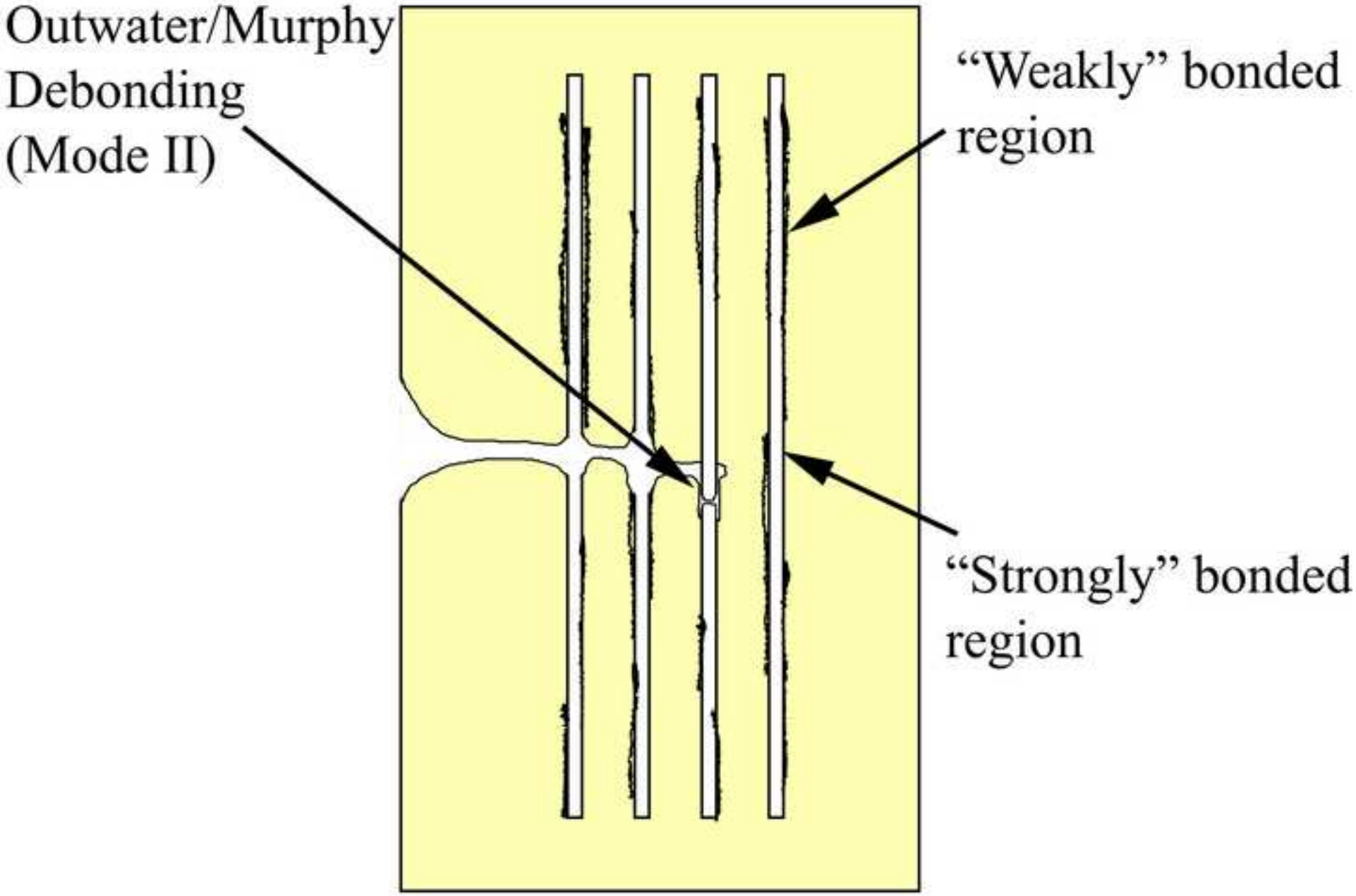

Figure 8b
Click here to download high resolution image

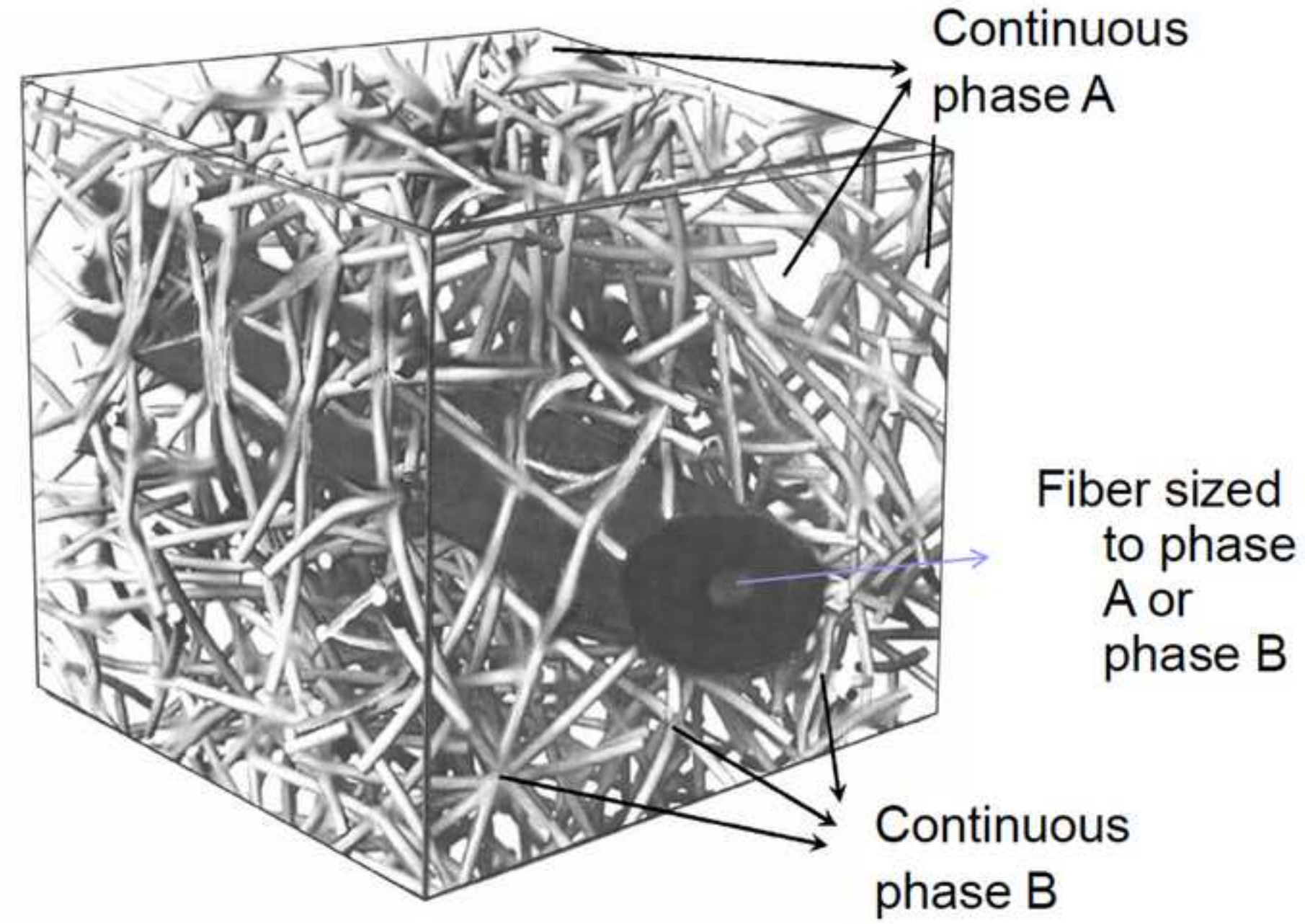

Figure 9

Click here to download high resolution image

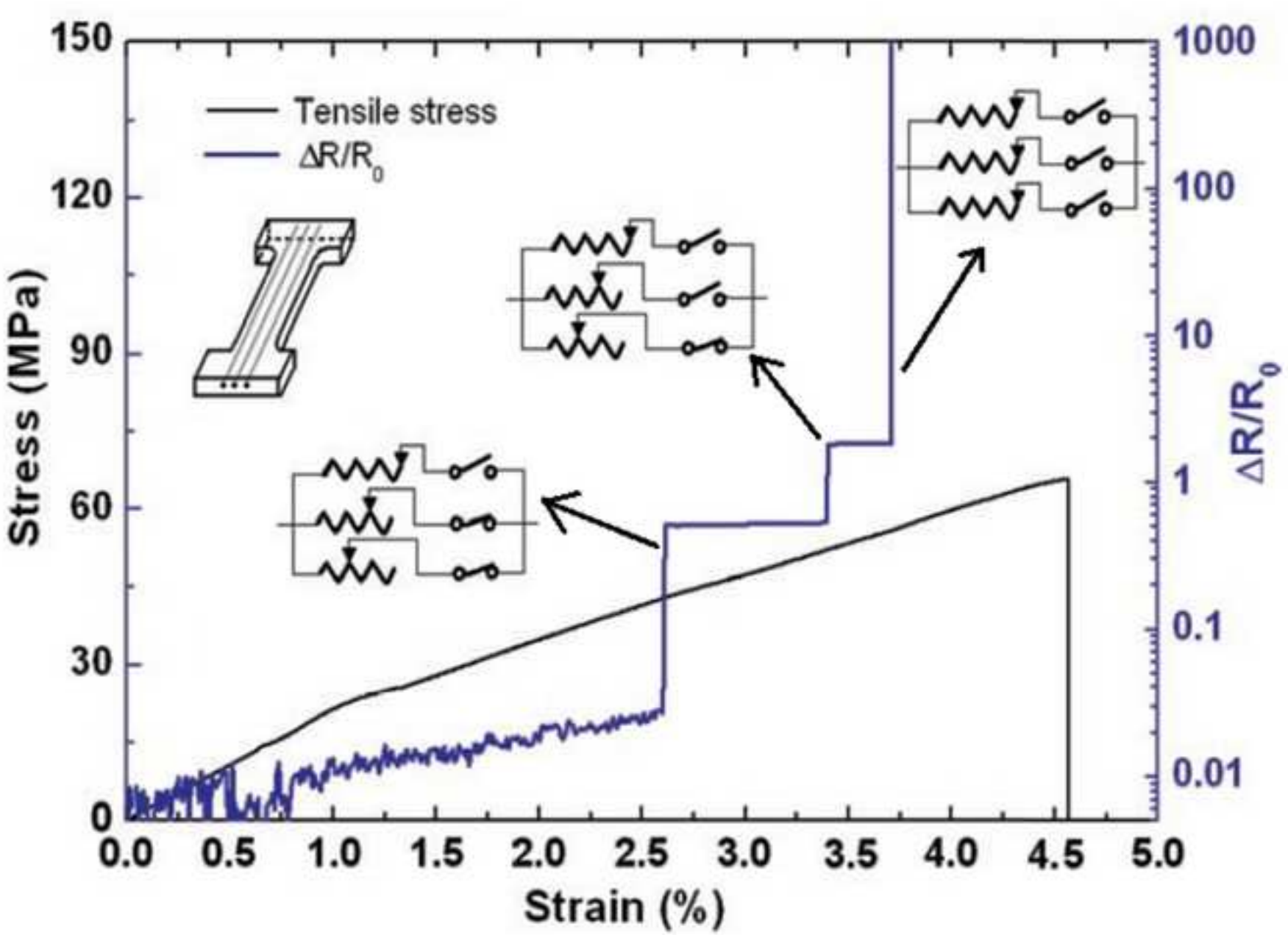

Figure 10a

Click here to download high resolution image

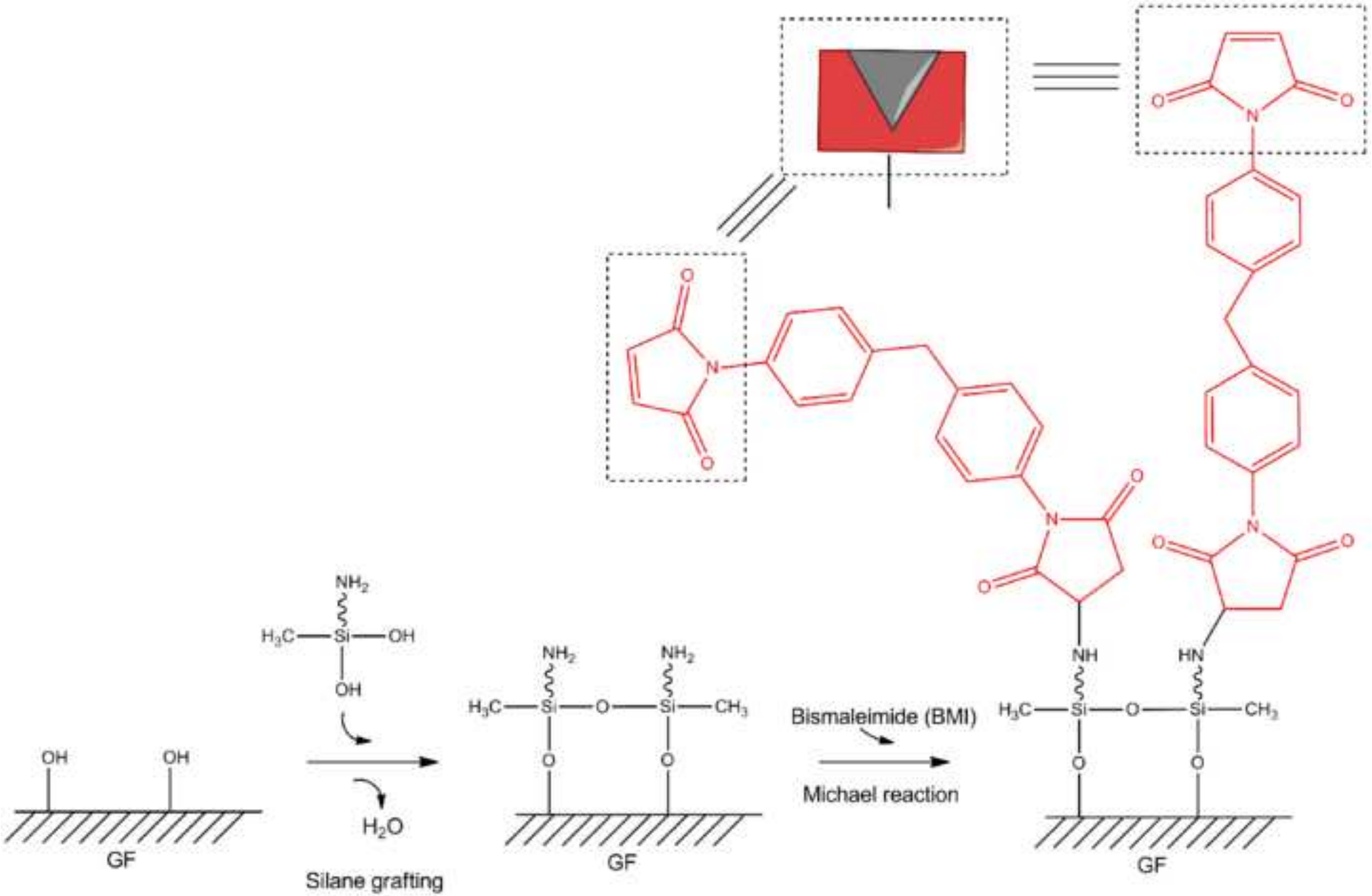

Figure 10b

Click here to download high resolution image

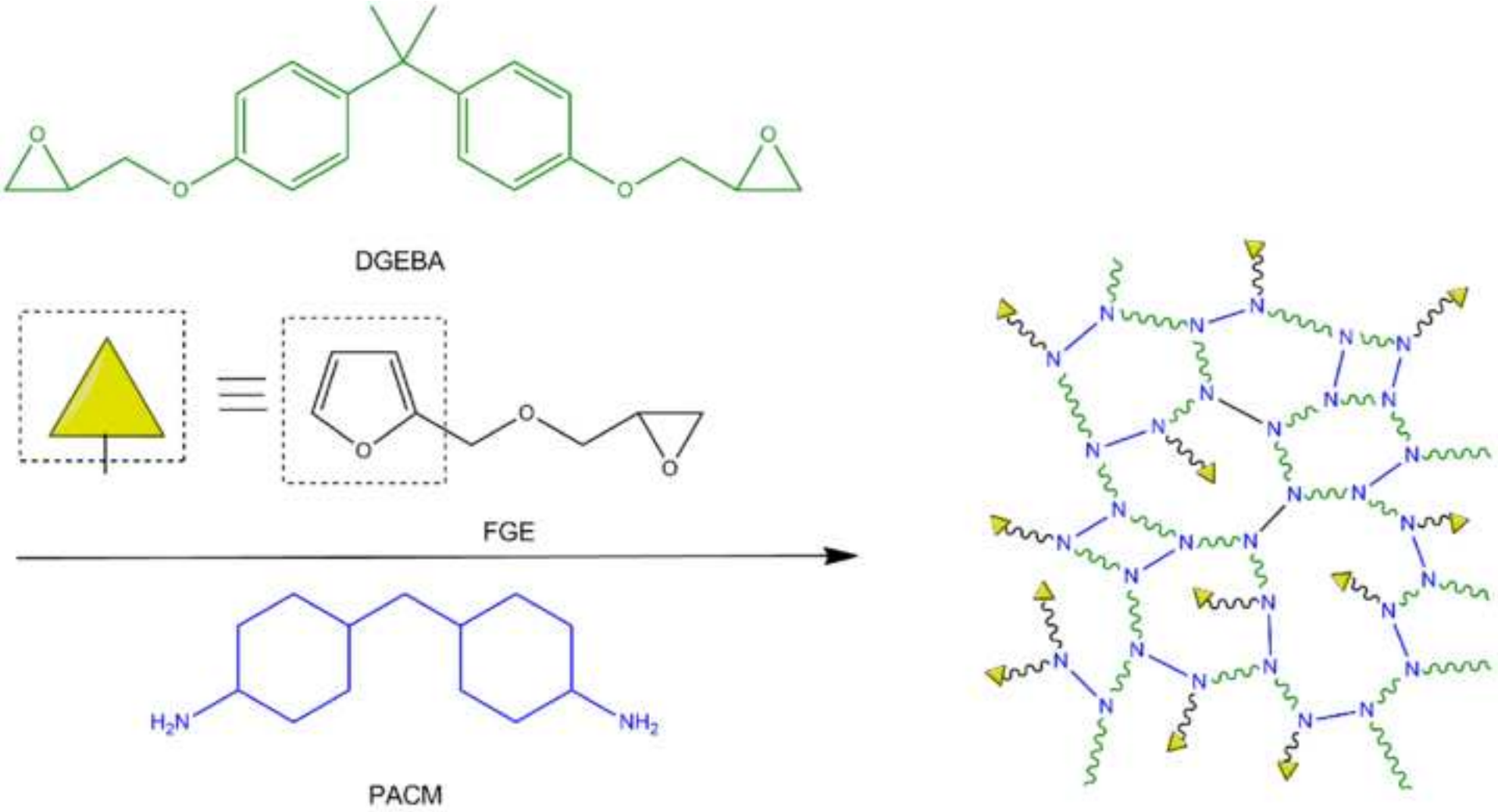

Figure 10c

Click here to download high resolution image

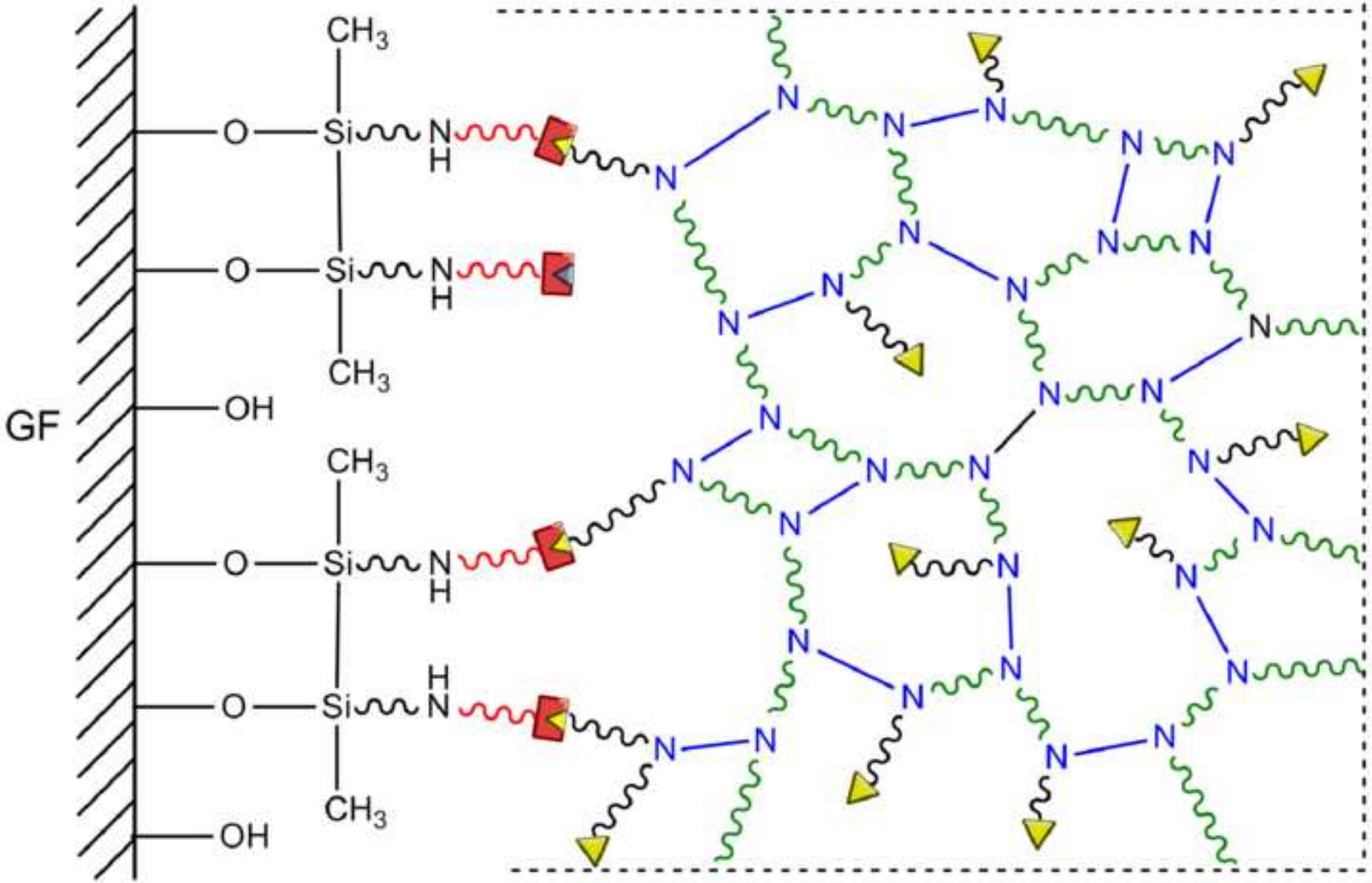

Figure 11

Click here to download high resolution image

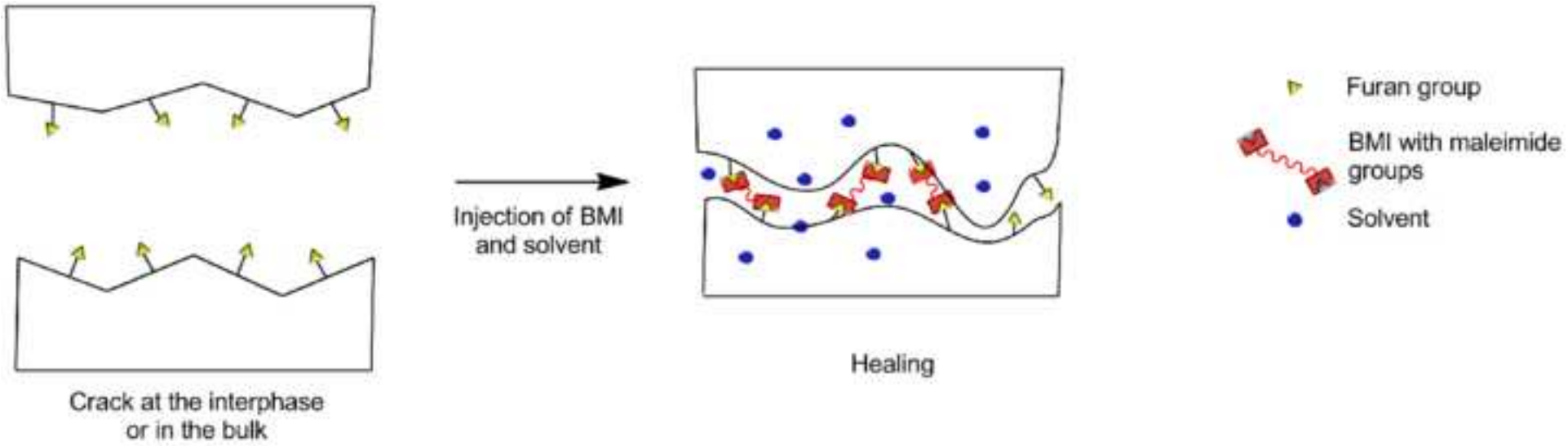

Figure 12

Click here to download high resolution image

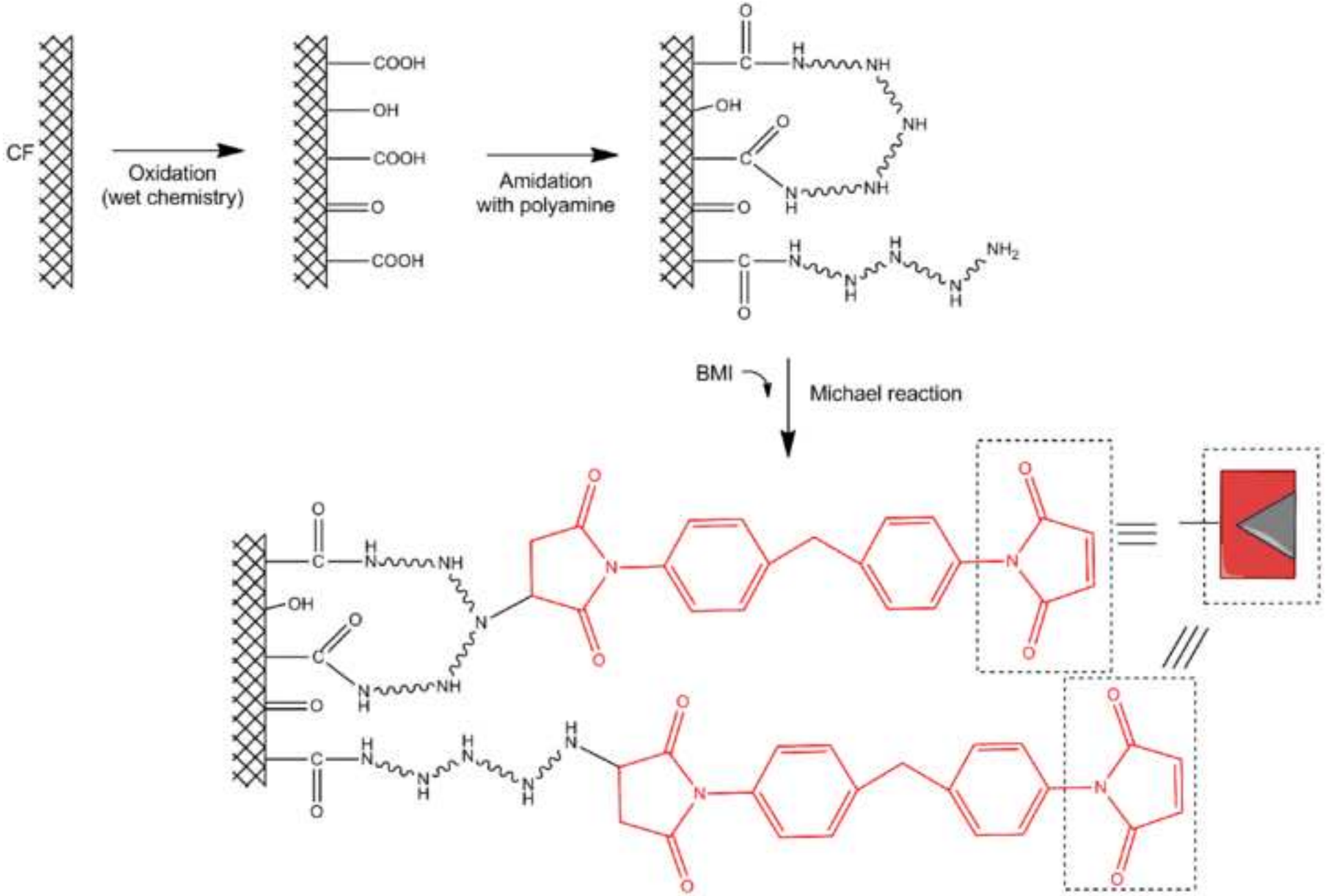

Figure 13

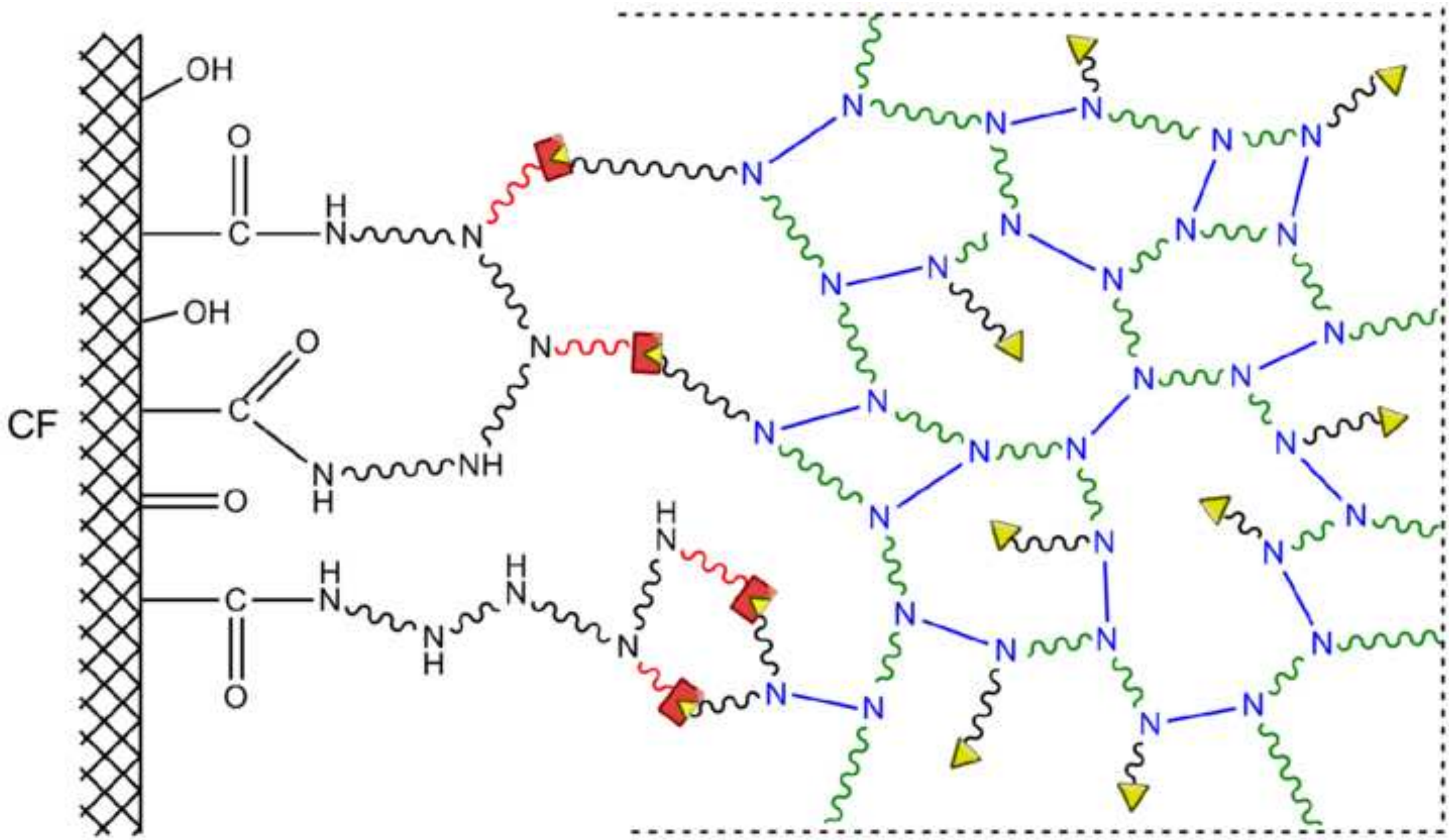

Figure 14

Click here to download high resolution image